台風セミナー2014 東京 2014.12.15-16

台風と地球温暖化

Part 1: これまでの研究のレビュー

Part 2: 現在の課題と議論

気象研究所客員研究員

杉　　正人

研究経歴

		所属	研究開発課題
1974	3年	気象庁仙台管区気象台	
1977	7.5年	気象庁予報部電子計算室	数値予報モデル開発、熱帯擾乱の予報
1984	2年	フロリダ州立大学	数値予報モデル開発、熱帯の数値予報
1986	2.5年	気象庁予報部数値予報課	数値予報モデル開発
1989	3年	気象研究所気候研究部	気候モデル開発
1992	4年	防災科学技術研究所気圏・水圏研究部	気候モデル開発、季節予報、台風と温暖化
1996	6年	気象研究所気候研究部	気候モデル開発、季節予報、台風と温暖化
2002	3年	気象庁気候・海洋気象部気候情報課	季節予報
2005	4年	気象研予報研究部	積雲対流、台風と温暖化
2009	5年	海洋研究開発機構	台風と温暖化、積雲対流
2014	?	気象研究所気候研究部	台風と温暖化、積雲対流

PART1

台風と地球温暖化に関する研究のレビュー

I.　1990-1995 （IPCC-SAR　まで）

II.　1996-2001　(IPCC-TAR　まで）

III.　2002-2007 （IPCC-AR4　まで）

IV.　2008-2013 （IPCC-AR5　まで）

I. 1990-1995 (IPCC-SAR まで)

Broccoli and Manabe (1990) GRL

Evans (1992) GRL

Ryan et al. (1992) GRL

Haarsma et al. (1993) CD

IWTC-3 (1993) Huatulco, Mexico

Lighthill et al. (1994) BAMS (← IWTC-3)

IPCC SAR (1995)

Broccoli and Manabe (1990) GRL

GEOPHYSICAL RESEARCH LETTERS, VOL 17, NO 11, PAGES 1917 1920, OCTOBER 1990

CAN EXISTING CLIMATE MODELS BE USED TO STUDY ANTHROPOGENIC CHANGES IN TROPICAL CYCLONE CLIMATE?

A. J. Broccoli and S. Manabe

Geophysical Fluid Dynamics Laboratory/NOAA

R15 4.5º x 7.5º with MLO 30 yrs
R30 2.25º x 3.75º with prescribed SST 5yrs

Broccoli and Manabe (1990) GRL

west and deepened gradually. The maps correspond to the time of maximum intensity, when the central pressure was 961 mb and the surface wind 47 m/s. The storm then crossed southern Japan before weakening over the Asian mainland.

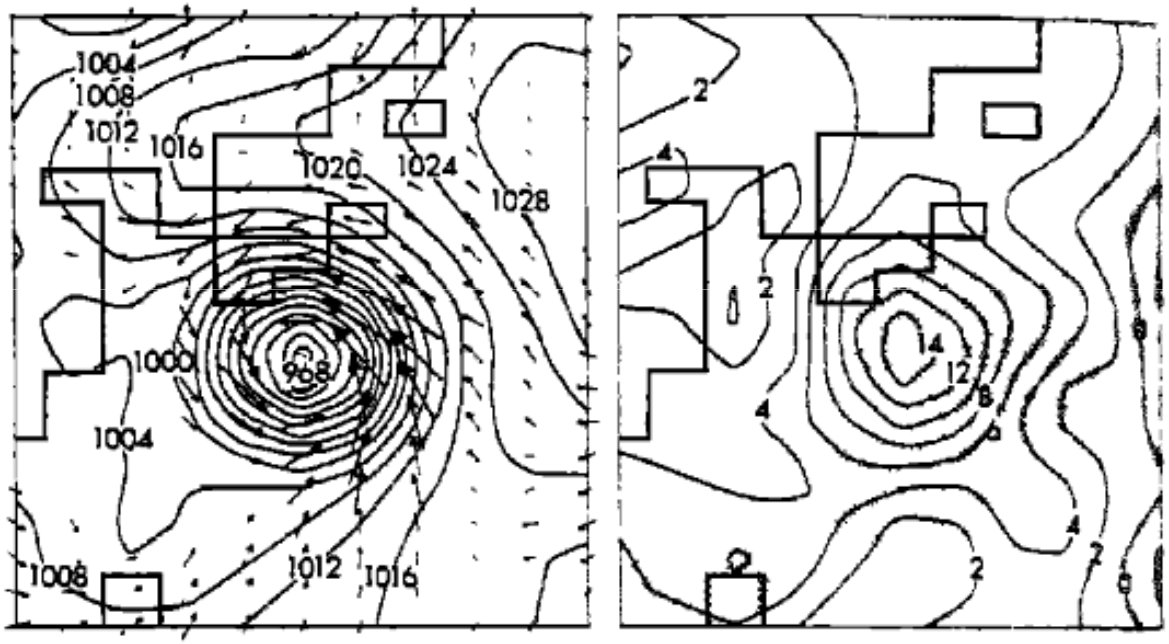

Fig. 1. Synoptic maps of [top] sea level pressure (in mb) and surface wind vectors, and [bottom] 350 mb temperature departure from zonal mean (deg) for an intense simulated tropical cyclone. The stippling on the bottom panel indicates 24-hour precipitation rates greater than 10 mm/day.

Broccoli and Manabe (1990) GRL

Table 1. Mean number of tropical cyclones reaching storm strength (surface winds >17 m/s) by region during the six-month "hurricane season" from the 1X integrations of each experiment. The observed annual mean number of storms (Frank, 1985) is given for comparison.

	R15 FC	R30 FC	R15 VC	R30 VC	Obs.
N.W. Pacific	20.7	20.4	30.2	40.6	26.1
N.E. Pacific	3.2	0.4	2.5	1.8	14.2
N. Atlantic/Caribbean	8.6	6.0	7.6	8.7	8.9
N. Indian	3.1	5.8	4.7	8.9	5.5
Australia/S. Pacific	13.9	15.6	20.8	29.6	16.4
S. Indian	10.8	4.0	10.5	8.2	9.0
S. Atlantic	8.0	2.8	4.7	4.0	0.0
N. Hemisphere	35.6	32.6	45.0	60.0	54.7
S. Hemisphere	32.7	22.4	36.0	41.8	25.4
Global	68.3	55.0	81.0	101.8	80.1

Broccoli and Manabe (1990) GRL

Table 2. Global number of tropical storms per six-month "hurricane season," number of storm-days, and average duration at of above tropical storm strength (days) from each integration. Percent changes resulting from the doubling of CO_2 are also shown. Asterisks indicate statistical significance at the 5% level. (No significance testing was done for the duration statistics.)

Experiment	Integration Segment	Number of Storms	Storm-Days	Average Duration
FC	R15FC-1X	68.3	117.2	1.72
	R15FC-2X	72.3	139.4	1.93
	% diff. (2X-1X)	+5.9	+18.9*	+12.2
	R30FC-1X	55.0	100.2	1.82
	R30FC-2X	56.6	116.2	2.05
	% diff. (2X-1X)	+2.9	+16.0	+12.6
VC	R15VC-1X	81.0	171.4	2.12
	R15VC-2X	75.8	148.9	1.96
	% diff. (2X-1X)	-6.4	-13.1*	-7.5
	R30VC-1X	101.8	245.3	2.41
	R30VC-2X	95.3	217.5	2.28
	% diff. (2X-1X)	-6.4	-11.3*	-5.7

Evans (1992) GRL

GEOPHYSICAL RESEARCH LETTERS, VOL. 19, NO. 14, PAGES 1523-1524, July 24, 1992

COMMENT ON "CAN EXISTING CLIMATE MODELS BE USED TO STUDY ANTHROPOGENIC CHANGES IN TROPICAL CYCLONE CLIMATE"

Jenni L. Evans

CSIRO Division of Atmospheric Research, Australia.

In summary, there is no reason why GCMs should not be able to simulate the tropical atmosphere and specifically, the tropical cyclone climatology. However, before comparisons are made between the populations of "tropical cyclones" in the control and greenhouse simulations of these models, the onus is on the modellers first to show that the genesis processes of the model vortices bear a reasonable physical relationship to those occurring in the atmosphere. Without this verification, no meaningful compar-

Broccoli and Manabe (1992) GRL

Reply to Evans

A. J. Broccoli and S. Manabe

Geophysical Fluid Dynamics Laboratory/NOAA

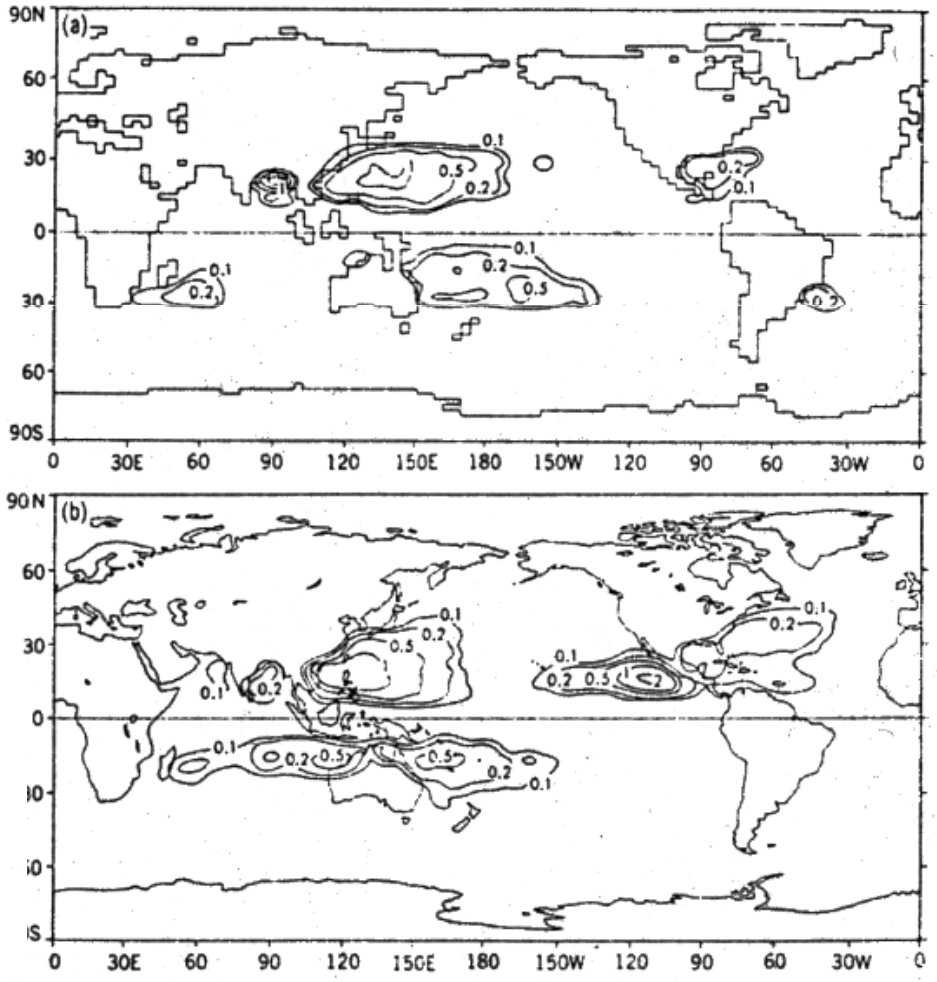

Fig. 1. Average annual tropical storm frequency within each 2.25° latitude by 3.75° longitude grid box. *Top:* Simulated (R30VC-1X integration). *Bottom:* Observed (National Climatic Data Center Consolidated Global Tropical Cyclone data base). Both maps have been smoothed spatially by using a 1-2-1 filter in each direction.

Ryan et al. (1992) GRL

TROPICAL CYCLONE FREQUENCIES INFERRED FROM GRAY'S YEARLY GENESIS PARAMETER: VALIDATION OF GCM TROPICAL CLIMATES

Brian F. Ryan, Ian G. Watterson and Jenni L. Evans

CSIRO Division of Atmospheric Research, Australia.

$$SGP = [(\zeta_r f \mid f \mid^{-1} + 5) \mid f \mid (S_z + 3)^{-1}] * [(E)(\frac{\partial \theta_e}{\partial p} + 5)^{\frac{(RH-40)}{30}}] \quad (1)$$

$\zeta_r f / \mid f \mid$ is in units of $10^{-6} s^{-1}$, $\mid f \mid$ in $10^{-5} s^{-1}$, S_z $^{-1}$ / (750 hPa), E in cal cm^{-2}, $\frac{\partial \theta_e}{\partial p}$ in K (500 hPa)$^{-1}$ H is the percentage mean RH between 500 and 700 The RH term is set to a maximum value of 1.0 at ve a relative humidity of 70%. If any of the compo-

$$YGP = SGP_{JFM} + SGP_{AMJ} + SGP_{AJS} + SGP_{OND}$$

Ryan et al. (1992) GRL

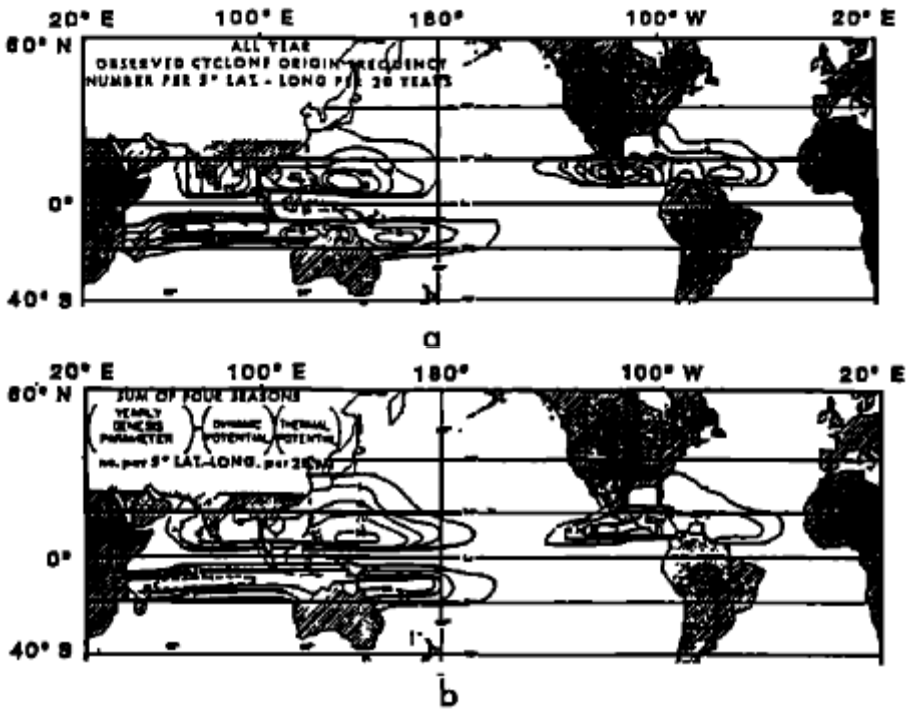

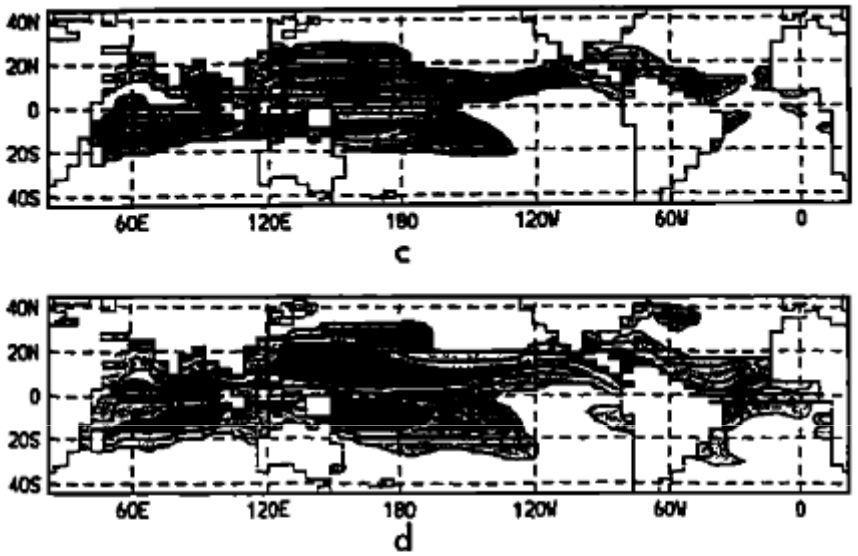

Figure 1: (a) observed global occurrence of tropical cyclogenesis over the period 1952 – 1971; (b) values of Gray's yearly genesis parameter (YGP) as calculated by him for the same period. (c) Global maps of YGP calculated from data from the CSIRO9 control run; and (d) the $2 \times CO_2$ simulation of the CSIRO9 model. In diagrams (c) and (d), shaded areas have YGP of at least 1, darker shading denotes regions of YGP above 30. YGP values of 1, 10, 30 and 100 are contoured.

Ryan et al. (1992) GRL

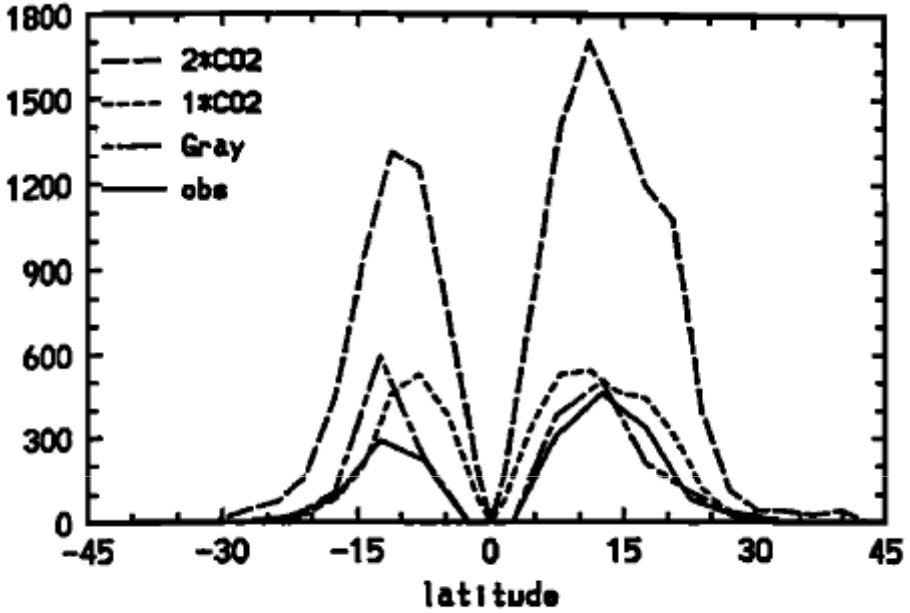

Figure 2: Zonal sums of: the annual distribution of observed tropical cyclogenesis from 1952 – 1971, the YGP calculated from Gray's data from 1952 – 1971, the YGP calculated from the CSIRO9 control run ($1 \times CO_2$), and the YGP calculated from the $2 \times CO_2$ CSIRO9 run.

Table 1: Ratio of $2 \times CO_2$ to $1 \times CO_2$ YGP.

Parameter	JFM	AMJ	JAS	OND
$\zeta_r f / \mid f \mid^{-1} + 5$	0.99	0.96	0.99	1.00
$(S_z + 3)^{-1}$	0.98	1.01	1.02	1.09
E	2.13	2.01	2.10	2.18
$\frac{\partial \theta_e}{\partial p} + 5)$	1.27	1.27	1.27	1.25
(RH-40)/30	1.09	1.08	1.06	1.07

$$Y = X_1 \cdot X_2 \cdot X_3 \cdot X_4 \cdot X_5$$

$$\ln Y = \ln X_1 + \ln X_2 + \ln X_3 + \ln X_4 + \ln X_5$$

$$\frac{\Delta Y}{Y} = \frac{\Delta X_1}{X_1} + \frac{\Delta X_2}{X_2} + \frac{\Delta X_3}{X_3} + \frac{\Delta X_3}{X_3} + \frac{\Delta X_3}{X_3}$$

	JFM	AMJ	JAS	OND
X1	−0.01	−0.04	−0.01	0
X2	−0.02	0.01	0.02	0.09
X3	1.13	1.01	1.1	1.18
X4	0.27	0.27	0.27	0.25
X5	0.09	0.08	0.08	0.07
Y	1.46	1.33	1.46	1.59

Haarsma et al. (1993) CD

Climate Dynamics (1993) 8:247–257

Climate Dynamics

Tropical disturbances in a GCM

RJ Haarsma[1], JFB Mitchell[2], CA Senior[2]

[1] Royal Netherlands Meteorological Institute, de Bilt, The Netherlands
[2] Hadley Centre, Bracknell, United Kingdom

Received May 31, 1991/Accepted August 26, 1992

2.5º x 3.75º with MLO 10 yrs

Haarsma et al. (1993) CD

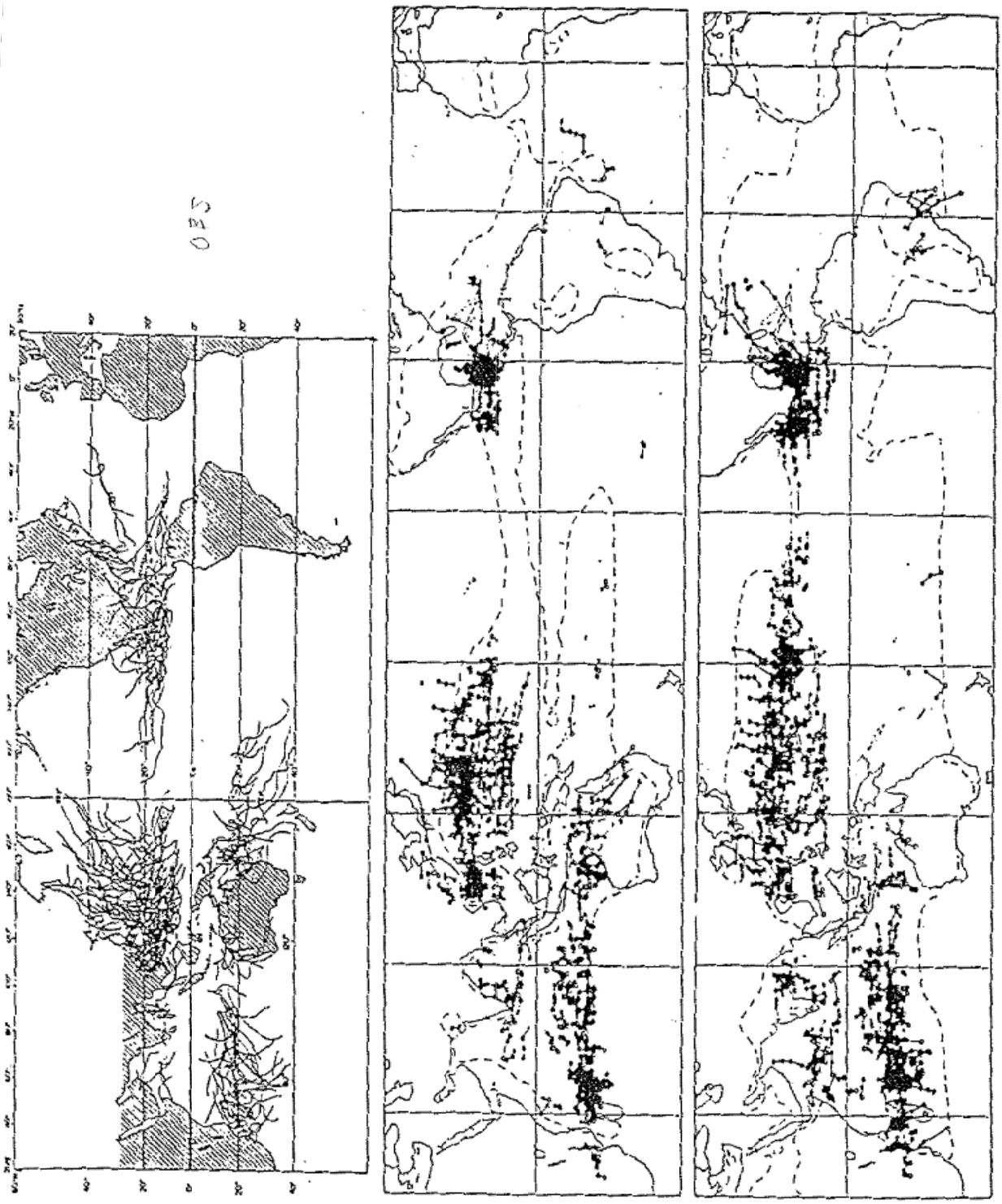

Fig. 3. a Observed tracks of tropical cyclones for a 3-year period, which contains one moderate El Niño (Gray 1976). b Simulated tropical disturbance tracks for a 5-year period. c As in b on doubling CO_2. The *dashed line* is the 26.5° C isotherm

Haarsma et al. (1993) CD

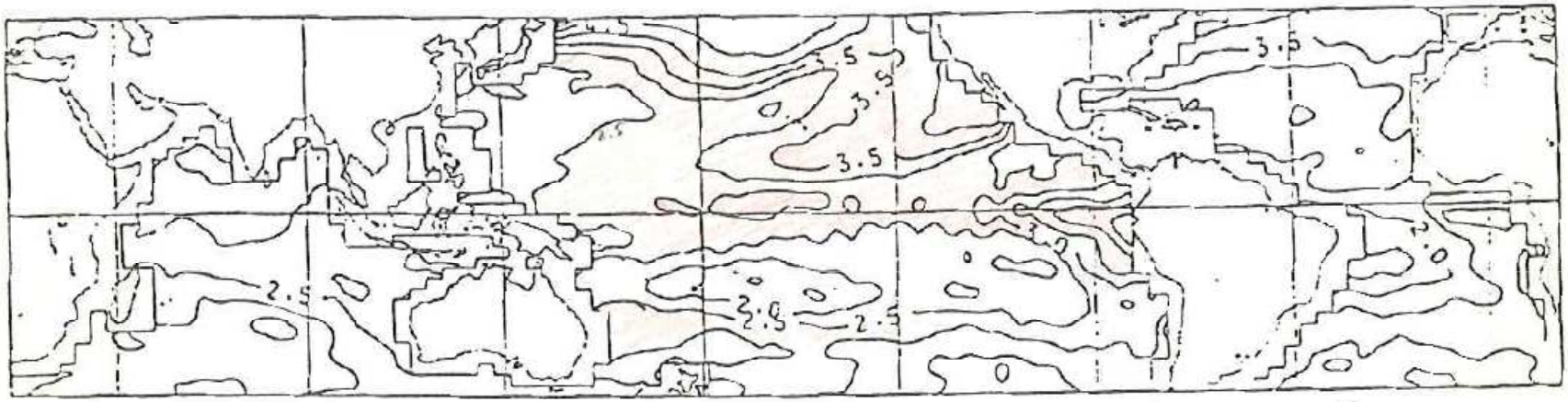

Fig. 8. Difference in SST between the doubled CO_2 and control simulation. Contour interval 0.5°C

Haarsma et al. (1993) CD

Table 1. Average number of tropical disturbance days (TDDs) per year for the different basins

Basin	$1 \times CO_2$	$2 \times CO_2$
Globe	301	447
NW Pacific	111	172
N Atlantic/NE Pacific	60	98
North Indian ocean	17	29
South Indian ocean	74	116
SW Pacific/Australian region	34	22
South Atlantic	5	10

Haarsma et al. (1993) CD

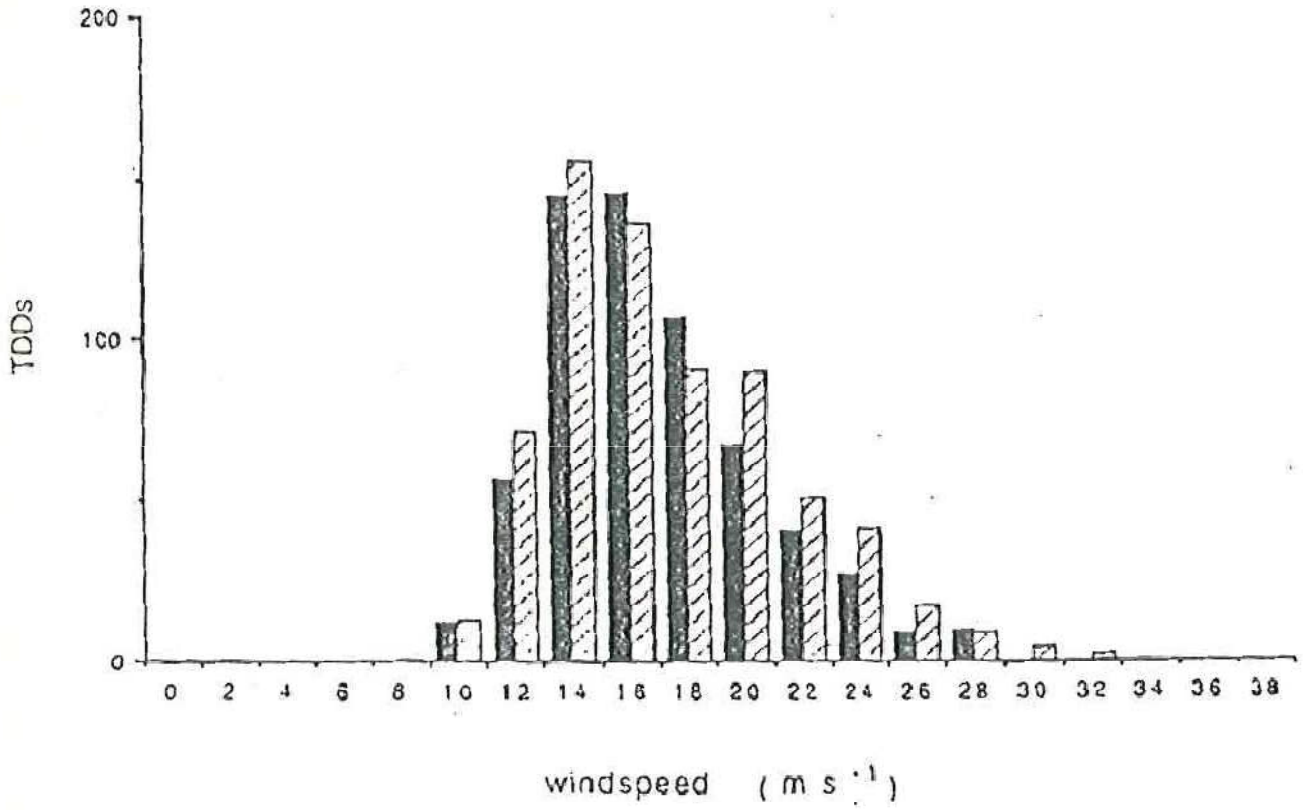

Fig. 9. Frequency distribution of windspeed for the NW Pacific. *Solid columns*: control simulation. *Cross-hatched columns*: on doubling CO_2

Lighthill et al. (1994) BAMS

meeting review

Global Climate Change and Tropical Cyclones

James Lighthill,* Greg Holland,+ William Gray,# Christopher Landsea,#
George Craig,@ Jenni Evans,& Yoshio Kurihara,** and Charles Guard++

(TC). Out of three methodologies available for addressing the question they employ two, discarding the third for reasons set out in the appendix.

In the first methodology, the authors enumerate reasons why, in tropical oceans, the increase in sea surface temperature (SST) suggested by climate change models might be expected to affect

In the second methodology, the authors study available historical records that have very large year-to-year variability in TC

Appendix. A third methodology

In this appendix, we consider quite briefly a third methodology that has been proposed (Broccoli and Manabe 1990; Haarsma et al. 1993; Manabe et al. 1994) for studying links between GCC and TCs. It is simply to run one of the climate models for different climate forcings and to count the number of transient tropical disturbances that can be discerned in each year, and then to study whether this number exhibits any change. If so, then this change is assumed to imply a similar change for TCs in the real atmosphere.

This seems to be a false analogy. Present climate models, for

At the same time, we acknowledge the clear possibility of future development of fine-grid climate models that would not necessarily be subject to the above criticisms. A future climate model with excellent model physics and with very high resolution might indeed be a suitable tool for studying how GCC may affect TC statistics.

II. 1996-2001 (IPCC-TAR まで)

Bengtsson et al. (1995, 1996) Tellus

Landsea (1997) Tellus

杉ほか(1995,1996) 気象学会予稿集

Sugi et al. (1996, 1997) WMO/TD

IWTC-4 (1998) Hainan, China

Henderson-Sellers et al. (1998) BAMS (← IWTC-6)

Knutson et a. (1998) Science

Yoshimura et al. (1999) AMS

Tsutsui et al. (1999) AMS

McDonald (1999) HC report

May (2000) DMI/DCC Report

IPCC TAR (2001)

Bengtsson et al. (1995) Tellus

Tellus (1995), 47A, 175–196
Printed in Belgium – all rights reserved

TELLUS
ISSN 0280–6495

Hurricane-type vortices in a general circulation model

By L. BENGTSSON*, M. BOTZET and M. ESCH, *Max-Planck-Institut für Meteorologie, Bundesstr. 55, D-20146 Hamburg, Germany*

(Manuscript received 3 January 1994; in final form 4 July 1994)

T106 (120km) AGCM with prescribed SST
5yr time slice present

Bengtsson et al. (1995) Tellus

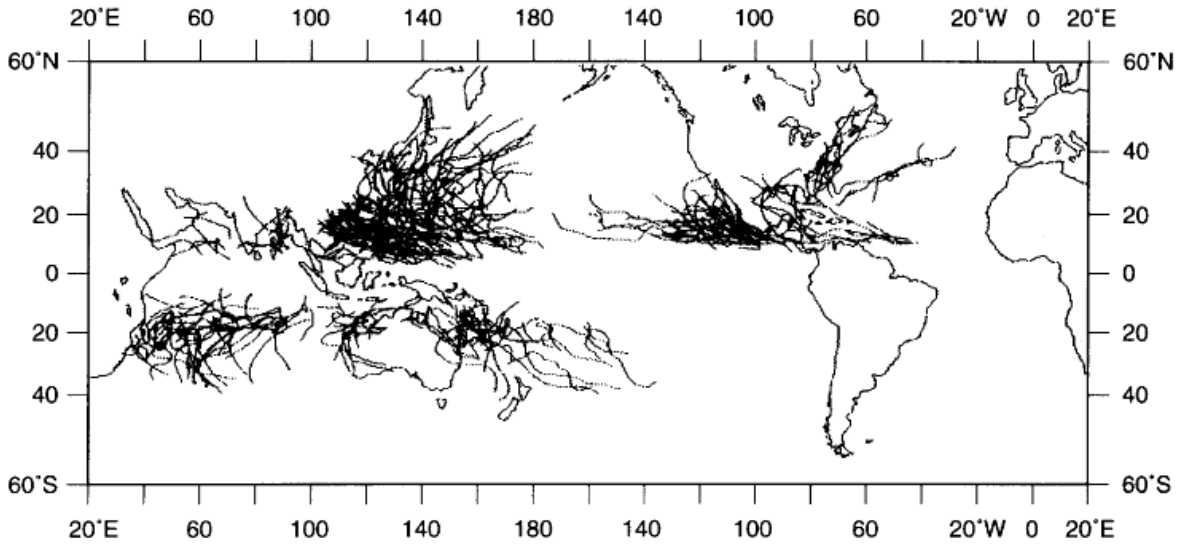

Fig. 10. Observed cyclone tracks over 3 years. According to Gray (1979)

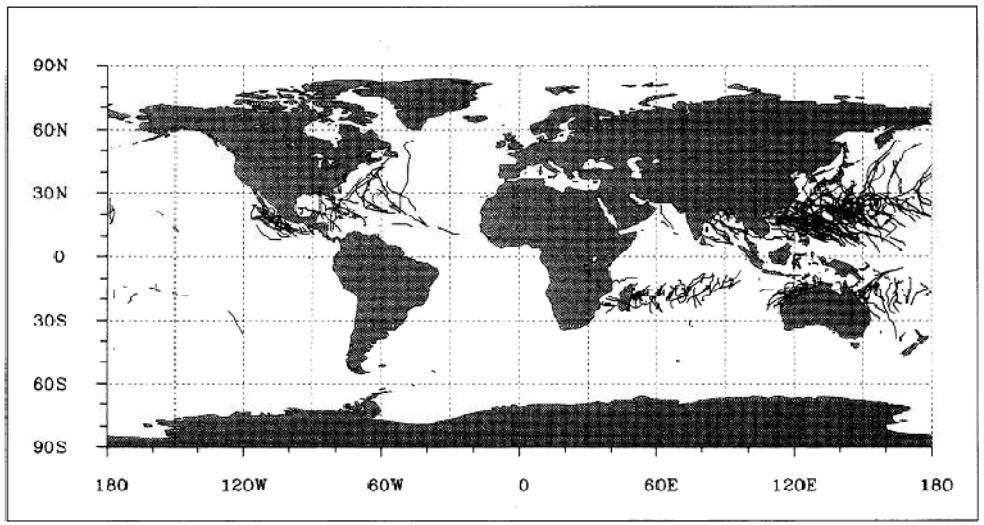

Fig. 9. Simulated cyclone tracks. The tracking is only indicated when the hurricanes satisfied the selection criteria. All tracks for 5 years. Colour notation as in Fig. 7.

Bengtsson et al. (1995) Tellus

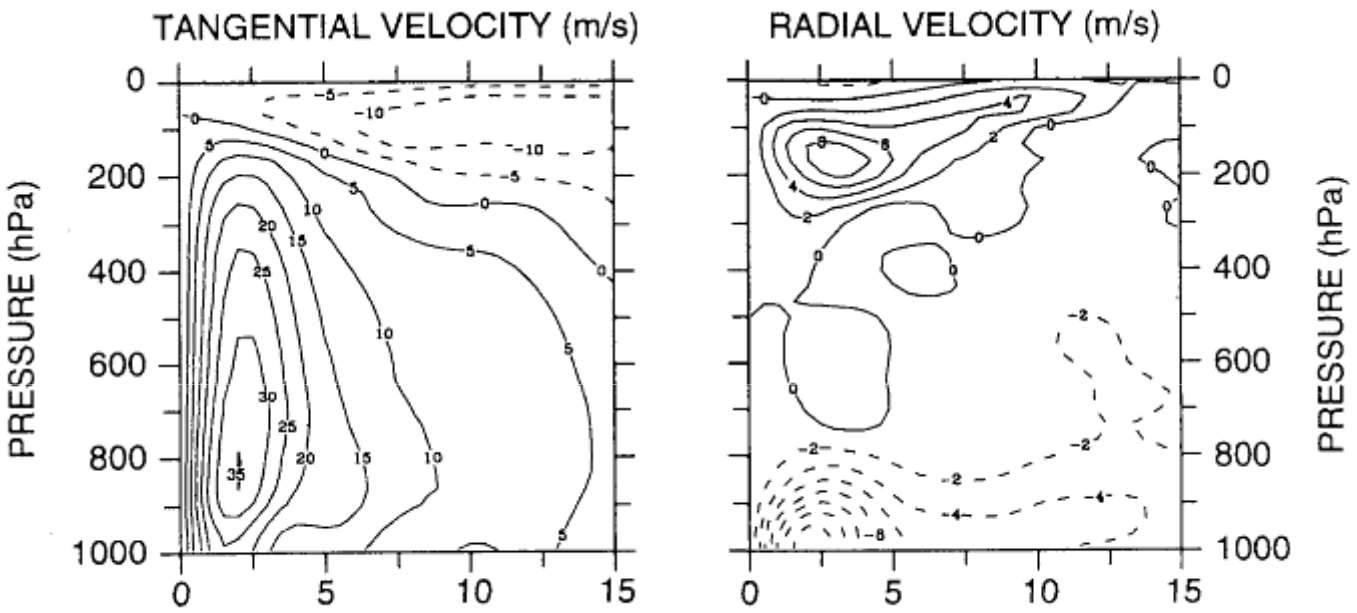

Bengtsson et al. (1995) Tellus

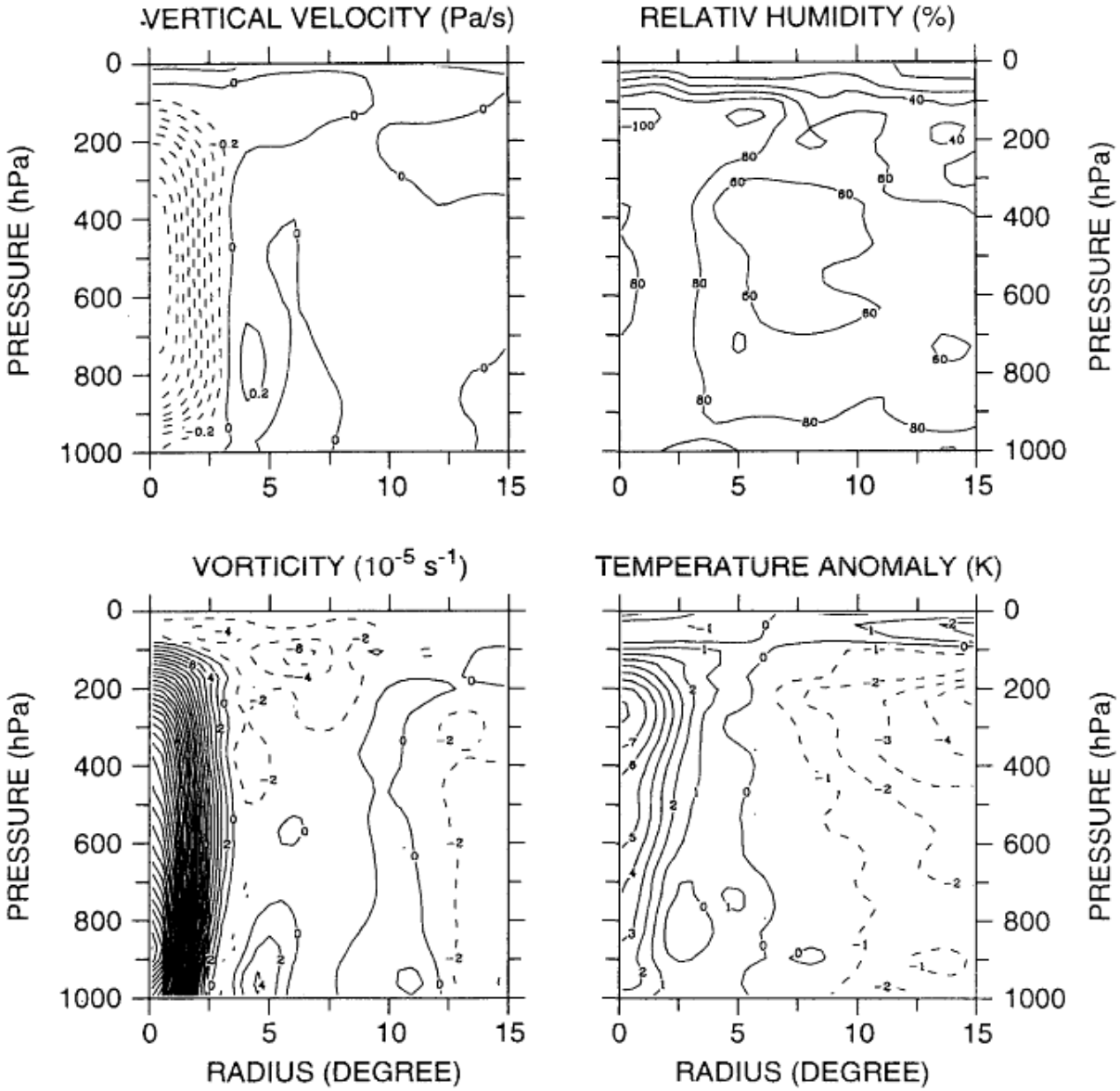

Fig. 4. 2-dimensional cross section of tangential wind (ms^{-1}), radial wind (ms^{-1}), vertical velocity (Pas^{-1}), relative humidity (%), velocity (10^{-5} s^{-1}) and temperature anomaly (K) for the maximum stage of the development at 15 August 12 UTC, year 1.

Bengtsson et al. (1996) Tellus

Tellus (1996), 48A, 57–73
Printed in Belgium – all rights reserved

TELLUS
ISSN 0280–6495

Will greenhouse gas-induced warming over the next 50 years lead to higher frequency and greater intensity of hurricanes?

By L. BENGTSSON*, M. BOTZET and M. ESCH, *Max-Planck-Institut für Meteorologie, Bundesstrasse 55, D-20146 Hamburg, Germany*

(Manuscript received 12 September 1994; in final form 22 June 1995)

T106 (120km) AGCM with prescribed SST
5yr time slice present and 2xCO2

Bengtsson et al. (1996) Tellus

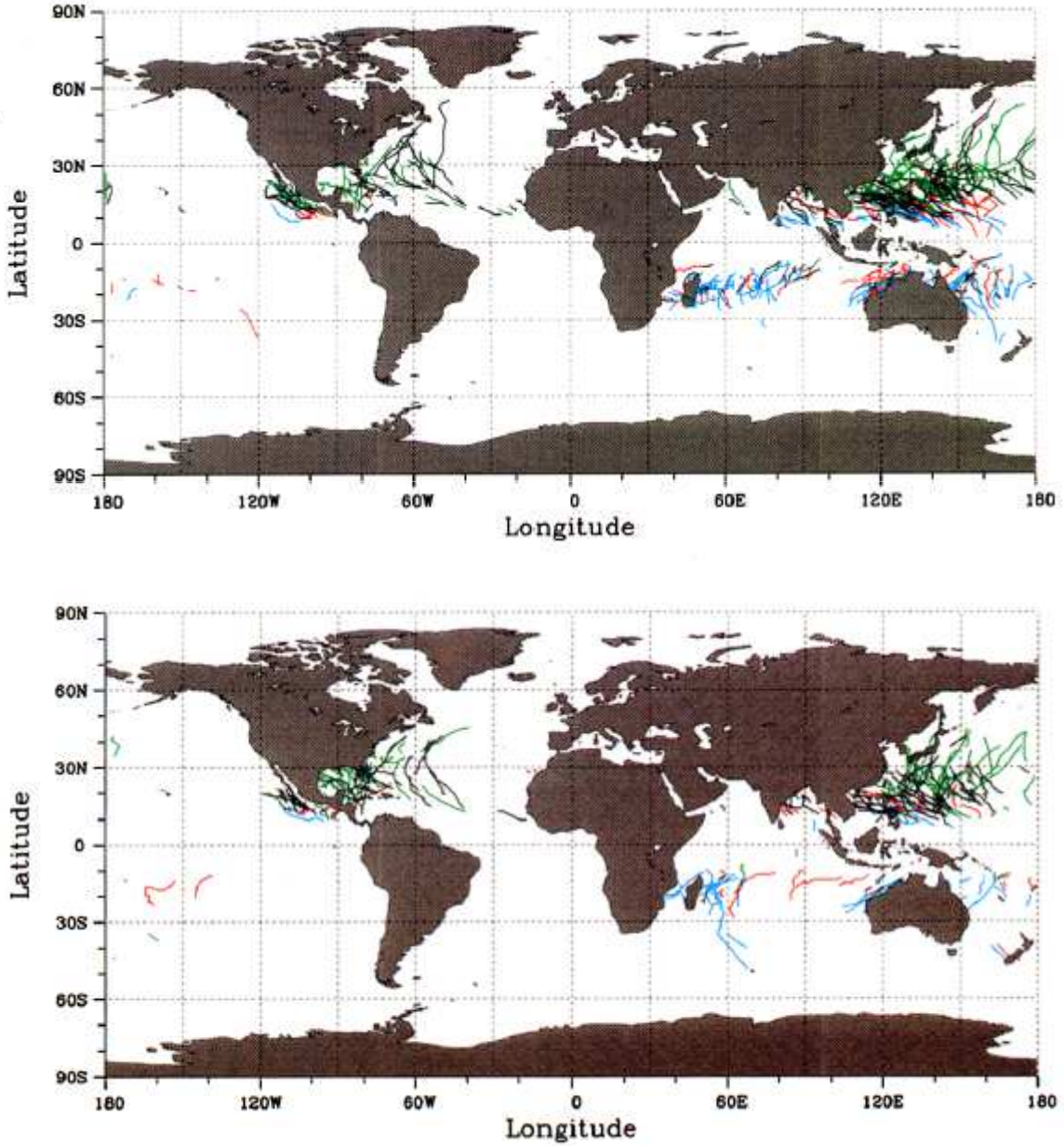

Bengtsson et al. (1996) Tellus

Table 3. *Number of simulated tropical cyclones by ocean basin and year*

Year	NWatl	NEPac	NWPac*	NInd.	SInd.*	Aust.*	S. Pac.	Others	Total
1	10	6	20	5	3	5	1	0	50
2	12	7	22	1	6	2	2	0	52
3	9	6	24	7	2	4	1	1	54
4	6	9	22	1	6	3	3	0	50
5	10	3	20	4	6	8	4	2	57
$2CO_2$									
total	47	31	108	18	23	22	11	3	263
average	9.4	6.2	21.6	3.6	4.6	4.4	2.2	0.6	52.6
range	6–12	3–9	20–24	1–7	2–6	2–8	1–4		
CTRL									
total	54	39	164	20	64	47	20	7	415
average	10.8	7.8	32.8	4.0	12.8	9.4	4.0	1.4	83.0
range	9–14	6–11	24–41	1–7	7–18	6–12	3–6		
OBS									
(1958–1977)	8.8	13.4	26.3	6.4	8.4	10.3	5.9	—	79.1
range	4–14	8–20	17–35	4–9	4–12	5–17	3–10		

The control simulations (present climate) and the observed number 1958–1977 according to Gray (1979) are shown on the bottom lines. For a specification of the areas, see B95. Others refer to hurricane developments elsewhere. Regions where the reduction of the number of storms are statistically significant (within the 97.5–99.0% confidence limit) are indicated by *.

Bengtsson et al. (1996) Tellus

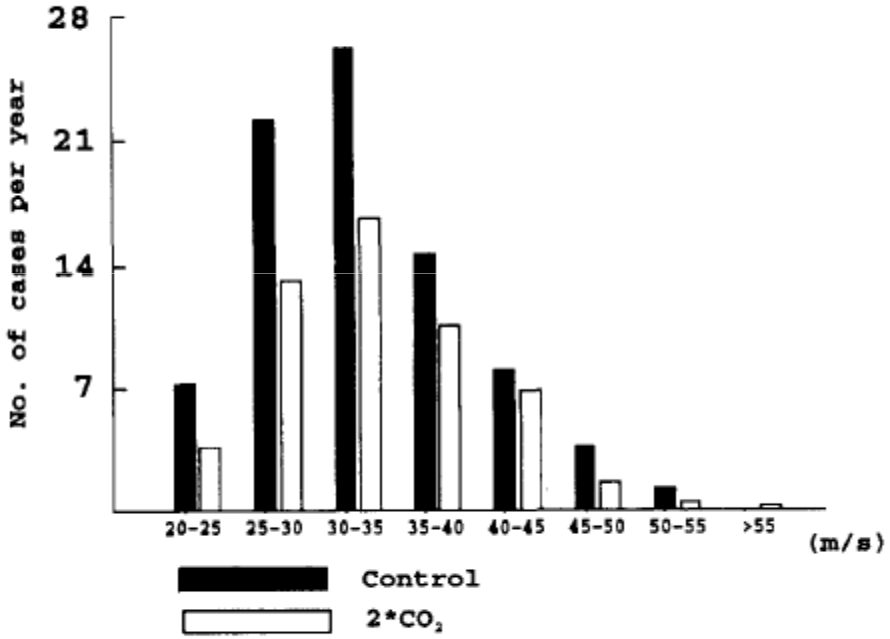

Fig. 5. Maximum windspeed obtained for each individual simulated tropical cyclone for present climate conditions (solid bars) and for the double CO_2 case (unfilled bars).

Bengtsson et al. (1996) Tellus

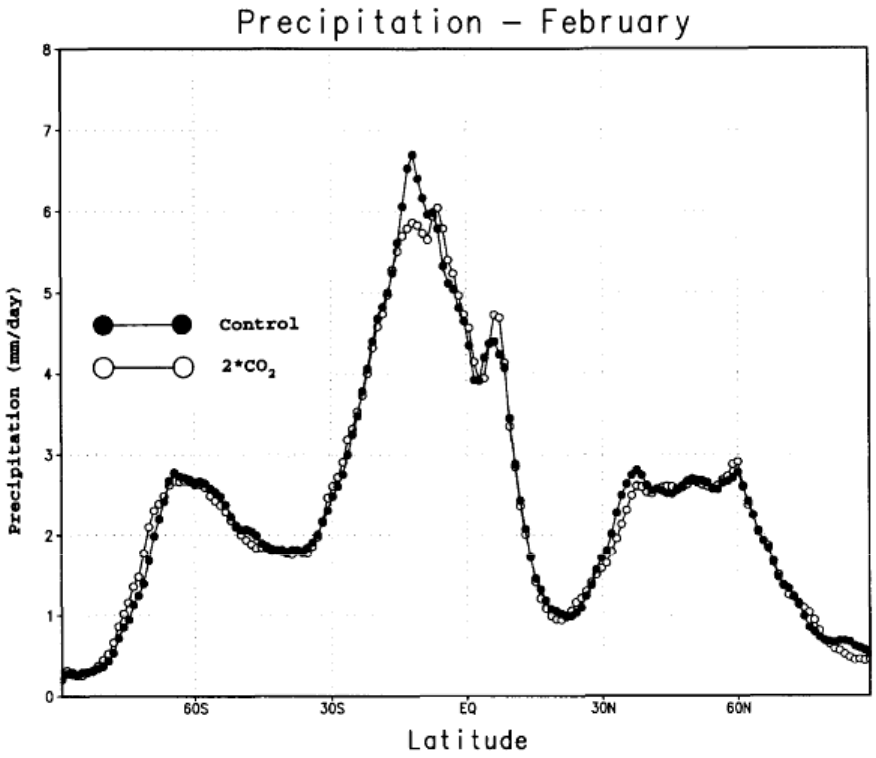

Fig. 12. Zonal cross section of precipitation during February. Present climate conditions (filled circles), double CO_2 climate (unfilled circles) unit mm/day.

There is a minor global decrease in the evaporation and precipitation in the double CO_2 experiment compared to the control. The largest differences are found over the Southern Indian Ocean in February, where evaporation is reduced

Landsea (1997) Tellus

Tellus (1997), 49A, 622–623
Printed in UK – all rights reserved

TELLUS
ISSN 0280–6495

Comments on "Will greenhouse gas-induced warming over the next 50 years lead to higher frequency and greater intensity of hurricanes?"

By CHRISTOPHER W. LANDSEA, *NOAA/AOML/Hurricane Research Division, 4301 Rickenbacker Causeway, Miami, FL, 33149, USA*

(Manuscript received 17 March 1997; in final form 20 May 1997)

The primary concern is the strong possibility of an incompatible flaw in the experimental design.

The main finding in BBE is that there were substantially fewer tropical cyclones globally in the doubled CO_2 than in the control run of undisturbed CO_2 conditions. BBE attribute this startling decrease in storm numbers to a weaker intertropical convergence zone (ITCZ) and hydrological cycle with an attendant decrease in synoptic scale vorticity, low–level convergence and moisture flux and an increase in vertical wind shear —

However, for the 60 years of integration of the enhanced CO_2 low resolution coupled ocean–atmosphere GCM, there was not a decrease in the ITCZ strength and hydrological cycle, but instead a strengthening of these features (Cubasch et al.,

Henderson-Sellers et al. (1998) BAMS

Tropical Cyclones and Global Climate Change: A Post-IPCC Assessment

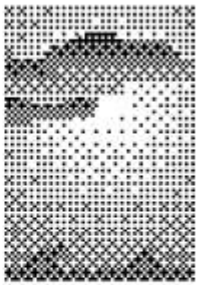

A. Henderson-Sellers,* H. Zhang,+ G. Berz,# K. Emanuel,@ W. Gray,& C. Landsea,**
G. Holland,+ J. Lighthill,++ S-L. Shieh,## P. Webster,@@ and K. McGuffie+

A strong caveat must be placed on analysis of results from current GCM simulations of the “tropical-cyclone-like” vortices. Their realism, and hence prediction skill (and also that of “embedded” mesoscale models), is greatly limited by the coarse resolution of current GCMs and the failure to capture environmental factors that govern cyclone intensity. Little, therefore, can be said about the potential changes of the distribution of intensities as opposed to maximum achievable intensity. Current knowledge and available techniques are too rudimentary for quantitative indications of potential changes in tropical cyclone frequency.

BAMS 1998

IPCC-TAR (2001)
Box 10.2: Tropical cyclones in current and future climates

In an early use of a high-resolution AGCM, a T106 ECHAM3 experiment simulated a decrease in tropical cyclones in the Northern Hemisphere and a reduction of 50% in the Southern Hemisphere (Bengtsson et al., 1996, 1997). However, the different hemispheric responses raised questions about the model's ability to properly represent tropical cyclones and methodological concerns about the experimental design were raised (Landsea, 1997). In a similar experiment, the JMA model also simulated fewer tropical cyclone-like vortices in both hemispheres (Yoshimura et al., 1999). A high resolution HadAM3a simulation reproduced the latter changes, giving changes in timing in the north-west Pacific and increases in frequency in the north-east Pacific and the north Indian basin (McDonald, 1999).

In conclusion, there is some evidence that regional frequencies of tropical cyclones may change but none that their locations will change. There is also evidence that the peak intensity may increase by 5% to *10% and precipitation rates may increase by 20%* to *30%. There is a need for much more work in this area to provide more robust results.*

III. 2002-2007 (IPCC-AR4 まで)

Sugi et al. (2002) JMSJ

McDonald (2005) CD

Oouchi (2006) JMSJ

IWTC-5 (2006)

WMO statement (2006) (← IWTC 5)

IPCC- AR4 (2007)

Sugi et al. (2002) JMSJ

Journal of the Meteorological Society of Japan, Vol. 80, No. 2, pp. 249–272, 2002

Influence of the Global Warming on Tropical Cyclone Climatology: An Experiment with the JMA Global Model

Masato SUGI, Akira NODA

Meteorological Research Institute, Tsukuba, Japan

and

Nobuo SATO

Japan Meteorological Agency, Tokyo, Japan

(Manuscript received 26 December 2000, in revised form 26 December 2001)

T106 (120km) AGCM with prescribed SST
10 yr time slice present and 2xCO2

Sugi et al. (2002) JMSJ

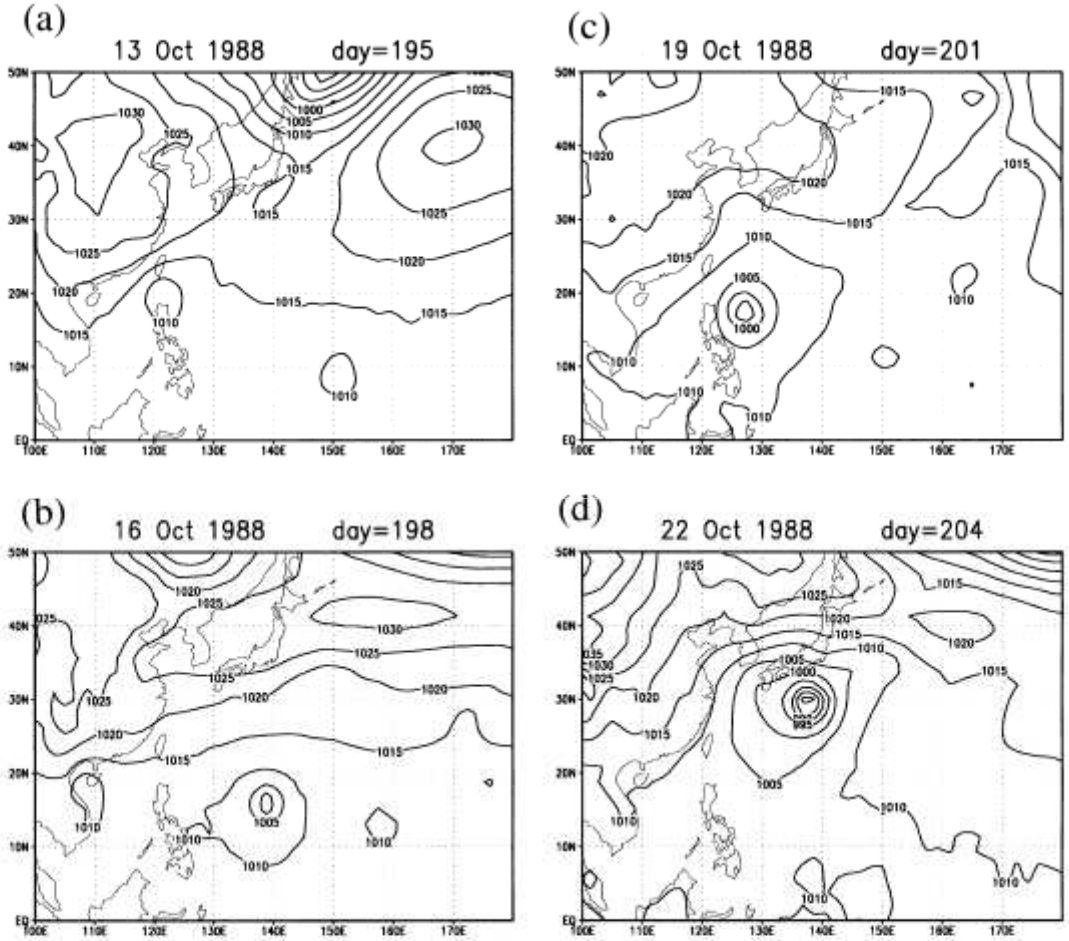

Fig. 1. A typhoon simulated with the T106 JMA global model. (a) A weak tropical depression was born on the day 195 of the simulation at around 9°N, 150°E. (b) The tropical depression moved west-north-westward and developed slowly. (c) It reached to the east of the Philippines on the day 201 and turned its direction to north-eastward, and further developed. (d) The simulated typhoon approached south of Japan on the day 204.

Sugi et al. (2002) JMSJ

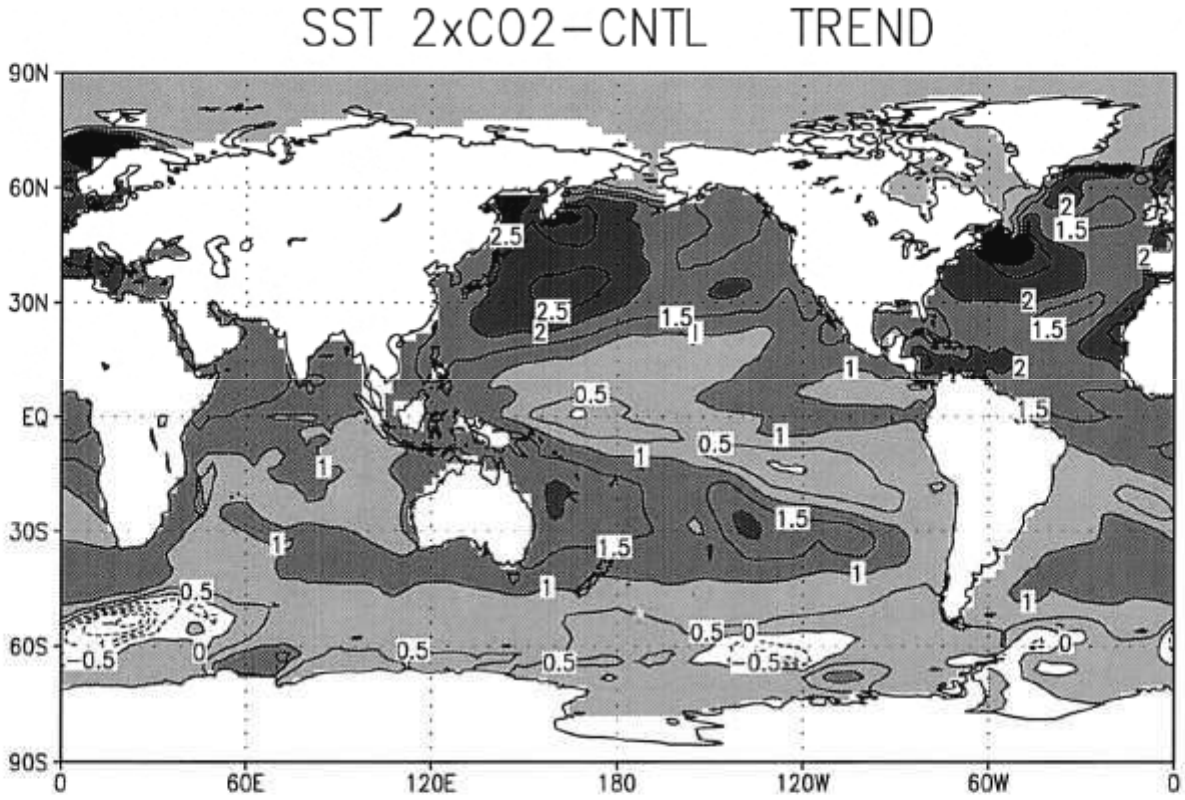

Fig. 2. The sea surface temperature change (°C) due to the global warming estimated by the linear trend of a transient CO2 experiment with the MRI-CGCM.

Sugi et al. (2002) JMSJ

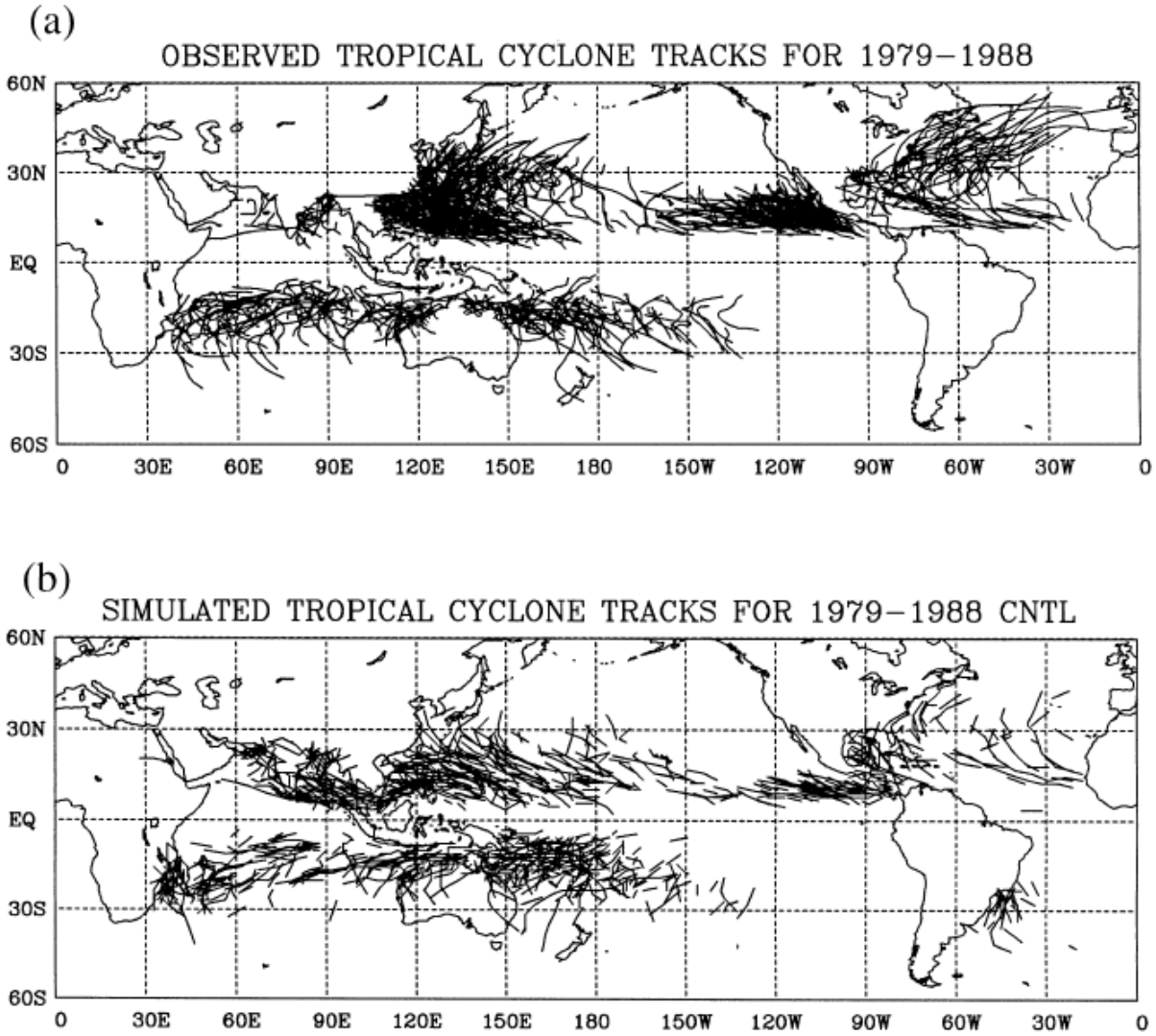

Sugi et al. (2002) JMSJ

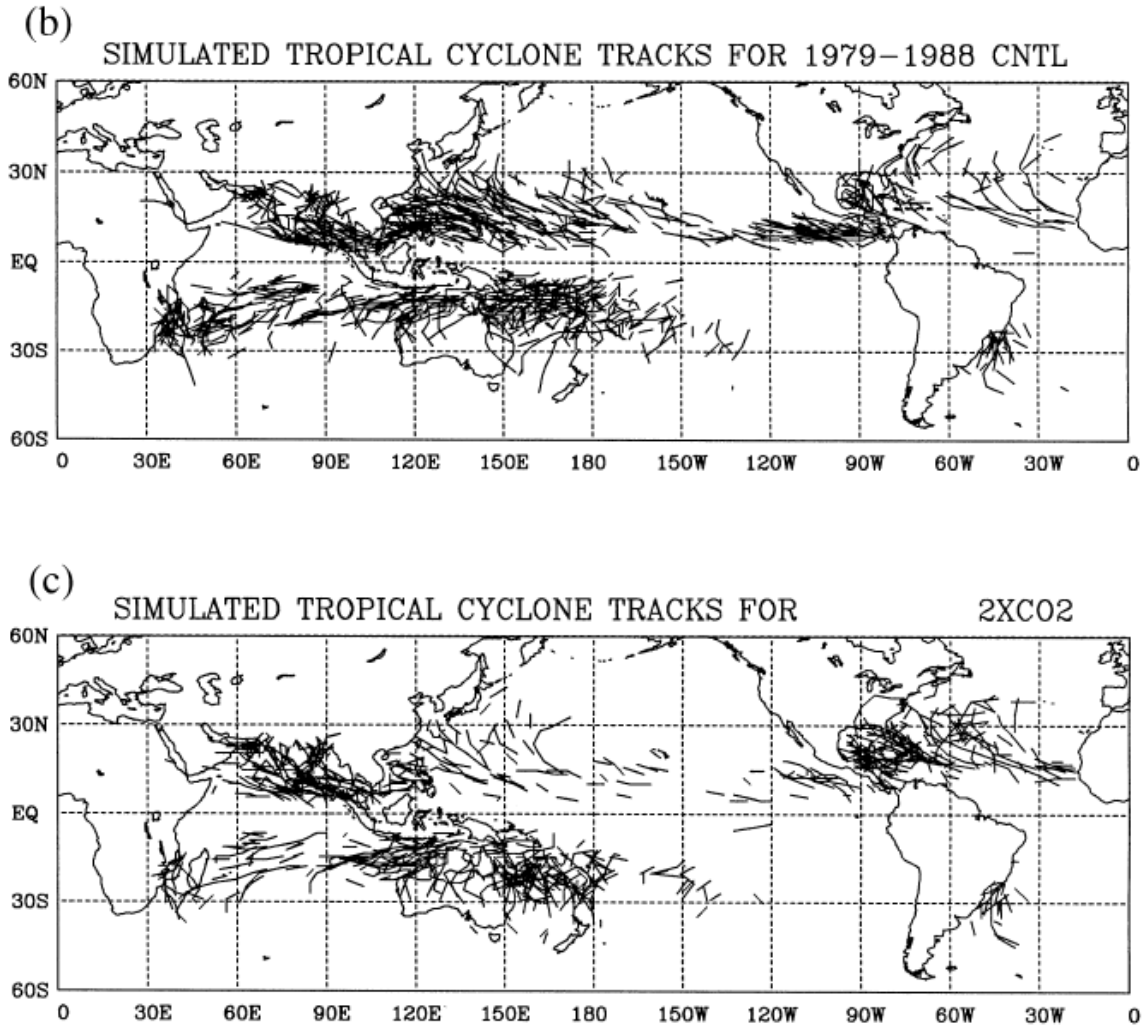

Sugi et al. (2002) JMSJ

Table 1. Number of tropical cyclones by ocean basin. Numbers in parenthesis show the standard deviations. Italic letter indicates that the value is not statistically significant at 95% confidence level.

Region	OBS 1979-1988	CNTL	2xCO2	Difference 2xCO2-CNTL	Ratio %
N Indian Ocean (–105°E)	3.9 (2.1)	10.6 (1.6)	11.6 (2.5)	*1.0*	109.4
NW Pacific (105°E –135°W)	27.4 (2.9)	21.9 (5.1)	7.5 (3.7)	-14.4	34.2
NE Pacific (135°W–)	16.1 (3.3)	6.3 (5.0)	2.1 (1.1)	*-4.2*	33.3
N Atlantic	9.1 (3.0)	7.4 (3.2)	11.9 (4.4)	4.5	160.8
S Indian Ocean (–105°E)	10.6 (3.6)	12.8 (4.1)	5.5 (3.1)	-7.3	43.0
SW Pacific (105°E –135°W)	14.0 (4.4)	26.0 (7.2)	17.9 (3.9)	-8.1	68.8
Other S Ocean (135°W–)	0.1(0.3)	3.1 (1.9)	2.0 (1.3)	*-1.1*	64.5
Northern Hemisphere	56.5 (7.2)	46.2 (9.0)	33.1 (6.3)	-13.1	71.6
Southern Hemisphere	24.7 (6.4)	41.9 (7.3)	25.4 (4.6)	-16.5	60.6
Global	81.2 (12.3)	88.1 (10.4)	58.5 (7.7)	-29.6	66.4

Sugi et al. (2002) JMSJ

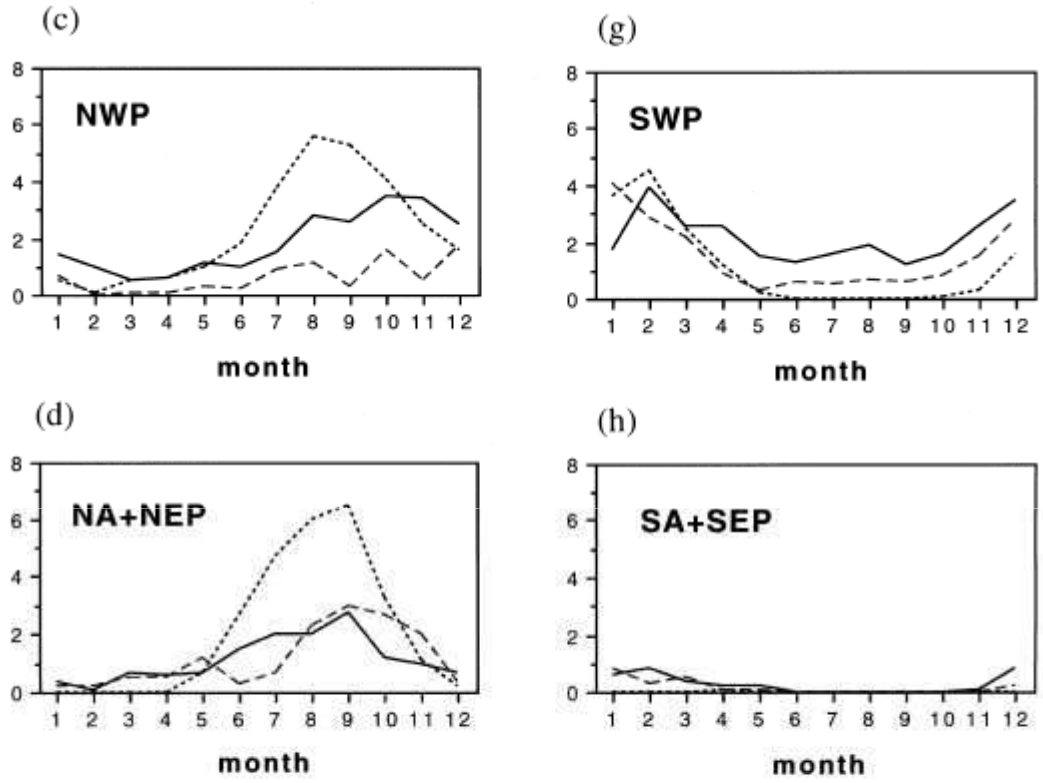

Fig. 4. Seasonal variation of tropical cyclone frequency by ocean basin. Dotted lines indicate the observed frequency. (a) Northern Hemisphere, (b) North Indian Ocean, (c) North Western Pacific, (d) North Atlantic and North East Pacific, (e) Southern Hemisphere, (f) South Indian Ocean, (g) South West Pacific, and (h) South Atlantic and South East Pacific (see Table 1 for the definition of regions). Solid and dashed lines show the frequencies of simulated tropical cyclones in the control experiment and the 2 × CO2 experiment, respectively.

Sugi et al. (2002) JMSJ

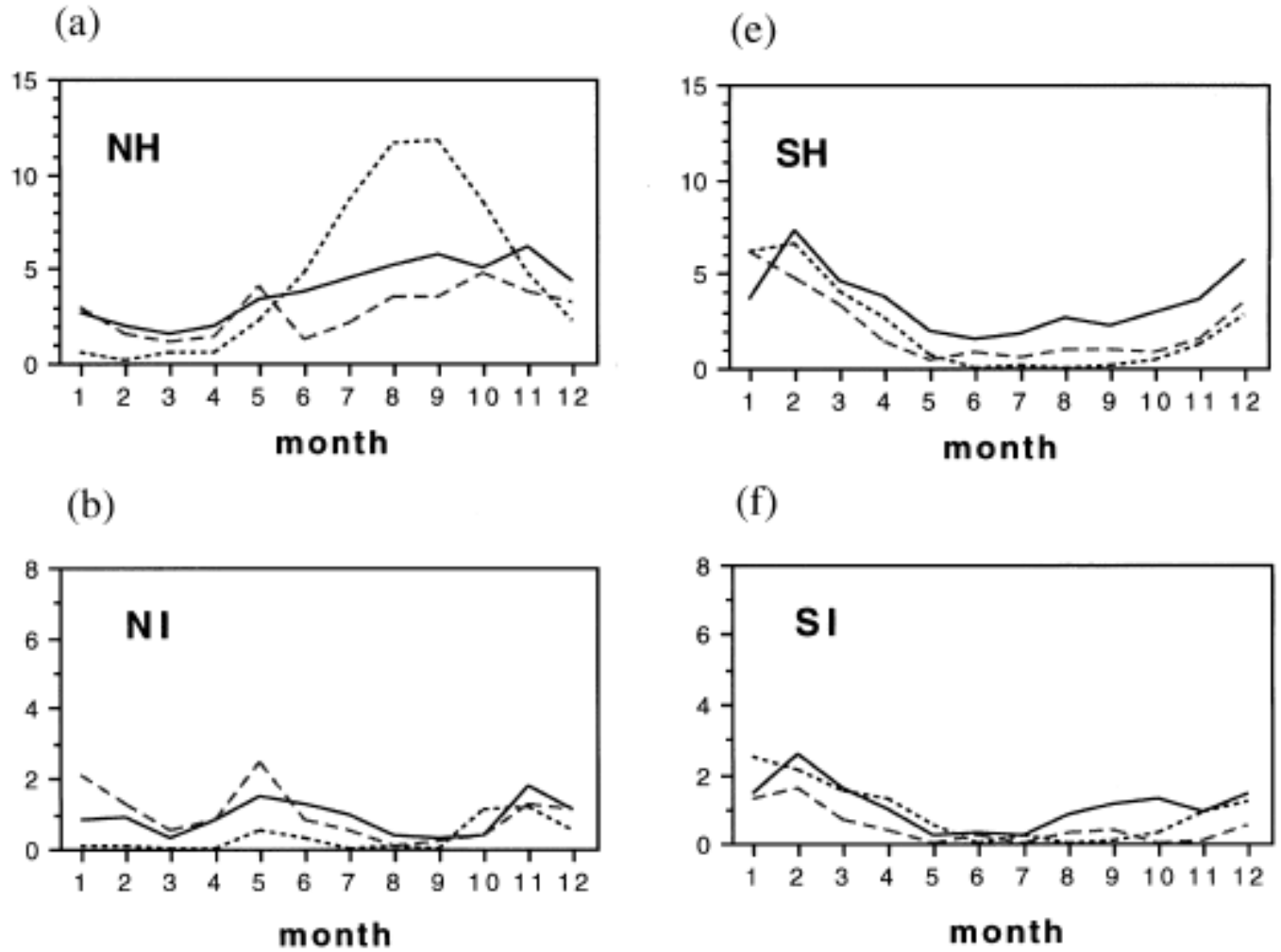

Sugi et al. (2002) JMSJ

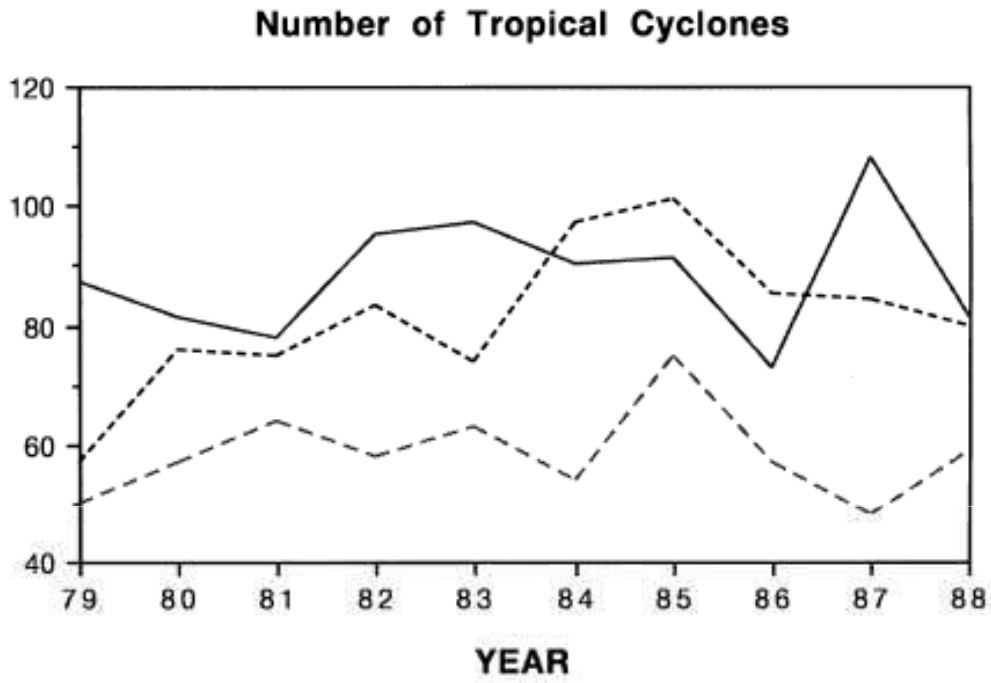

Fig. 5. Inter-annual variation of tropical cyclone frequency. Dotted curve indicates the observed frequency based on the US Navy Best Track Deataset. Solid and dashed lines show the frequencies of simulated tropical cyclones in the control experiment and the $2 \times CO2$ experiment, respectively.

Sugi et al. (2002) JMSJ

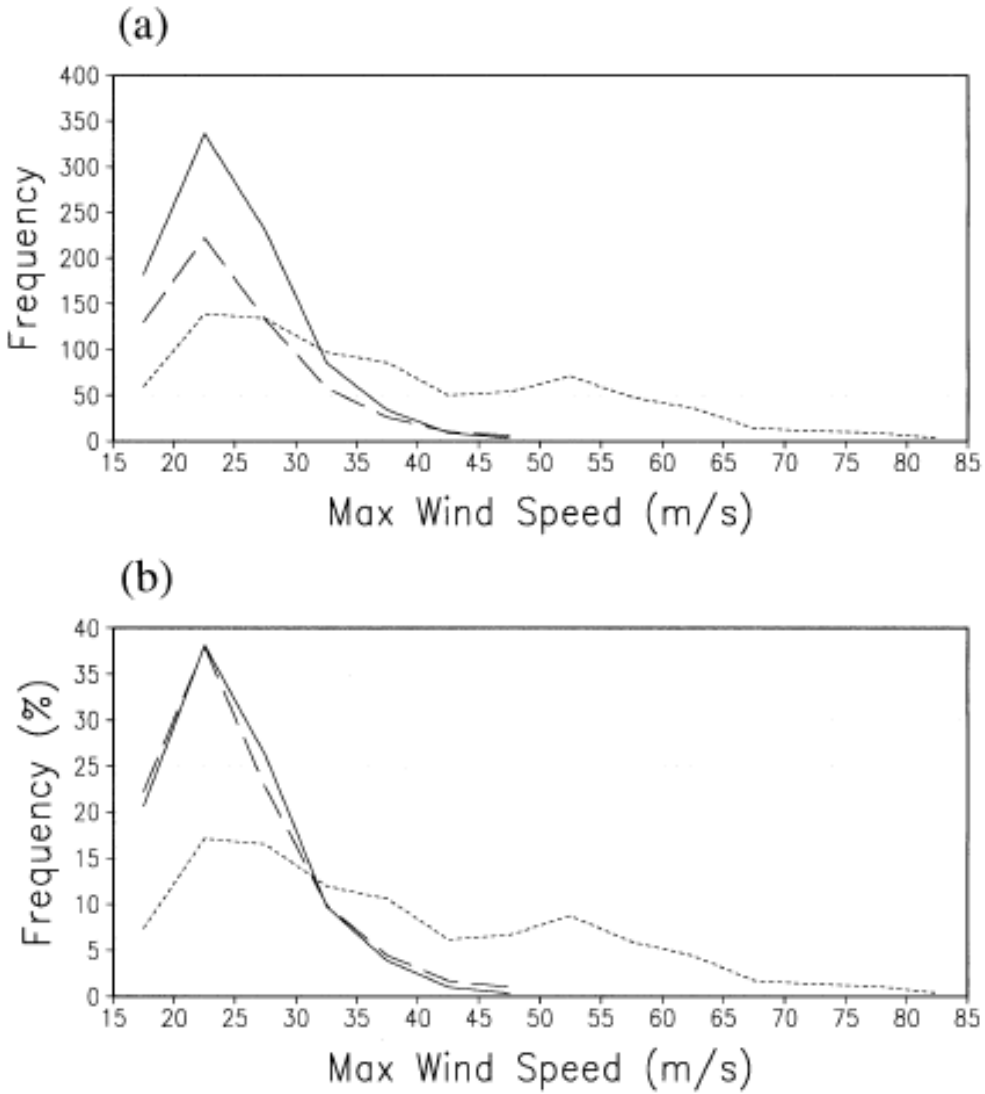

Sugi et al. (2002) JMSJ

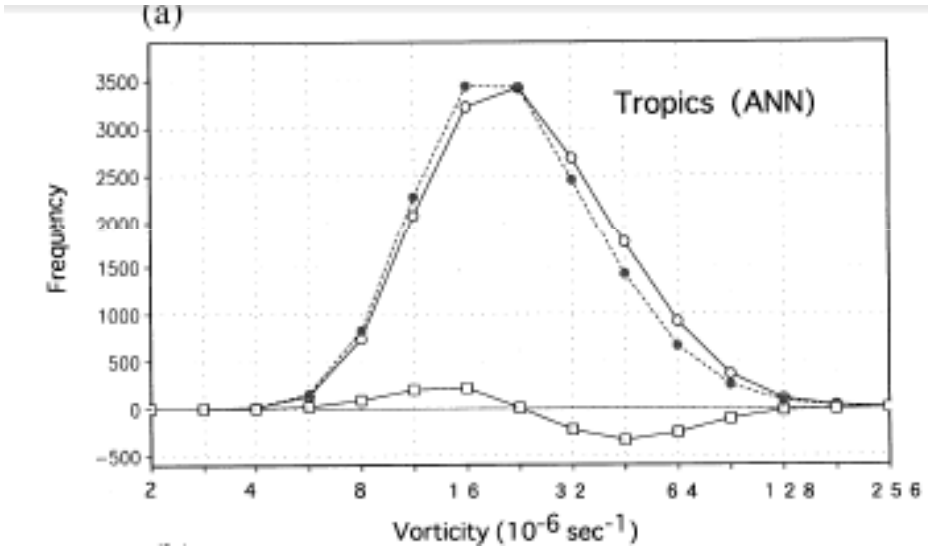

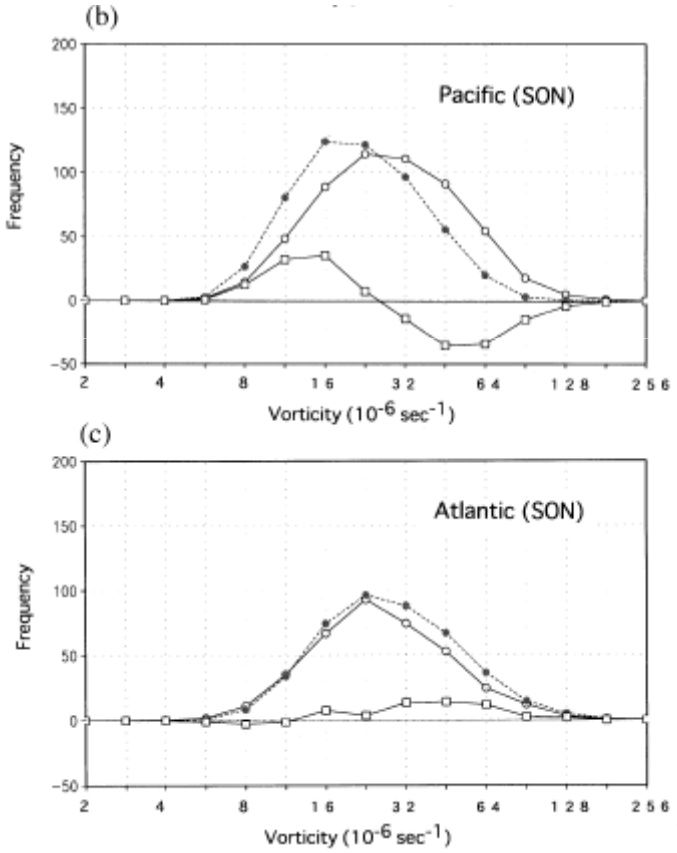

Sugi et al. (2002) JMSJ

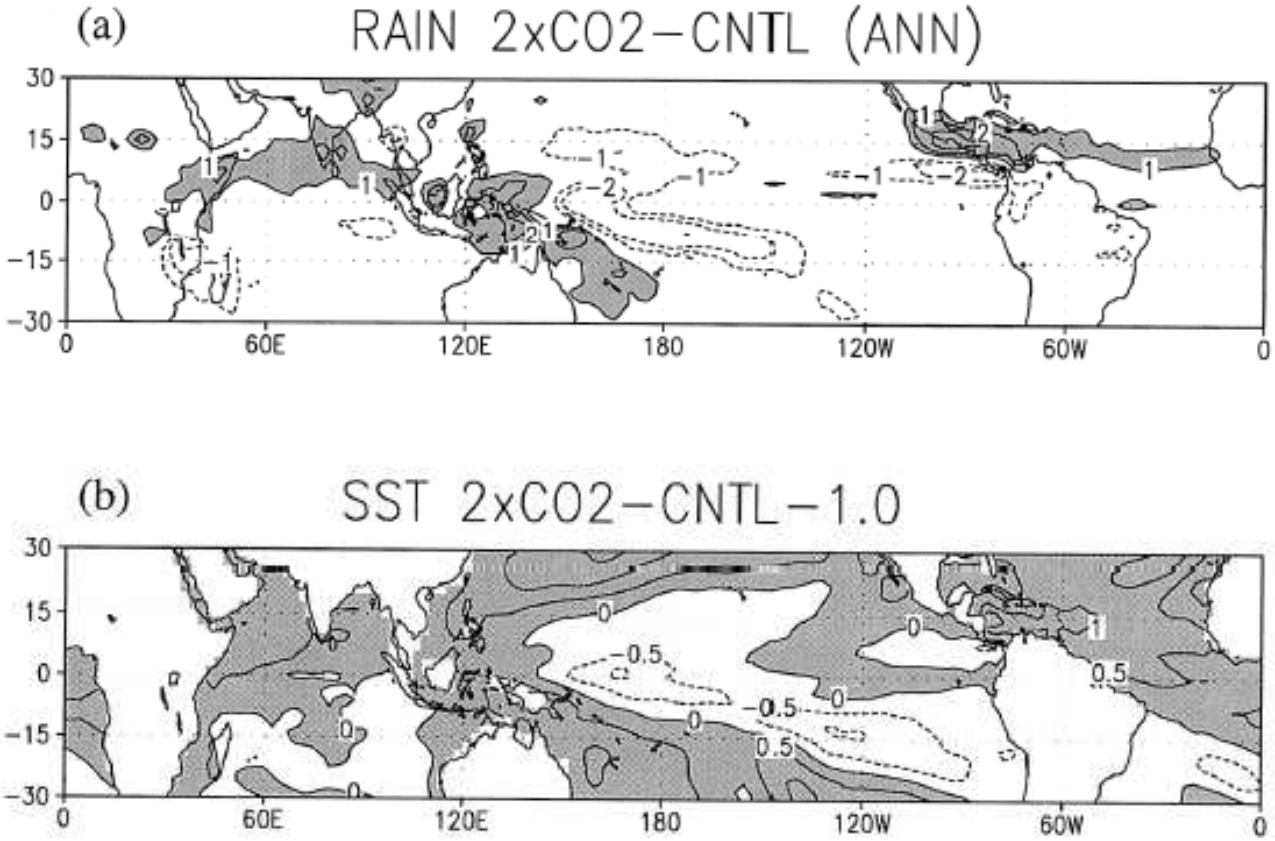

Fig. 8. (a) Annual mean precipitation intensity difference (mm/day) between the control experiment and the 2 × CO2 experiment. (b) Annual mean SST difference (°C) between the control experiment and the 2 × CO2 experiment. One degree is subtracted from the SST difference.

Sugi et al. (2002) JMSJ

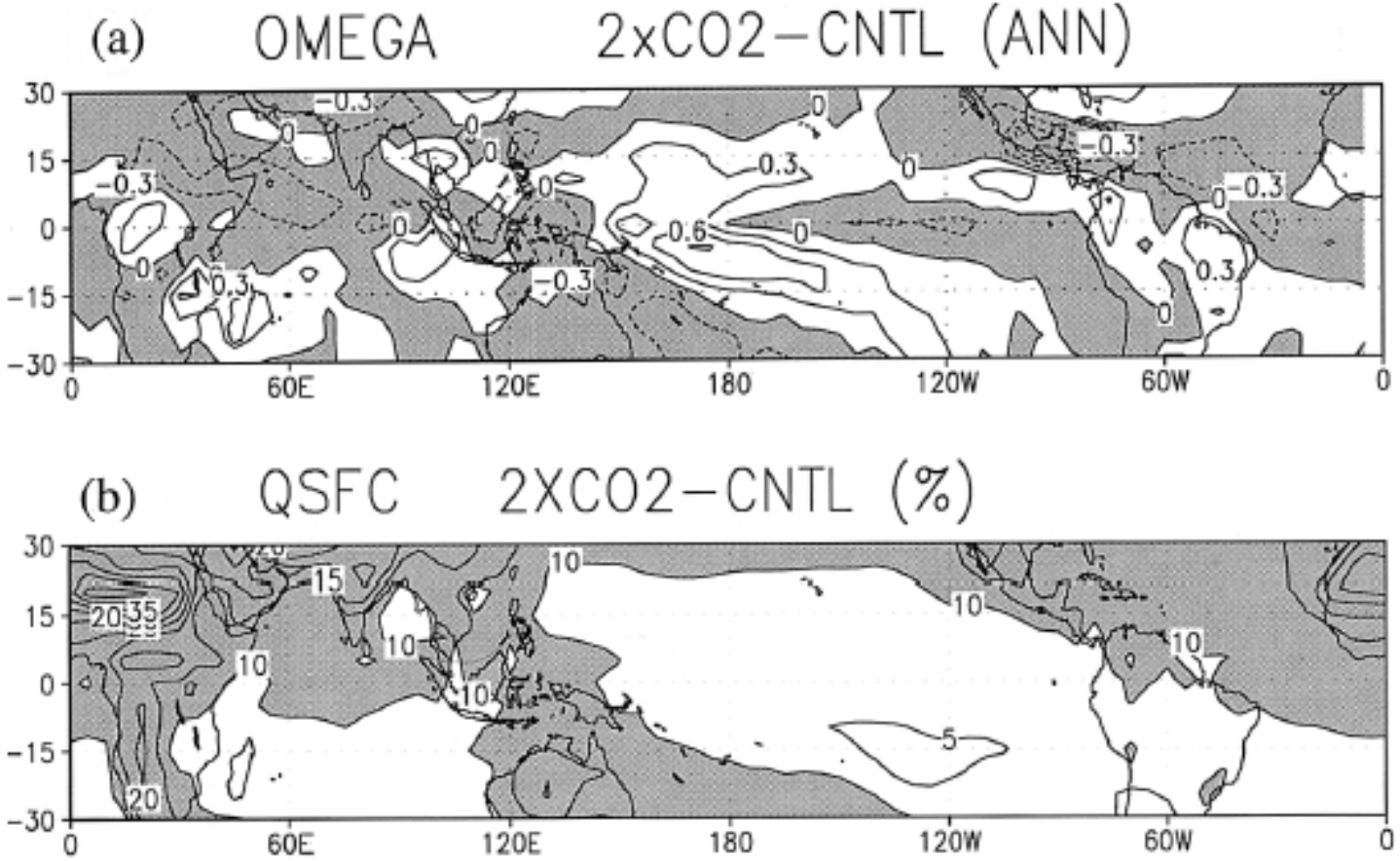

Sugi et al. (2002) JMSJ

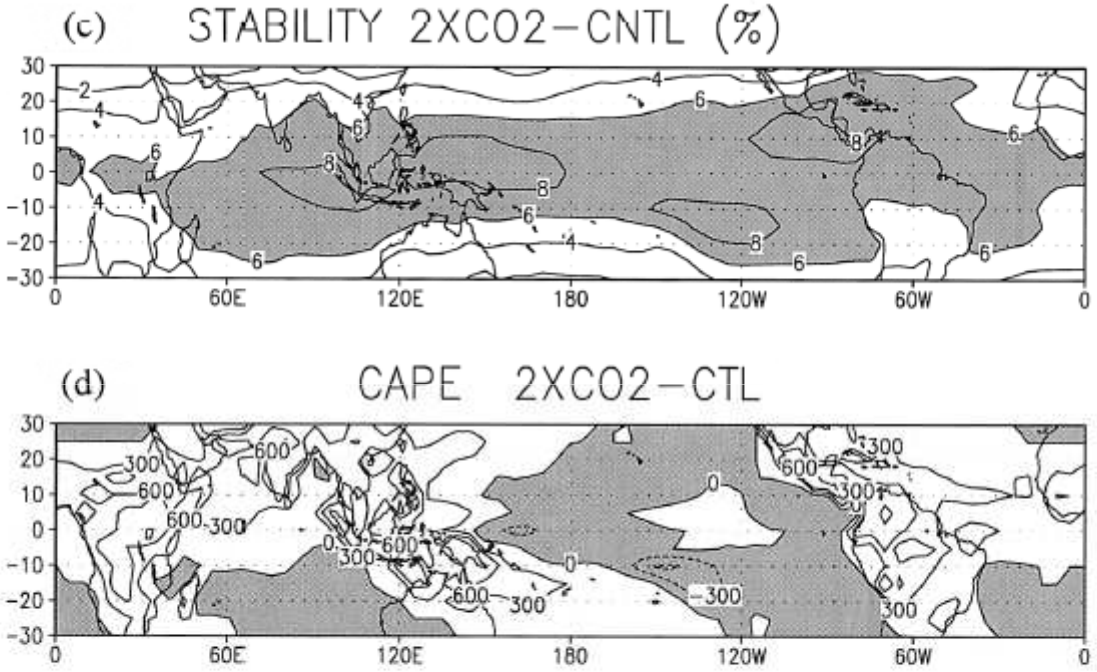

Fig. 9. Differences in the annual mean quantities related to tropical circulation between the control experiment and the $2 \times CO2$ experiment. (a) vertical p-velocity at 500 hPa (hPa/h), (b) surface specific humidity (difference in %) , (c) dry static stability (difference in %), (d) CAPE (J kg^{-1}).

Sugi et al. (2002) JMSJ

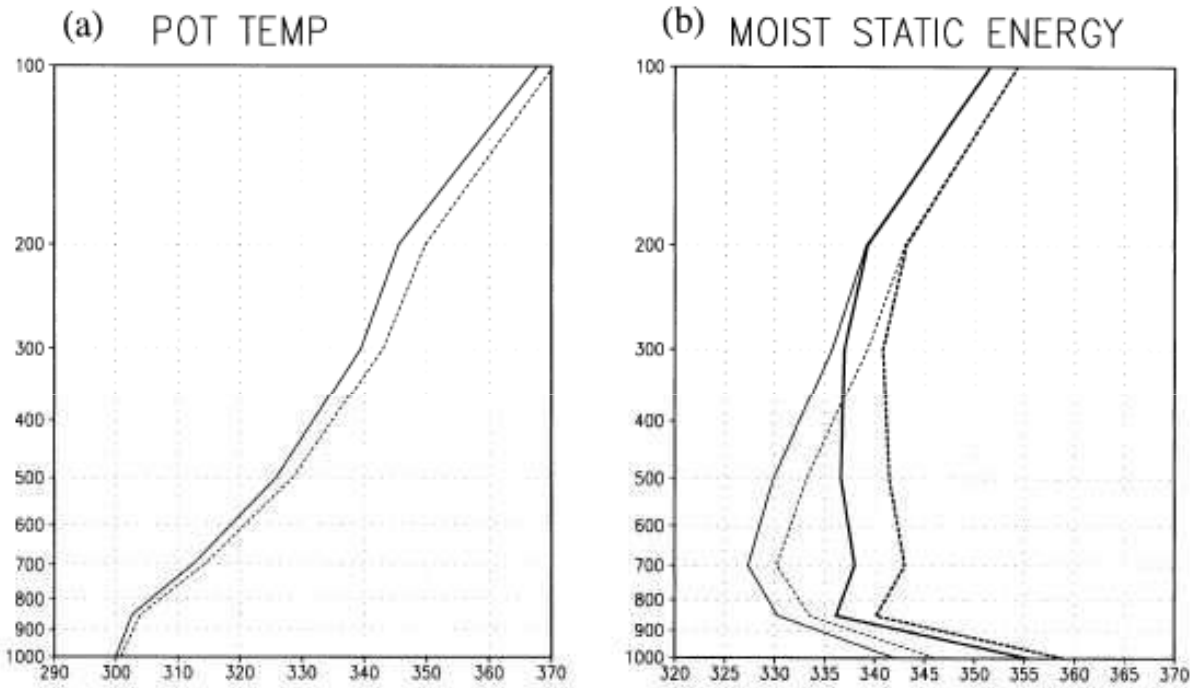

Fig. 10. Annual mean vertical profile of (a) potential temperature (K), and (b) moist static energy (10^3 J kg^{-1}) at 10°N, 160°E. Solid and dashed lines indicate the control experiment and $2 \times CO2$ experiments. Thick lines in (b) show the saturated moist static energy.

Sugi et al. (2002) JMSJ

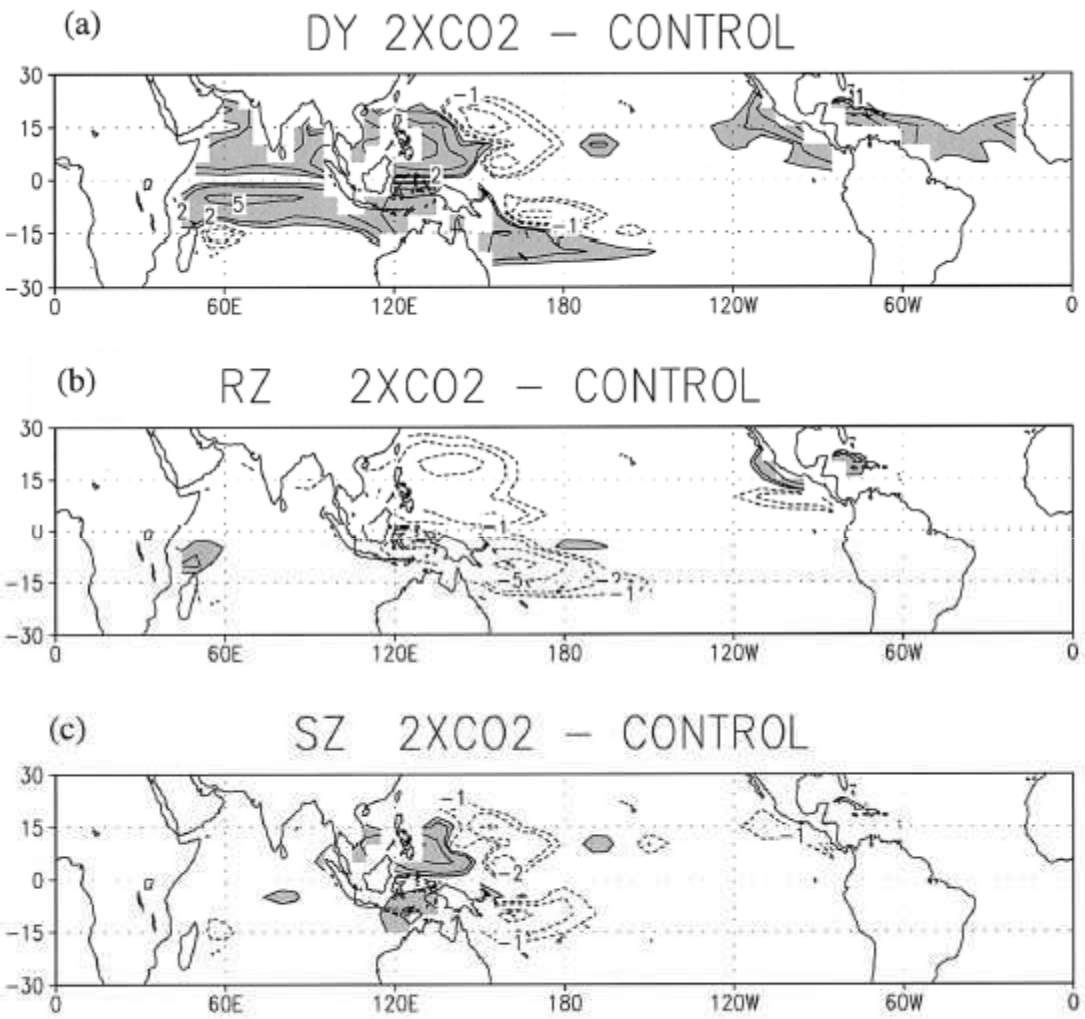

$$Y = X_1 \cdot X_2 \cdot X_3 \cdot X_4 \cdot X_5$$

$$\frac{\Delta Y}{Y} = \frac{\Delta X_1}{X_1} + \frac{\Delta X_2}{X_2} + \frac{\Delta X_3}{X_3} + \frac{\Delta X_3}{X_3} + \frac{\Delta X_3}{X_3}$$

$$DY = RZ + SZ + E + ST + RH$$

DY: change in YGP
RZ: change in vorticity
SZ: change in shear
E: change in ocean thermal energy
ST: change in stability
RH: change in relative humidity

Fig. 11. (a) Difference in the YGP between the control experiment and 2 × CO2 experiment. (b)–(f) Contributions to the difference in YGP from the changes in constituting factors: (b) relative vorticity, (c) vertical shear of horizontal wind.

Sugi et al. (2002) JMSJ

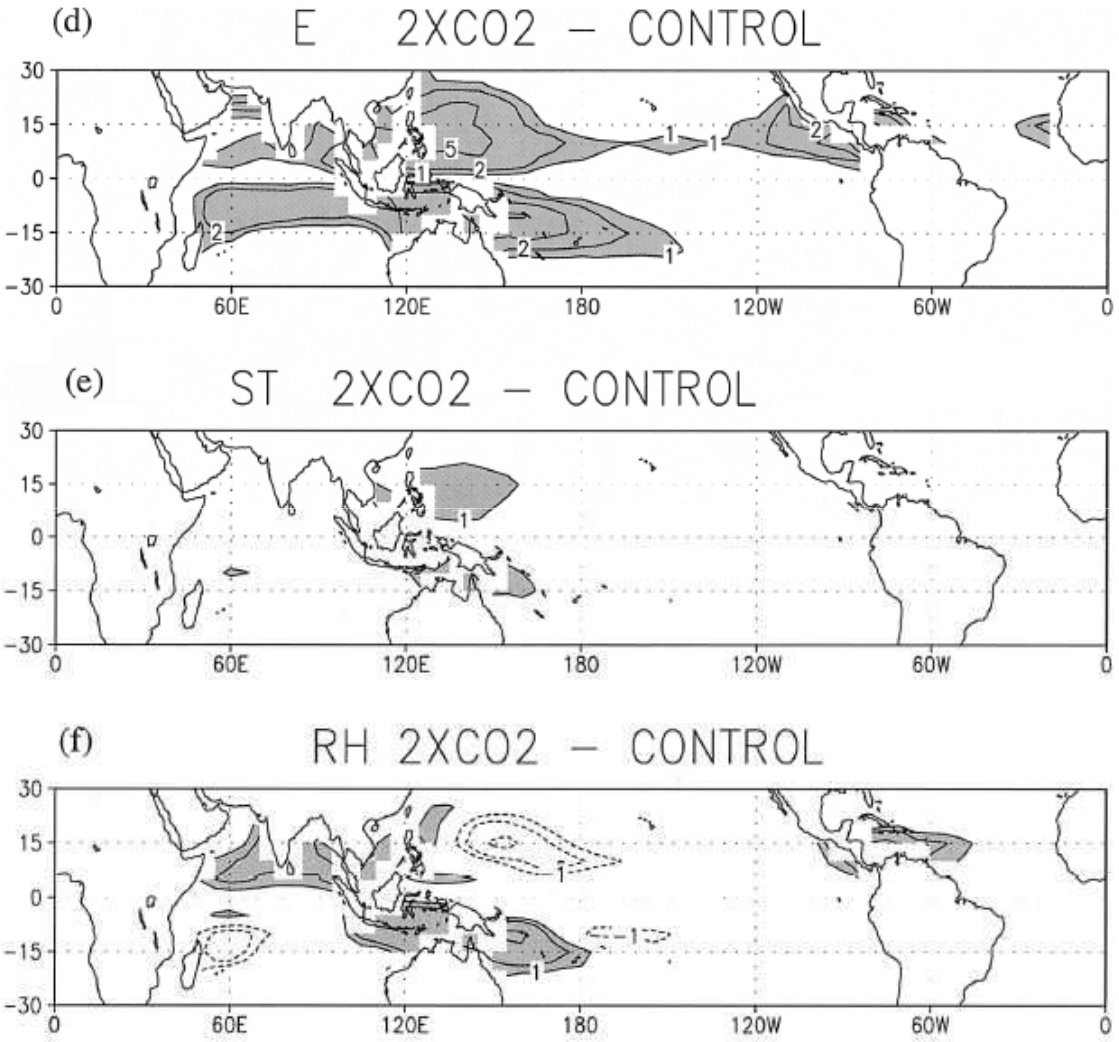

Fig. 11. (d) ocean thermal energy (SST), (e) moist instability, (f) relative humidity.

Sugi et al. (2002) JMSJ

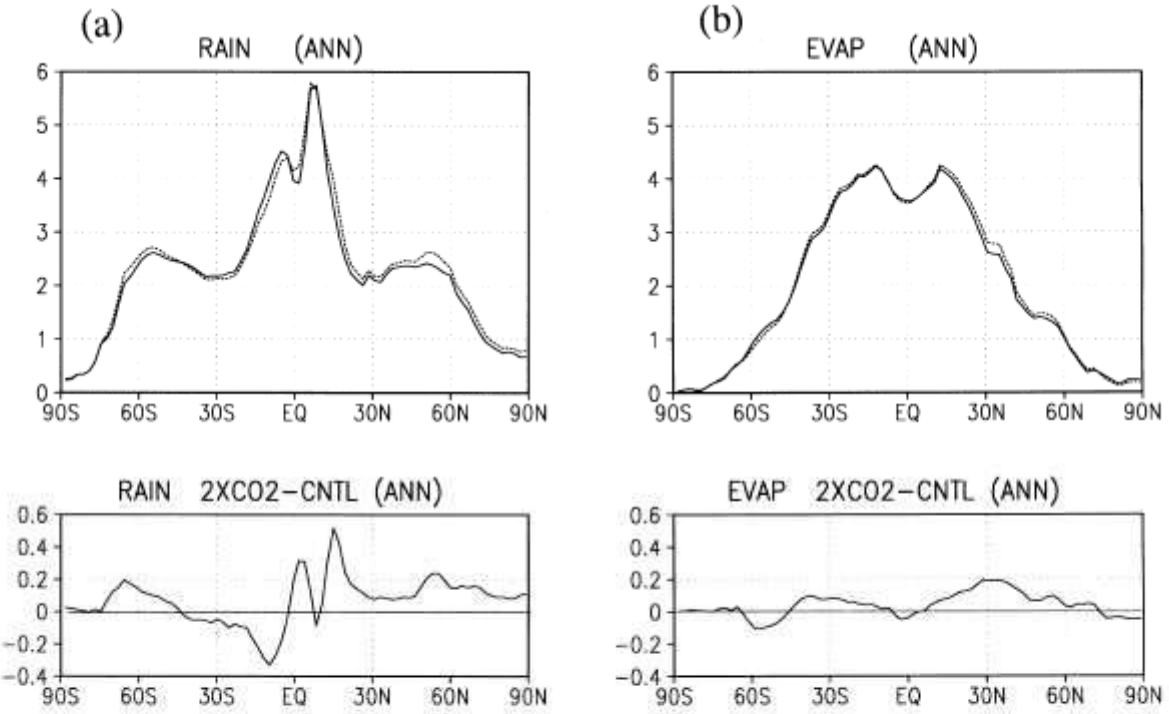

Fig. 12. (a) Zonally averaged annual mean precipitation (mm/day) in the control experiment and 2 × CO2 experiment, and their difference. (b) Zonally averaged annual mean evaporation (mm/day) in the control experiment and 2 × CO2 experiment, and their difference. Solid and dotteded curves in the top panels indicate the control experiment and 2 × CO2 experiment, respectively. The difernce is shown in the bottom panels.

Sugi et al. (2002) JMSJ

Table 2. Variables related to tropical circulation

Variables	CNTL	2xCO2	Difference %
Precipitation	3.43	3.47	+ 1.0
Evaporation	3.78	3.83	+ 1.4
Radiative Cooling	101.0	102.0	+ 1.0
Stability	47.2	49.8	+ 5.5
Mass flux	1.429	1.337	- 6.4
Precipitable Water	3.35	3.81	+ 13.7

Sugi et al. (2002) JMSJ

Table 3. Tropical mass fluxes

	CNTL		2xCO2		Difference (%)	
	Mass flux	Area	Mass flux	Area	Mass flux	Area
Instantaneous						
Upward	1.429	0.438	1.337	0.440	- 6.4	0.46
Downward	1.403	0.562	1.284	0.560	- 8.5	- 0.36
Monthly mean						
Upward	0.697	0.438	0.672	0.438	- 3.6	0.0
Downward	0.672	0.562	0.638	0.562	- 5.1	0.0
Annual mean						
Upward	0.497	0.462	0.487	0.473	- 2.0	2.3
Downward	0.472	0.538	0.453	0.527	- 4.0	- 2.0

Sugi et al. (2002) JMSJ

The wakening of tropical circulation due to global warming may be understood by energy balance of the tropical atmosphere. The approximate energy equation in the tropics may be expressed as,

$$\omega \frac{\partial \theta}{\partial p} \approx \frac{\theta}{T} \frac{Q}{C_p}, \tag{1}$$

(Holton 1979; Kuntson and Manabe 1995). Here we consider a schematic tropical circulation as shown in Fig. 13. Then, the energy balance in the upward motion region and downward motion region at 500 hPa may be written as,

$$M_u \left| \frac{\partial \theta}{\partial p} \right| \approx \frac{\theta}{T} \frac{1}{C_p} (Q_c - Q_R) A_u, \tag{2}$$

$$M_d \left| \frac{\partial \theta}{\partial p} \right| \approx \frac{\theta}{T} \frac{1}{C_p} Q_R A_d, \tag{3}$$

where $M_u(M_d)$ and $A_u(A_d)$ are the mass flux,

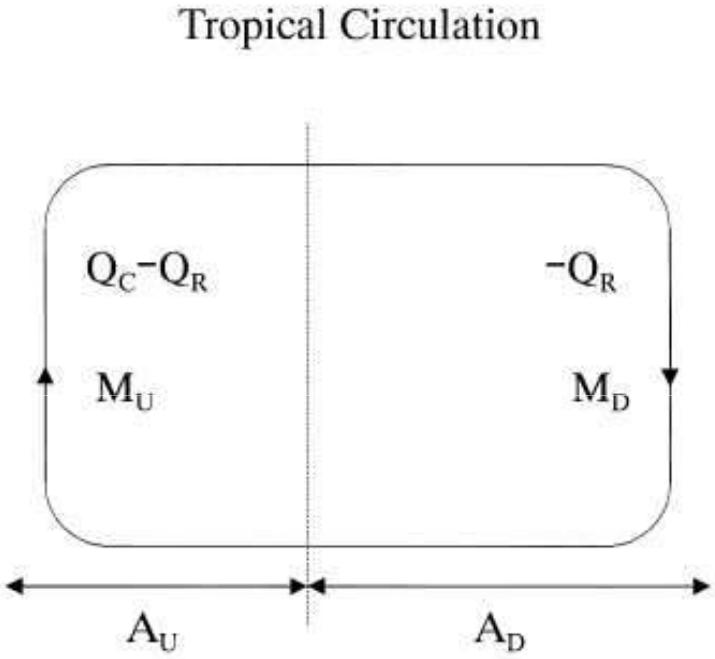

Fig. 13. A schematic diagram showing the energy balance of tropical circulation.

Sugi et al. (2002) JMSJ

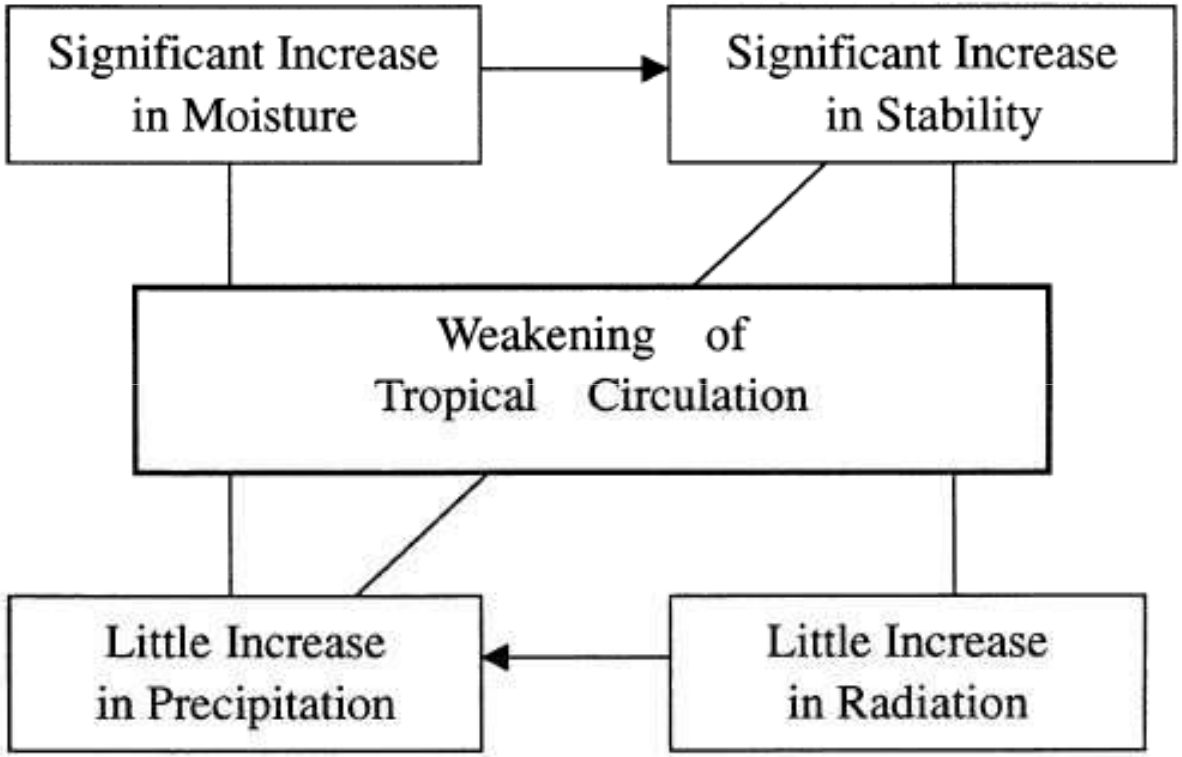

Fig. 14. Changes in quantities related to tropical circulation on doubling CO2.

Sugi et al. (2002) JMSJ

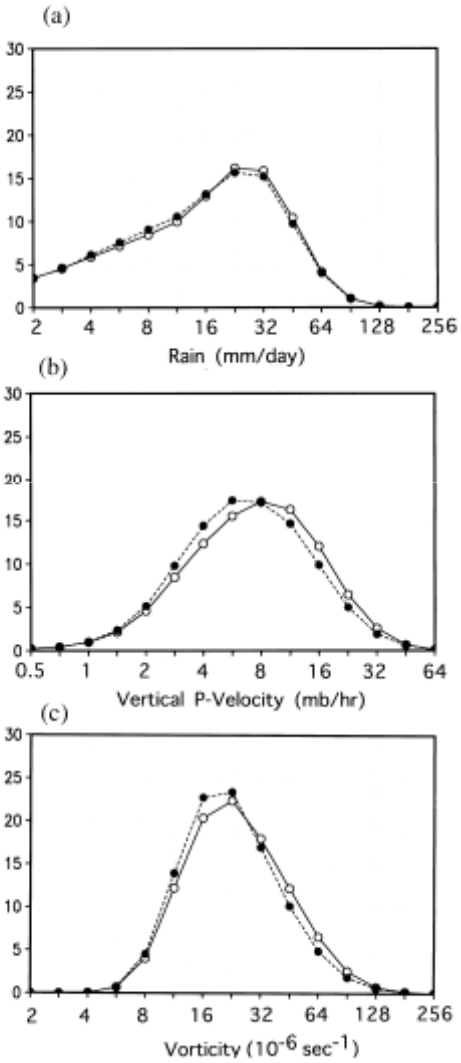

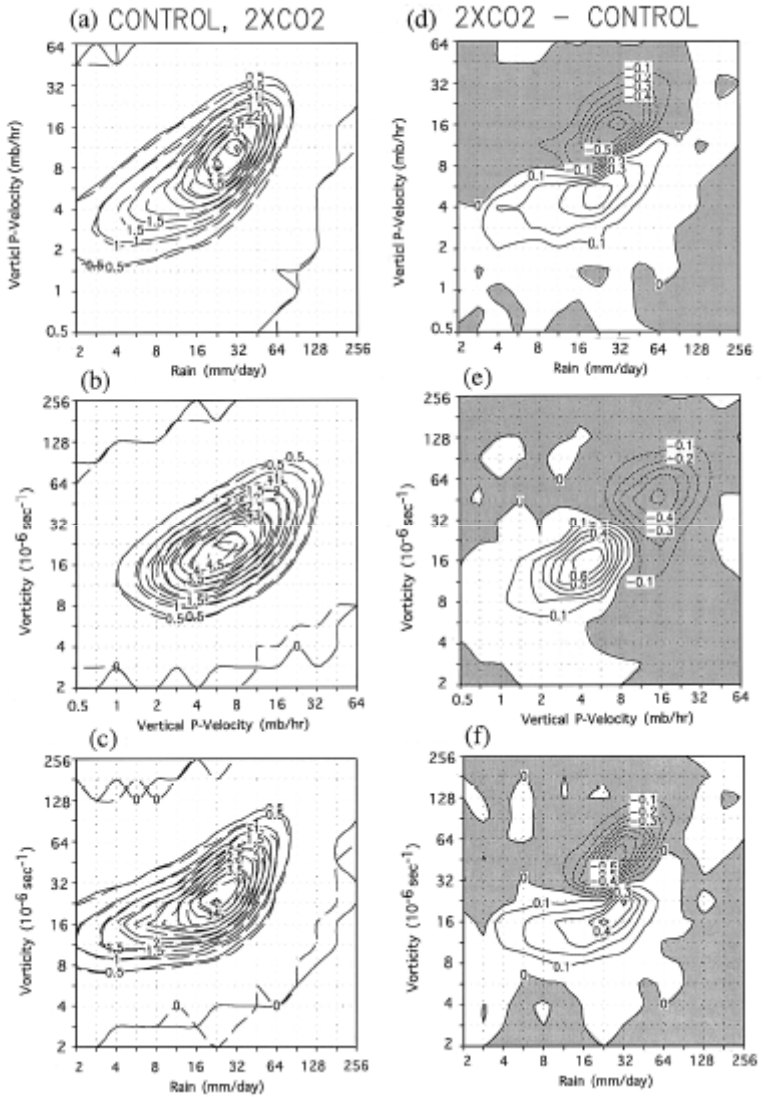

McDonald et al. (2005) CD

Climate Dynamics (2005) 25: 19–36
DOI 10.1007/s00382-004-0491-0

R. E. McDonald · D. G. Bleaken · D. R. Cresswell
V. D. Pope · C. A. Senior

Tropical storms: representation and diagnosis in climate models and the impacts of climate change

Received: 20 August 2002 / Accepted: 22 October 2004 / Published online: 18 May 2005

0.83º x 1.25º with prescribed SST 17 yrs

McDonald et al. (2005) CD

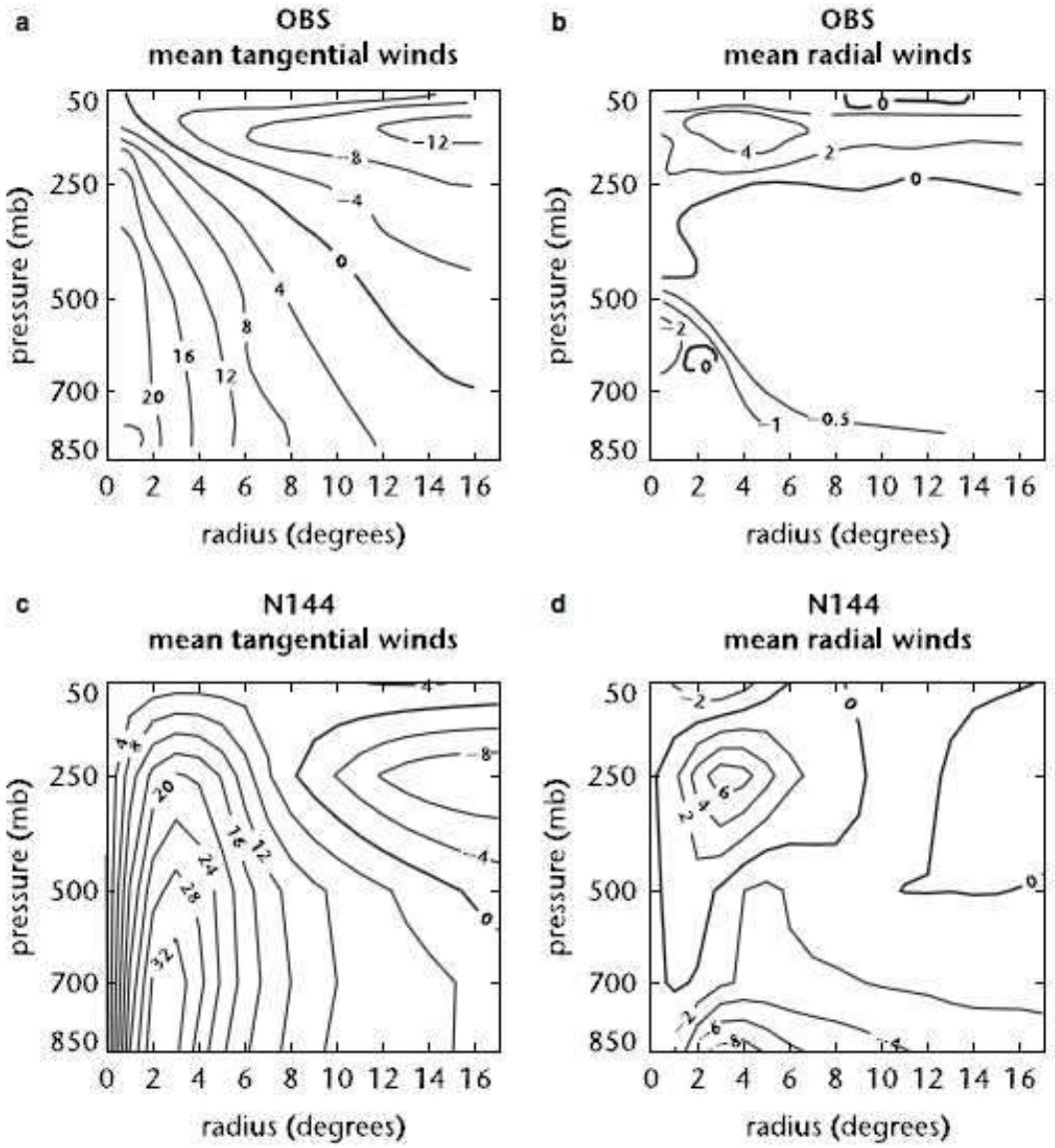

Fig. 1 Two-dimensional cross section of wind for a mean observed typhoon wind structure (adapted from Gray (1979)), for one of the strongest tropical storms from the N144 experiment (located in the SW Pacific to the North of Australia) and for one of the strongest tropical storms from the N48 experiment (located in the Northwest Pacific near to Japan). **a** Observed tangential winds for a mean typhoon (from Gray (1979)), **b** observed radial winds for a mean typhoon (from Gray (1979)), **c** N144 mean tangential winds, **d** N144 mean radial winds, **e** N48 mean tangential winds, and **f** N48 mean radial winds. The contour interval in **a**, **c** and **e** is 4 ms^{-1} and the contour interval in **b**, **d** and **f** is 2 ms^{-1}

McDonald et al. (2005) CD

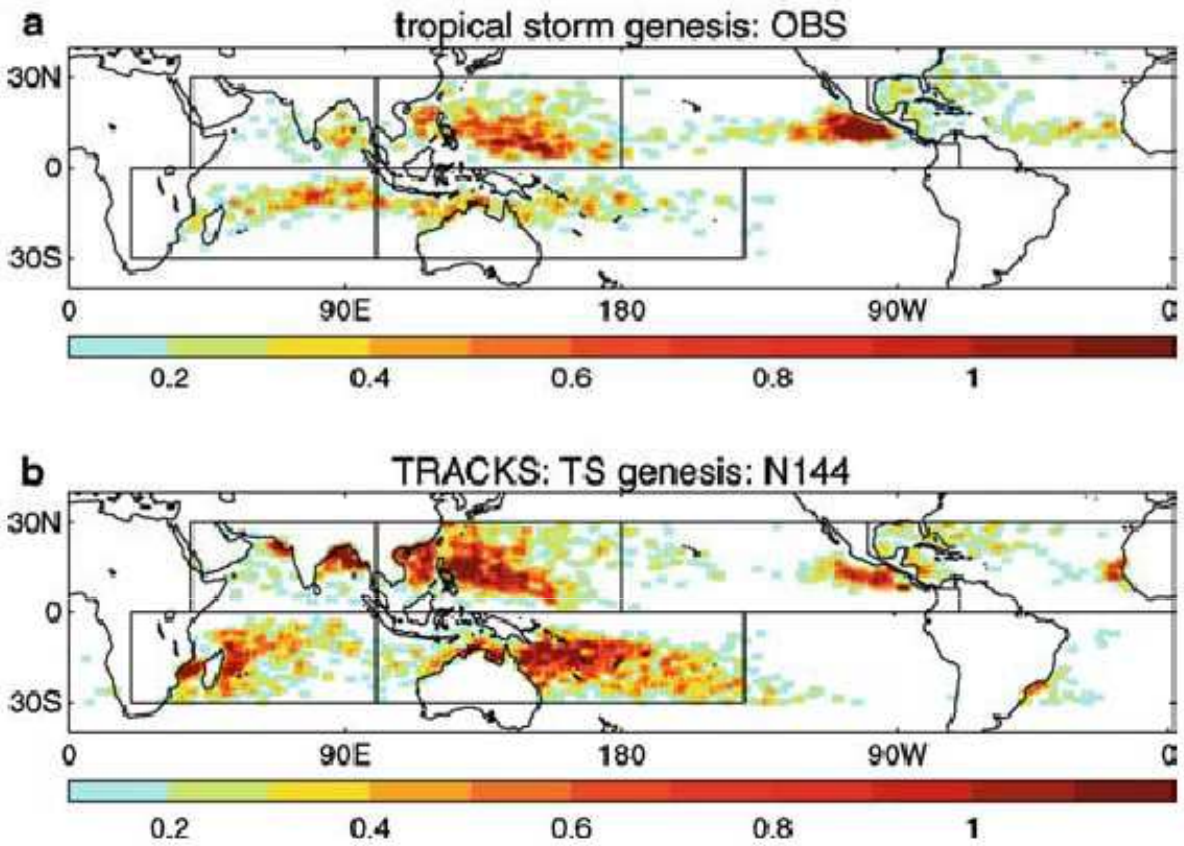

Fig. 2 Density of tropical storm genesis for: **a** OBS (17 years, 1 December 1978 to 1 December 1995) and **b** N144 (17 years, 1 December 1978 to 1 December 1995). For OBS the genesis point is the first point in the 'best track' data and to be included in our analysis an observed tropical storm must attain a wind speed of 17 ms^{-1} at some point during its life. For N144 the TSs are diagnosed using TRACKS and the point at which cyclogenesis occurs is defined as the grid point where the magnitude of the relative vorticity at the centre becomes at least 5.0×10^{-5} s^{-1}. The

McDonald et al. (2005) CD

Table 2 Annual mean and standard deviation (in parenthesis) of number of tropical storms per season in each ocean basin for WARM (15-year mean) and the differences and percentage changes of WARM minus N144

	Tropics 30°S–30°N	Northern Hemisphere 0–30°N	Southern Hemisphere 0–30°S	North Indian	Northwest Pacific	Northeast Pacific	North Atlantic	Southwest Indian	Southwest Pacific
WARM	135 (6.7)	69 (8.5)	67 (9.5)	17 (4.8)	28 (8.8)	18 (7.2)	6 (2.6)	24 (4.4)	39 (6.8)
WARM-N144	**−9.2**	−2.3	**−7.0**	**5.1**	**−12.2**	**8.0**	**−2.6**	2.1	**−8.3**
%change (%)	6	3	10	45	30	78	32	10	18

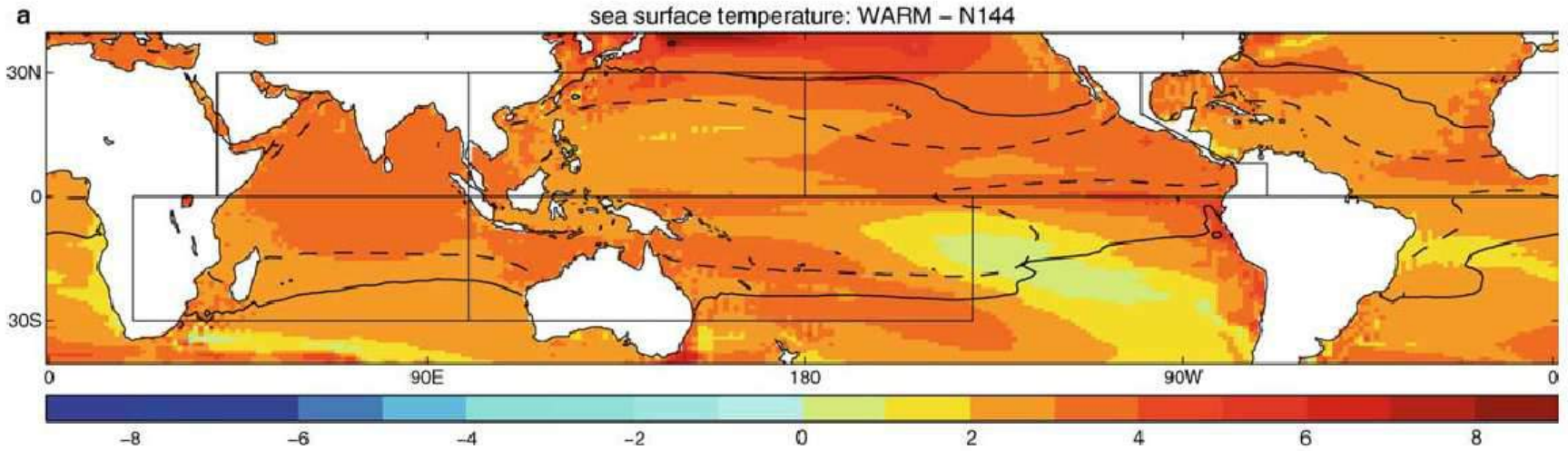

McDonald et al. (2005) CD

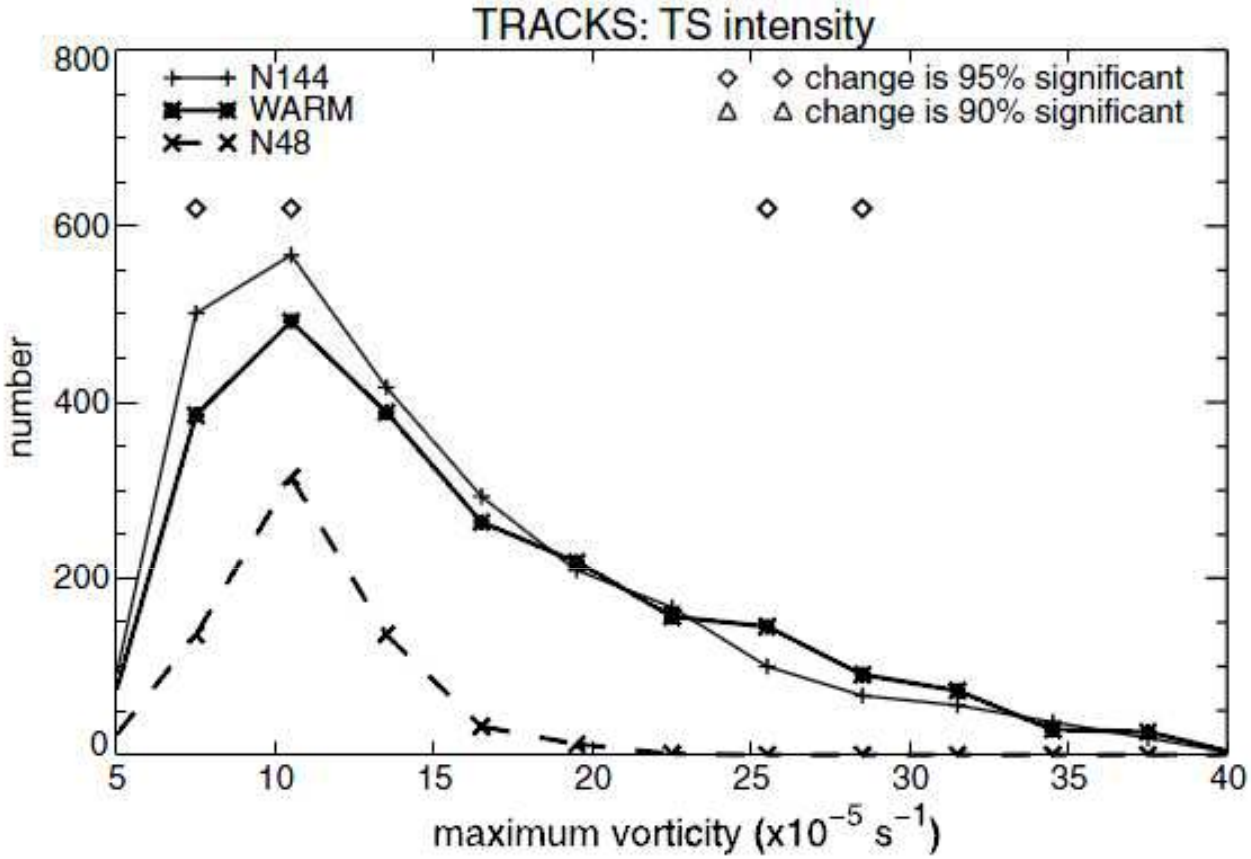

Fig. 8 Frequency distribution of the maximum magnitude of relative vorticity at the TS centre for all TSs in N144 (17 years, *plus and thin solid lines*), WARM (15 years scaled to 17 years, *asterisk and bold solid line*), and N48 (17 years, 1 December 1978 to 1 December 1995 *multi and bold dashed lines*). The units of magnitude of relative vorticity are 10^{-5} s^{-1}. We use a 2-sided

Oouchi et al. (2006) JMSJ

Journal of the Meteorological Society of Japan, Vol. 84, No. 2, pp. 259–276, 2006

Tropical Cyclone Climatology in a Global-Warming Climate as Simulated in a 20 km-Mesh Global Atmospheric Model: Frequency and Wind Intensity Analyses

Kazuyoshi OOUCHI

Advanced Earth Science and Technology Organization, Earth Simulator Center, Yokohama, Japan

Jun YOSHIMURA, Hiromasa YOSHIMURA

Meteorological Research Institute, Tsukuba, Japan

Ryo MIZUTA

Advanced Earth Science and Technology Organization, Tsukuba, Japan

Shoji KUSUNOKI and Akira NODA

Meteorological Research Institute, Tsukuba, Japan

(Manuscript received 30 April 2005, in final form 15 November 2005)

Oouchi et al. (2006) JMSJ

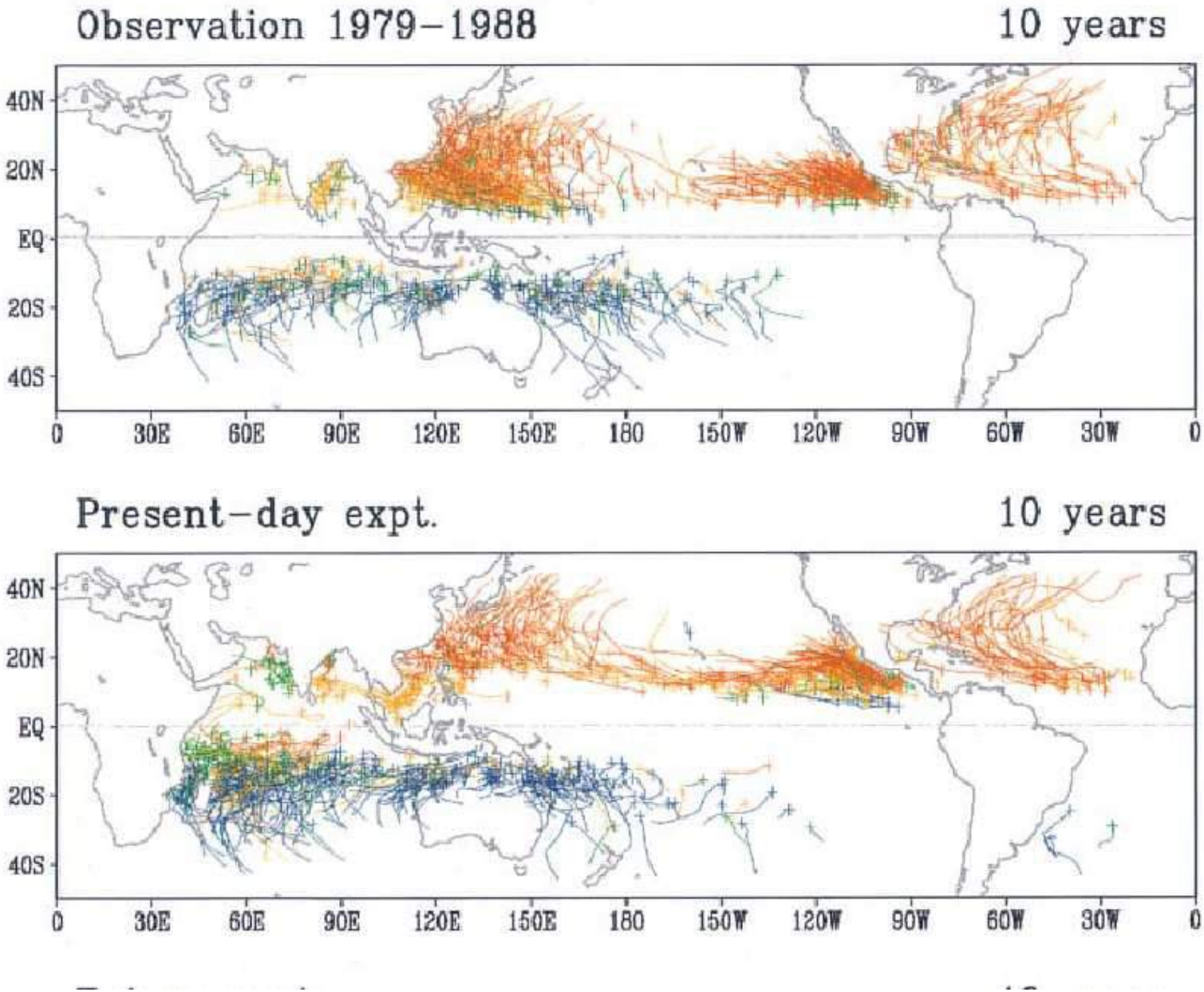

Oouchi et al. (2006) JMSJ

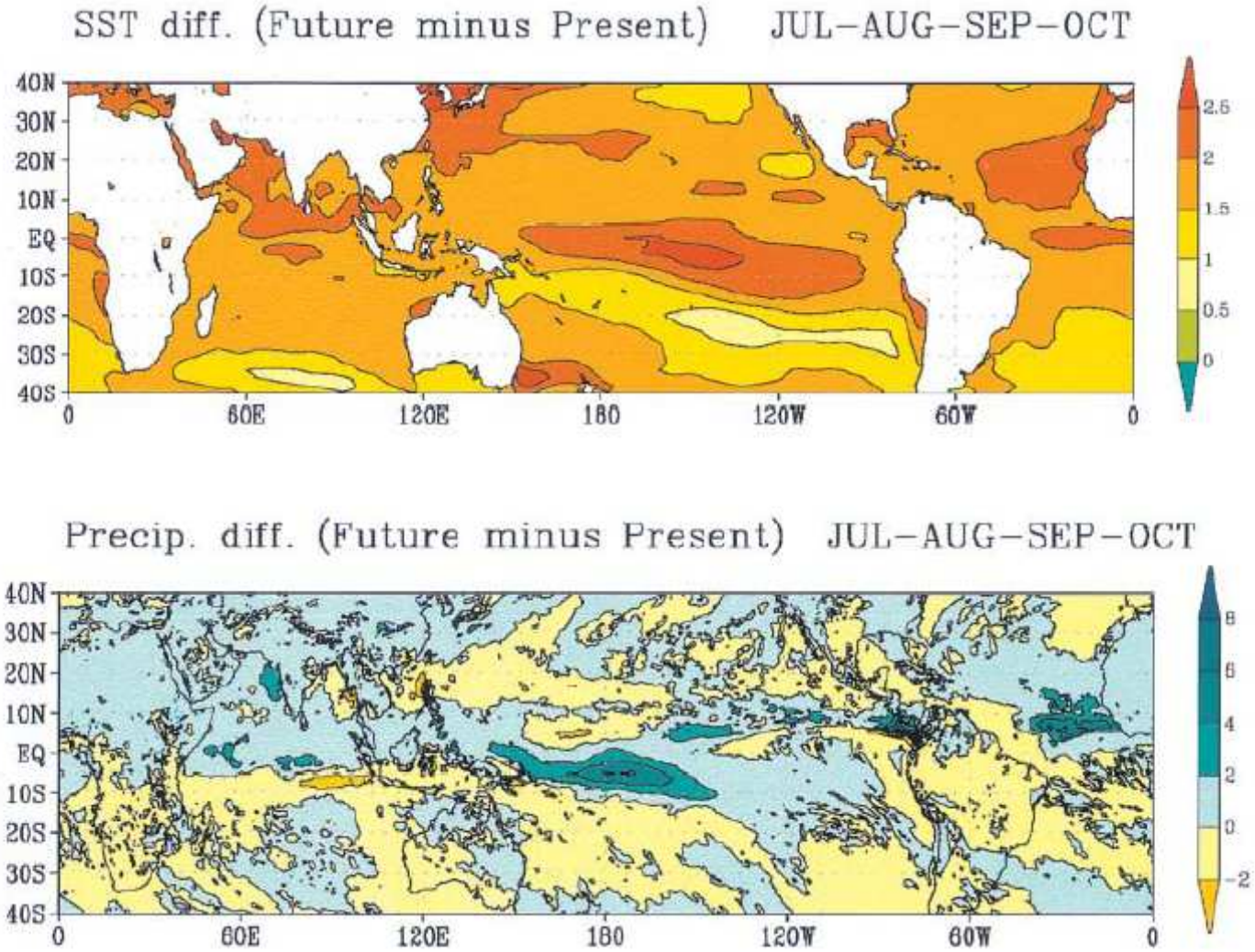

Fig. 3. Difference between the future and the present-day experiments (future minus present-day) in the sea surface temperature (upper) and precipitation amount (lower) derived from the average in the boreal tropical-cyclone season (July, August, September, and October) for the entire integration years.

20kmメッシュ全球大気モデルによる温暖化予測　　Oouchi et al. 2006, JMSJ

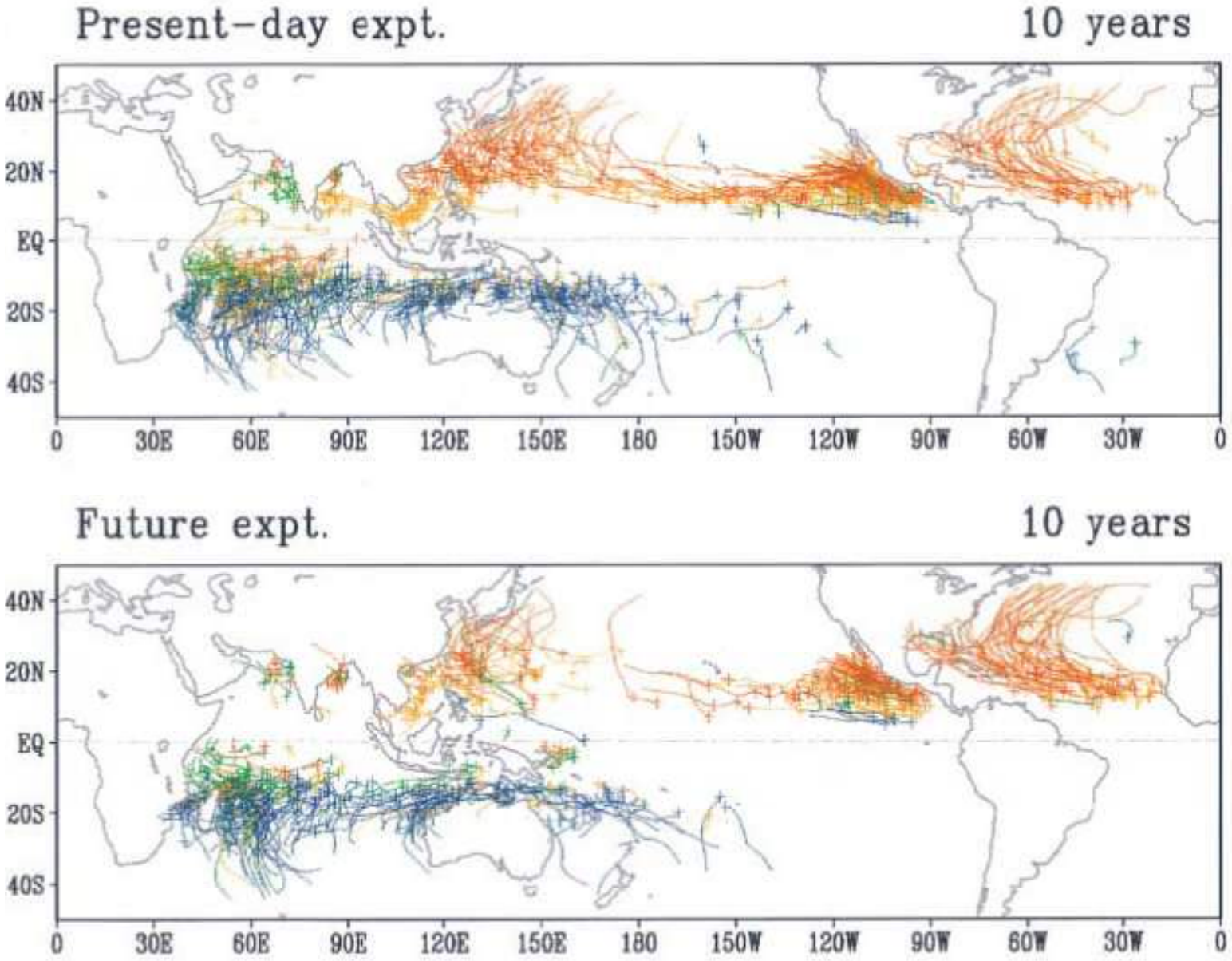

熱帯低気圧の強度別頻度分布

Oouchi et al. (2006) JMSJ

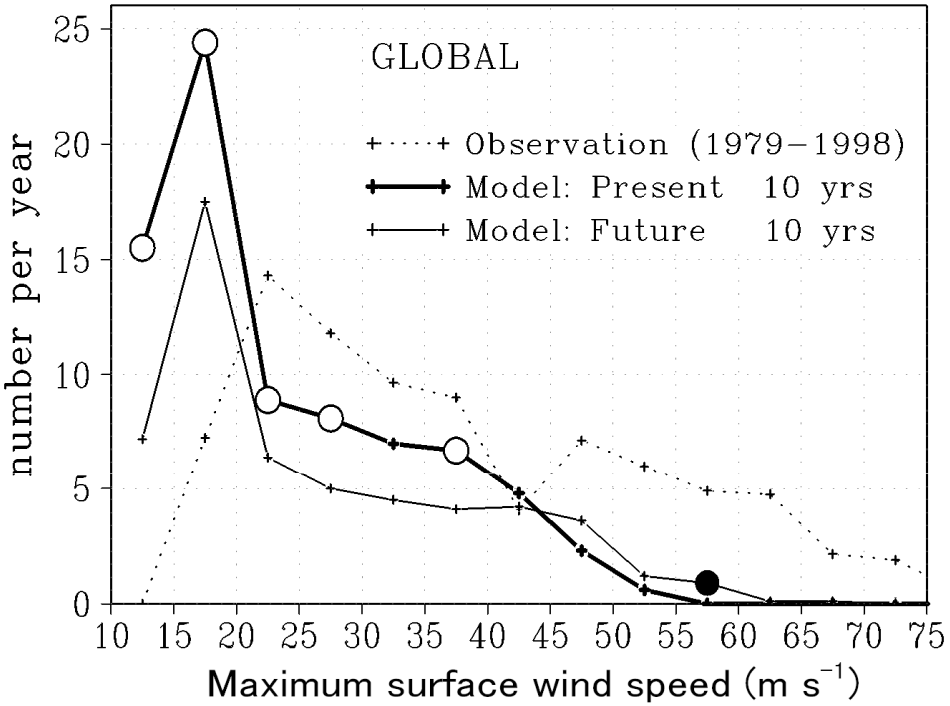

広範なモデル予測によれば、熱帯域の海面水温上昇に伴って、将来の熱帯低気圧（台風及びハリケーン）の強度は増大し、最大風速や降水強度は増加する可能性が高い。それと比べて世界的に熱帯低気圧の発生数が減少するとの予測については信頼性が低い。(IPCC AR4 WG1 SPM　2007)

Oouchi et al. (2006) JMSJ

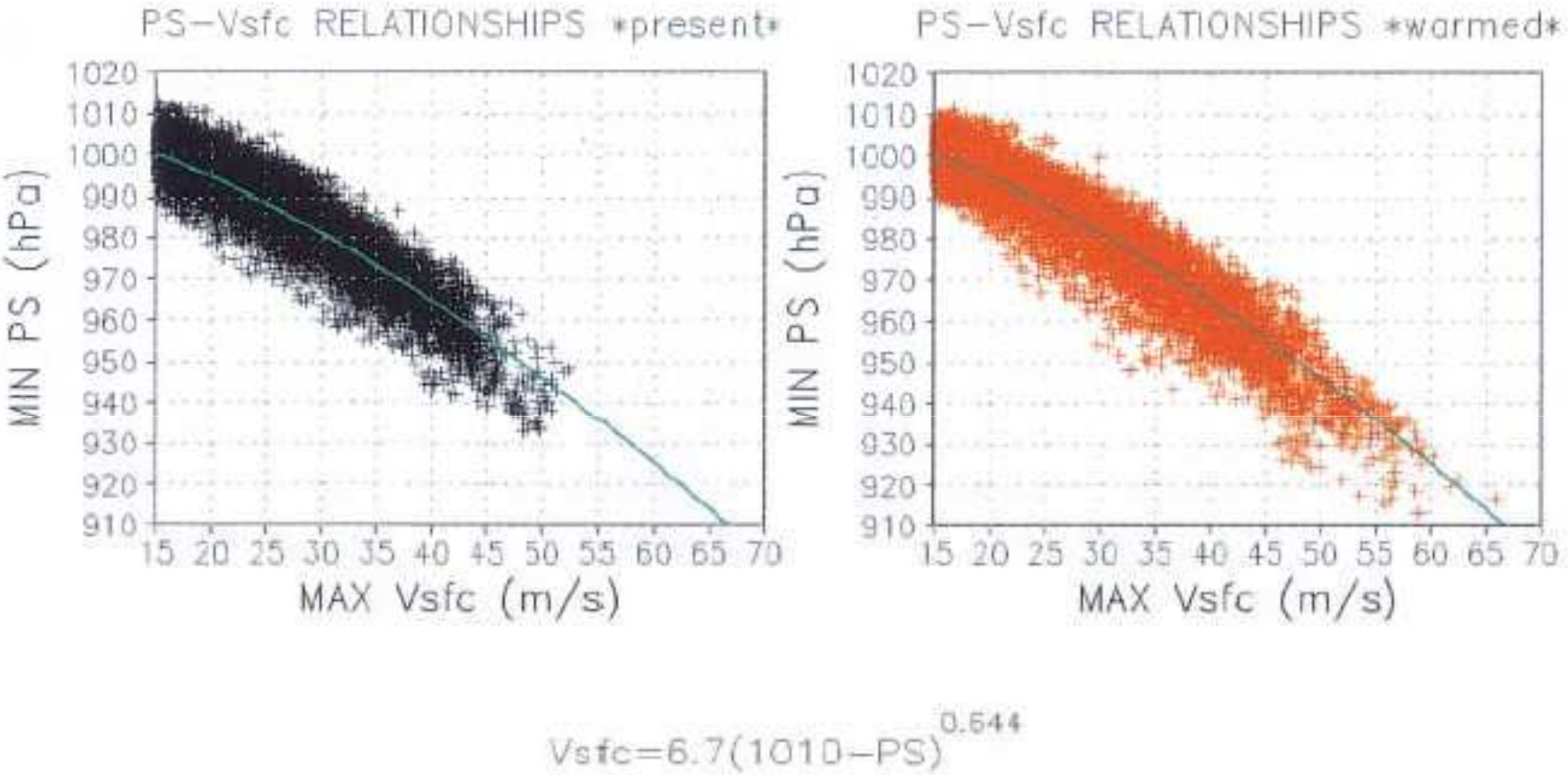

Fig. 5. Scattered diagram of minimum surface pressure versus maximum surface wind speed for all the simulated tropical cyclones in the (left) present-day experiment and (right) warmed climate experiment. Blue line is the nonlinear regression line of "surface wind (Vsfc in knot) and surface pressure (mb)" relationship from Atkinson and Holliday (1977).

Danish Climate Centre

DMI, Ministry of Transport

A time-slice experiment with the ECHAM4 A-GCM at high resolution: The simulation of tropical storms for the present-day and of their change for the future climate

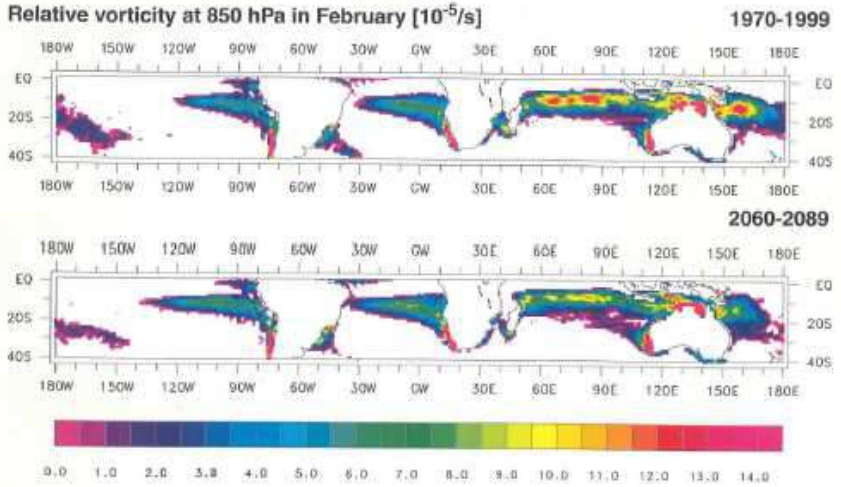

Wilhelm May
Danish Meteorological Institute and Danish Climate Centre

Rapport 00-5

May (2000) DCC/DNI Report

T106 (120km) AGCM with prescribed SST 30 yr time slice present and 2xCO2

Table 4:

Area	Ratio (%)	Ratio (%) B96
Globe	77.1	68.2
N Hemisphere	78.1	74.7
S Hemisphere	74.2	43.3
NW Atlantic	59.3	87.0
NE Pacific	76.9	79.5
NW Pacific	74.0	65.9
N Indian	122.8	90.0
S Indian	64.2	35.9
Australia	90.3	46.8
S Pacific	52.4	55.0
Others	60.0	42.9

Ratio between the numbers of tropical storms for TSL_2 (2060-2089) and TSL_1 (1970-1999) as well as the relative change in the number of tropical storms according to Bengtsson et al. (1996) distinguishing between different regions.

中高解像度全球大気モデル実験における
温暖化に伴う熱帯低気圧の数の変化

Reference	Model	Resolution	Experiment	Global	NWP	NA
Bengtsson et al. 1996 May 2000	ECHAM4	120km	5y x 2 30y x 2	63% 77%	66% 74%	87% 59%
Sugi et al. 2002	JMA8911	120km	10y x 2	66%	34%	161%
McDonald et al. 2005	HadAM3	100km	15y x 2	94%	79%	75%
Oouchi et al. 2006	JMA/MRI	20km	10y x 2	70%	62%	134%

IWTC 6 Statement (2006)

16.
Currently there is large overall uncertainty in future changes in tropical cyclone frequency as projected by climate models with future greenhouse gases. The most recent results obtained from medium and high resolution GCM indicate a consistent signal of fewer tropical cyclones globally in a warmer climate (Sugi et al., 2002; McDonald et al., 2005; Bengtsson et al., 2006; Oouchi et al., 2006) , with some regions showing increases in some simulations, though these findings are still not conclusive. Based on the model simulations, the broad geographic regions of cyclogenesis and therefore also the regions affected by tropical cyclones are not expected to change significantly.

Most models used for such global warming experiments have not been examined extensively concerning their ability to reproduce known historical variations (interannual to interdecadal) in tropical cyclone activity in various basins. While these models generally produce weak tropical cyclone-like storms in roughly the correct locations and seasons, many in the hurricane research community are sceptical of the tropical cyclogenesis process in these low-resolution models, which calls into question the reliability of their future projections.

IPCC-AR4 (2007) SPM

Based on a range of models, it is *likely* that future tropical cyclones (typhoons and hurricanes) will become more intense, with larger peak wind speeds and more heavy precipitation associated with ongoing increases of tropical sea surface temperatures. There is less confidence in projections of a global decrease in numbers of tropical cyclones. The apparent increase in the proportion of very intense storms since 1970 in some regions is much larger than simulated by current models for that period.

IV. 2008-2013 （IPCC-AR5まで）

Bengtsson et al. (2007) Tellus [Resolution]
Emanuel et al. (2008) BAMS [Downscaling CMIP3]
Knutson et al. (2008) Nature GS [18km N Atl.]
Gualdi et al. (2008) JCLI [Coupled model]
Zhao et al. (2009) JCLI [50 km HiRAM]
Sugi et al. (2009) SOLA [Resolution]
Bender et al. (2010) Science [9km N Atl.]
Knutson et al. (2010a) Nature GS (→ IWTC-7)
Knutson et al. (2010b) World Scientific (← IWTC-6)
IWTC-7 (2010) (← Knutson et al. 2010a)
Murakami et al. (2012a) CD [60km MRI-AGCM]
Murakami et al. (2012b) JCLI [20km MRI-AGCM]
IPCC- AR5 (2013)

Bengtsson et al. (2007) Tellus

Tellus (2007), 59A, 539–561
Printed in Singapore. All rights reserved

TELLUS

How may tropical cyclones change in a warmer climate?

By LENNART BENGTSSON[1,2], KEVIN I. HODGES[1*], MONIKA ESCH[2], NOEL KEENLYSIDE[3], LUIS KORNBLUEH[2], JING-JIA LUO[4] and TOSHIO YAMAGATA[4],
[1]*Environmental Systems Science Centre, University of Reading, Whiteknights, PO Box 238, Reading, RG6 6AL, UK;* [2]*Max Planck Institute for Meteorology, Bundesstraße 53, 20146 Hamburg, Germany;* [3]*Leibniz Institute of Marine Sciences, IFM-GEOMAR, Düsternbrooker Weg 20, D-24105 Kiel, Germany;* [4]*Climate Variations Research Program, Frontier Research Center for Global Change (FRCGC), 3173-25 Showamachi, Kanazawa-ku, Yokohama City, Kanagawa 236-0001, Japan*

(Manuscript received 22 January 2007; in final form 13 April 2007)

T63-T319 (200-40km) prescribed SST
30yr (20yr for T319)

Bengtsson et al. (2007) Tellus

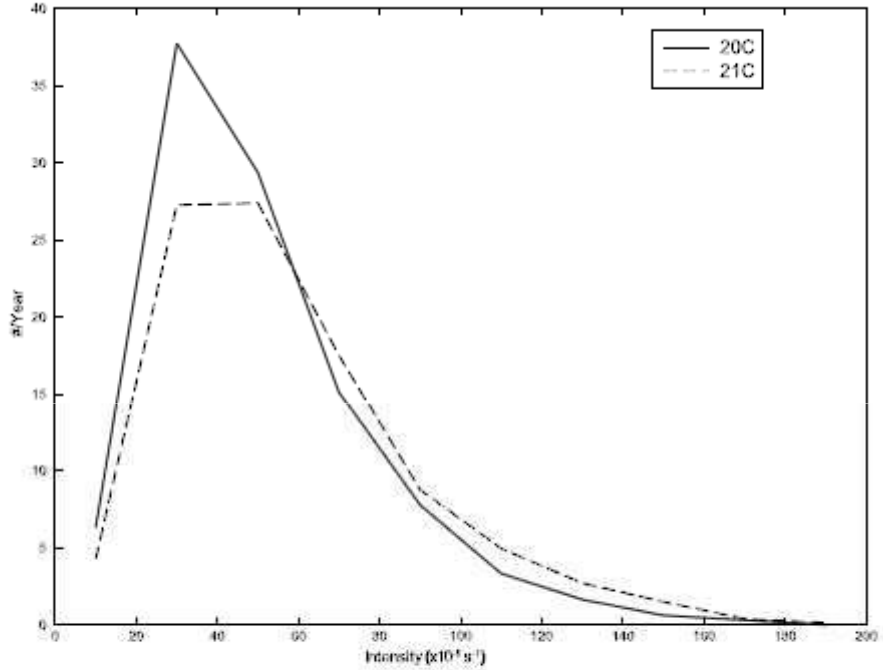

Fig. 8. T213 distributions of maximum attained intensity for NH, TC based on 850 hPa relative vorticity for 20C and 21C. Bin widths are 2×10^{-4} s^{-1}.

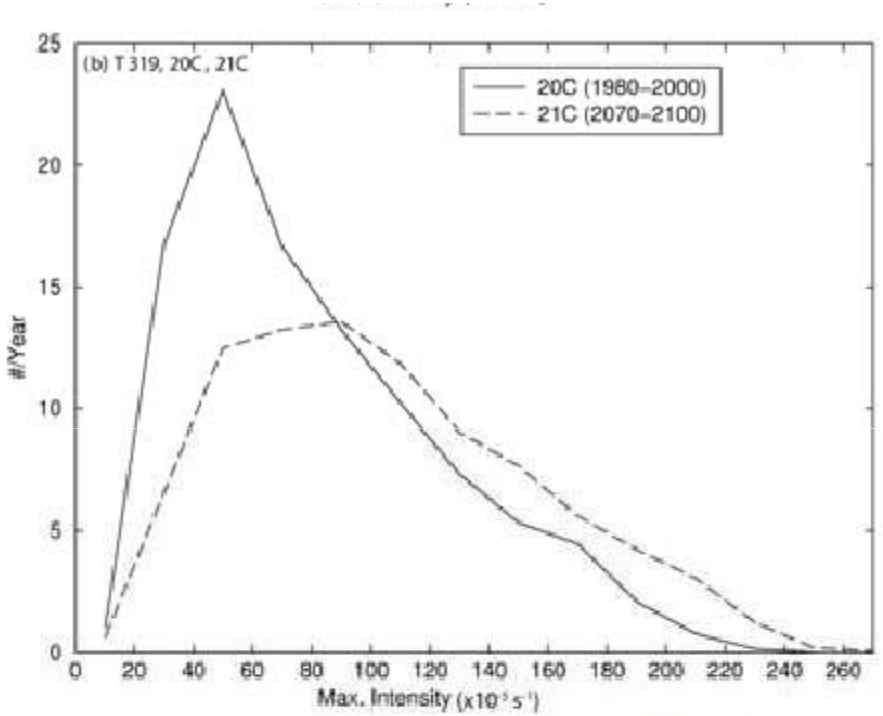

Fig. 15. Maximum attained intensity distributions for NH, TC based on the 850 hPa relative vorticity for (a) all resolutions, T63, T213 and T319, bin widths 1.0×10^{-4} s^{-1}, (b) T319, 20C and 21C, bin widths 2.0×10^{-4} s^{-1}.

Bengtsson et al. (2007) Tellus

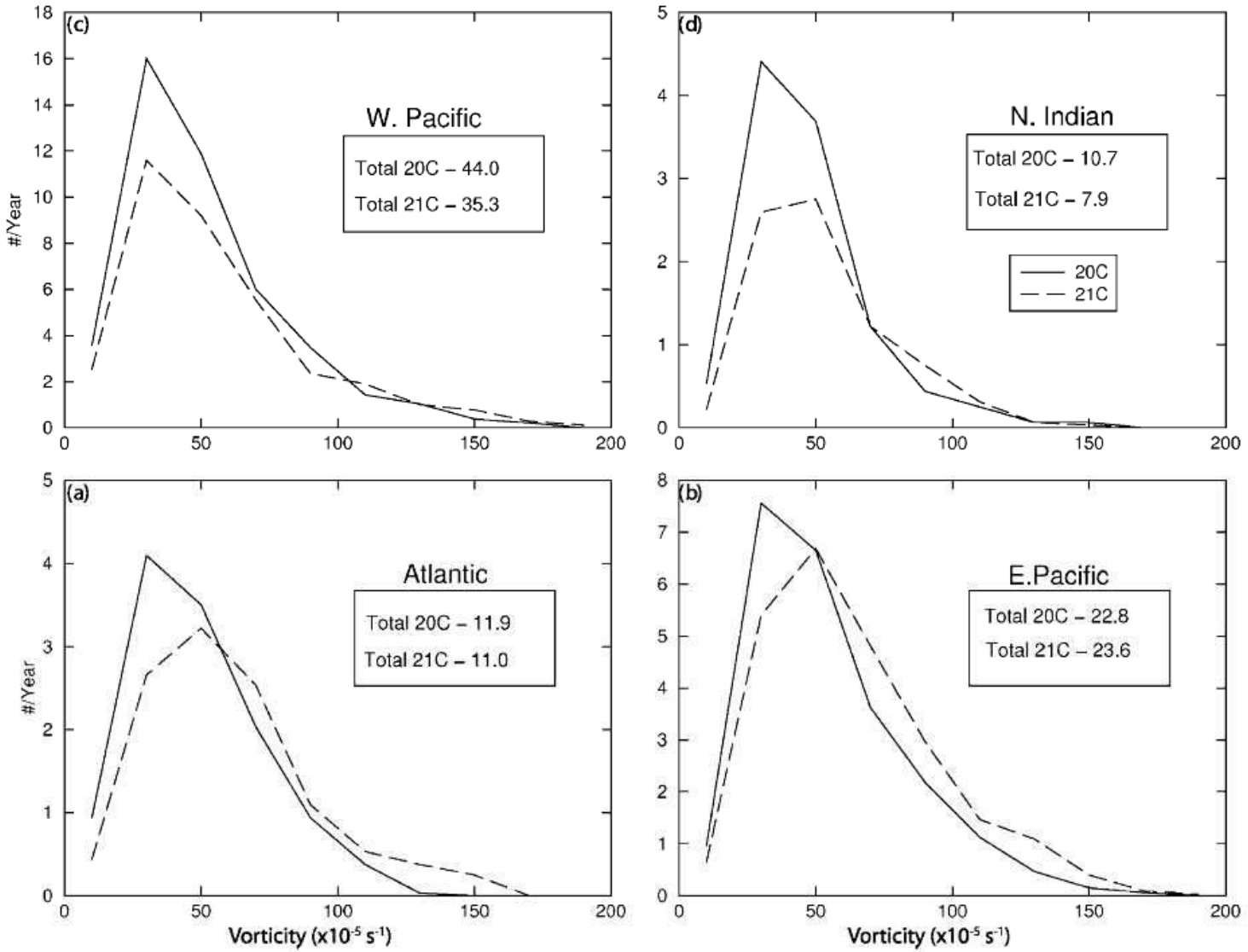

Fig. 12. T213 regional distributions of maximum attained intensity based on 850 hPa relative vorticity for 20C and 21C for (a) Atlantic, (b) eastern Pacific, (c) western Pacific and (d) north Indian ocean. Bin widths are 2×10^{-4} s^{-1}. Inset boxes show the total number per year for each region and for 20C and 21C, respectively.

Bengtsson et al. (2007) Tellus

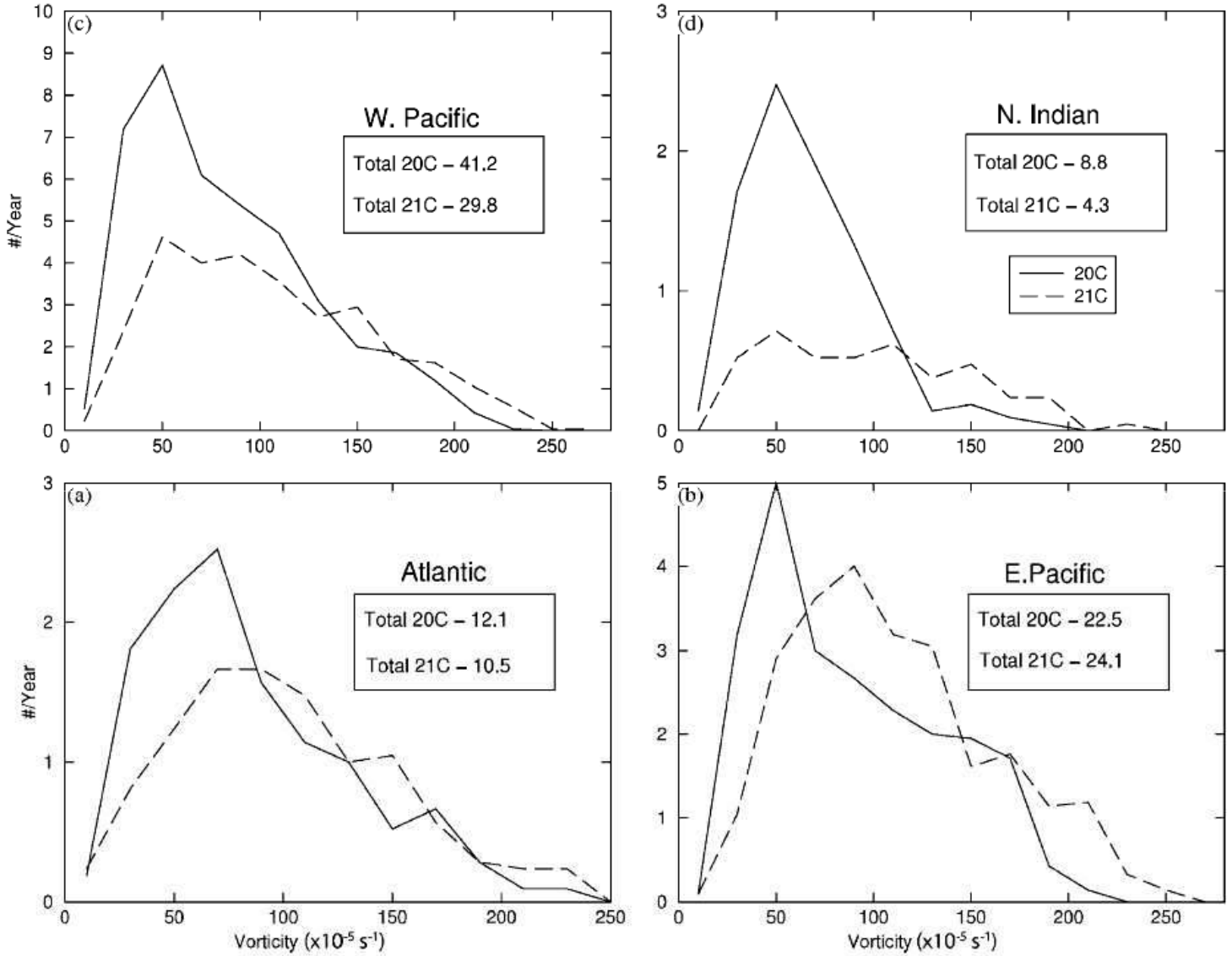

Fig. 16. T319 regional distributions of maximum attained intensity based on 850 hPa relative vorticity for 20C and 21C for (a) Atlantic, (b) eastern Pacific, (c) western Pacific and (d) north Indian ocean. Bin widths are 2×10^{-4} s^{-1}. Inset boxes show the total number per year for each region and for 20C and 21C, respectively.

Emanuel et al. (2008) BAMS

HURRICANES AND GLOBAL WARMING

Results from Downscaling IPCC AR4 Simulations

BY KERRY EMANUEL, RAGOTH SUNDARARAJAN, AND JOHN WILLIAMS

A new technique for deriving hurricane climatologies from global data, applied to climate models, indicates that global warming should reduce the global frequency of hurricanes, though their intensity may increase in some locations.

Downscaling CMIP3 models using CHIPS model.
Random seeding of warm core vortex with max wind 12m/s.

Emanuel et al. (2008) BAMS

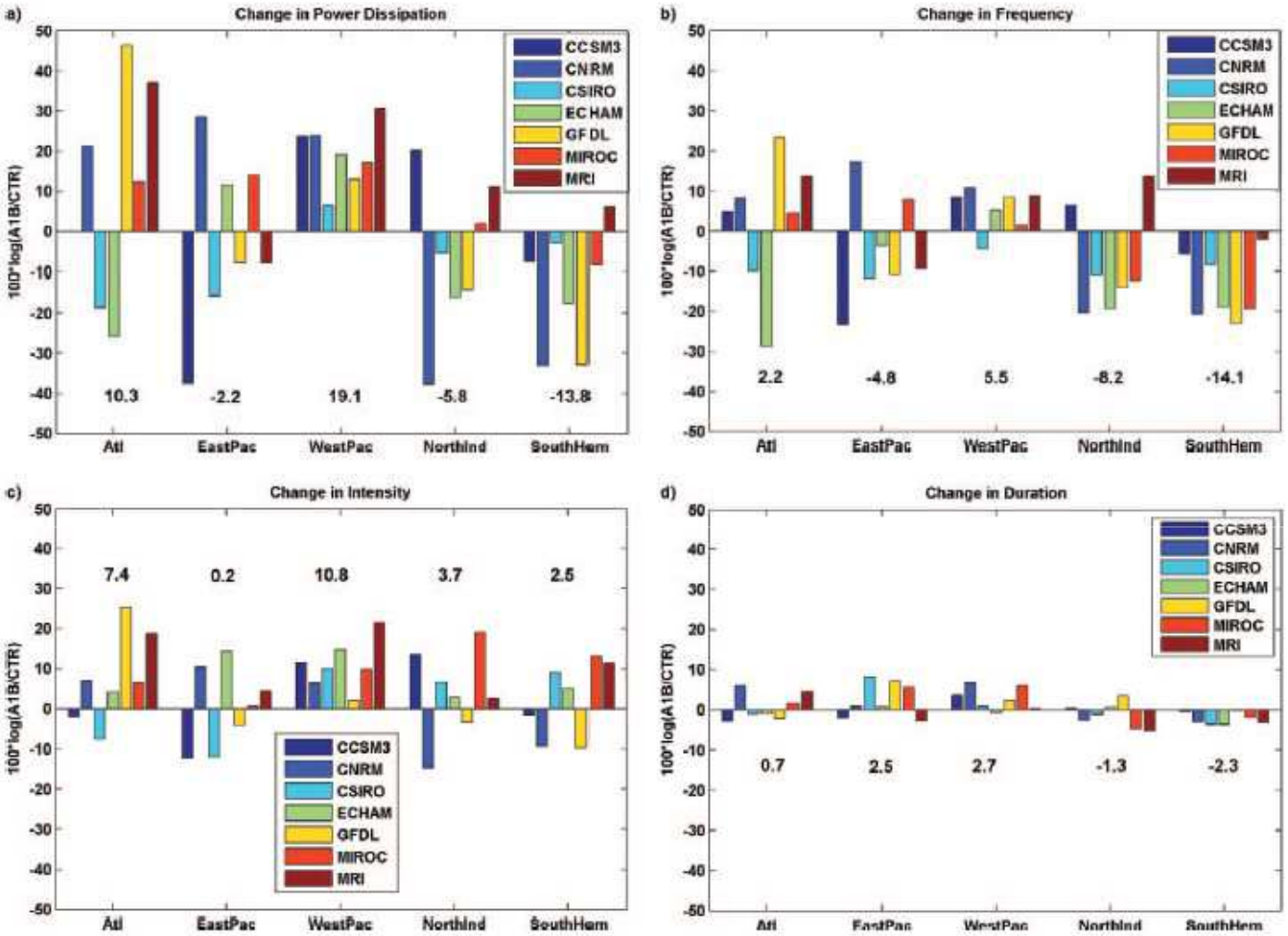

FIG. 8. Change in basinwide tropical cyclone (a) power dissipation, (b) frequency, (c) intensity, and (d) duration from the last 20 yr of the twentieth century to the last 20 yr of the twenty-second century, as predicted by running 2,000 synthetic events in each basin in each period of 20 yr. The different colors correspond to the different global climate models, as given in the legends. See text for definitions of intensity and duration. The change here is given as 100 multiplied by the logarithm of the ratio of twenty-second- and twentieth-century quantities. Note that (a) is the sum of (b)–(d). The values of the changes averaged across all models are given by the numbers in black.

Emanuel et al. (2008) BAMS

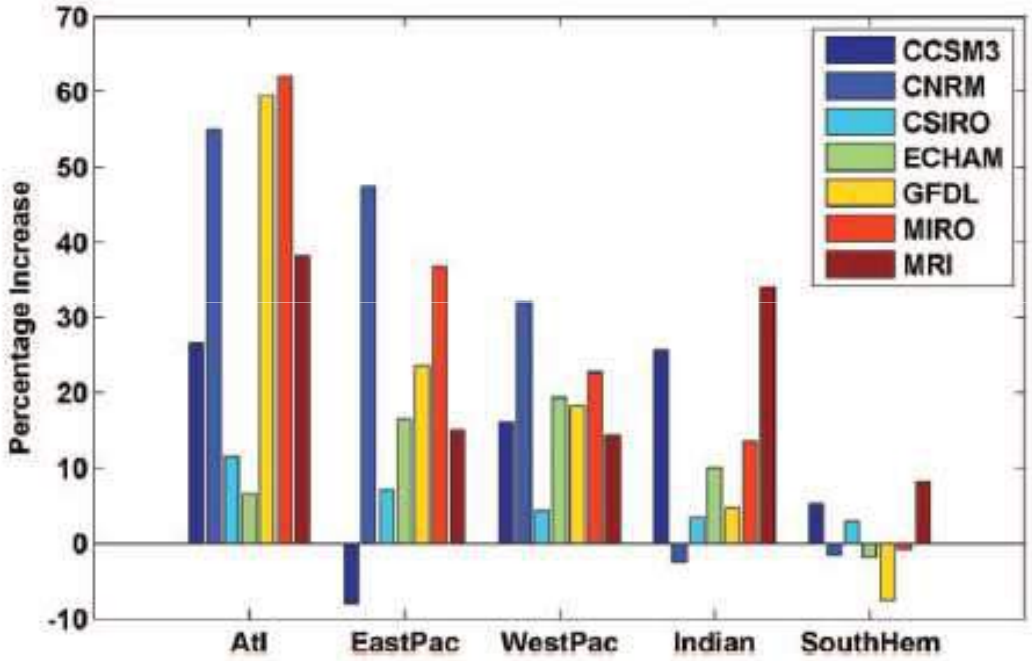

FIG. 10. Percentage increase in basin-wide tropical cyclone frequency from the last 20 yr of the twentieth century to the last 20 yr of the twenty-second century, as predicted by running 2,000 synthetic events in each basin in each period of 20 yr. The different colors correspond to the different global climate models, as given in the legends. In this experiment, the saturation mixing ratio q^* was held to a fixed constant value in (4); this should be contrasted with Fig. 8b in which q^* was permitted to vary with climate change.

Knutsonl et al. (2008) Nature GS

LETTERS

Simulated reduction in Atlantic hurricane frequency under twenty-first-century warming conditions

THOMAS R. KNUTSON*, JOSEPH J. SIRUTIS, STEPHEN T. GARNER, GABRIEL A. VECCHI AND ISAAC M. HELD

NOAA/Geophysical Fluid Dynamics Laboratory, Princeton, New Jersey 08542, USA
*e-mail: Tom.Knutson@noaa.gov

Downscaling N Atlantic hurricanes
using 18km resolution regional model (ZETAC)
without cumulus parameterization

Knutsonl et al. (2008) Nature GS

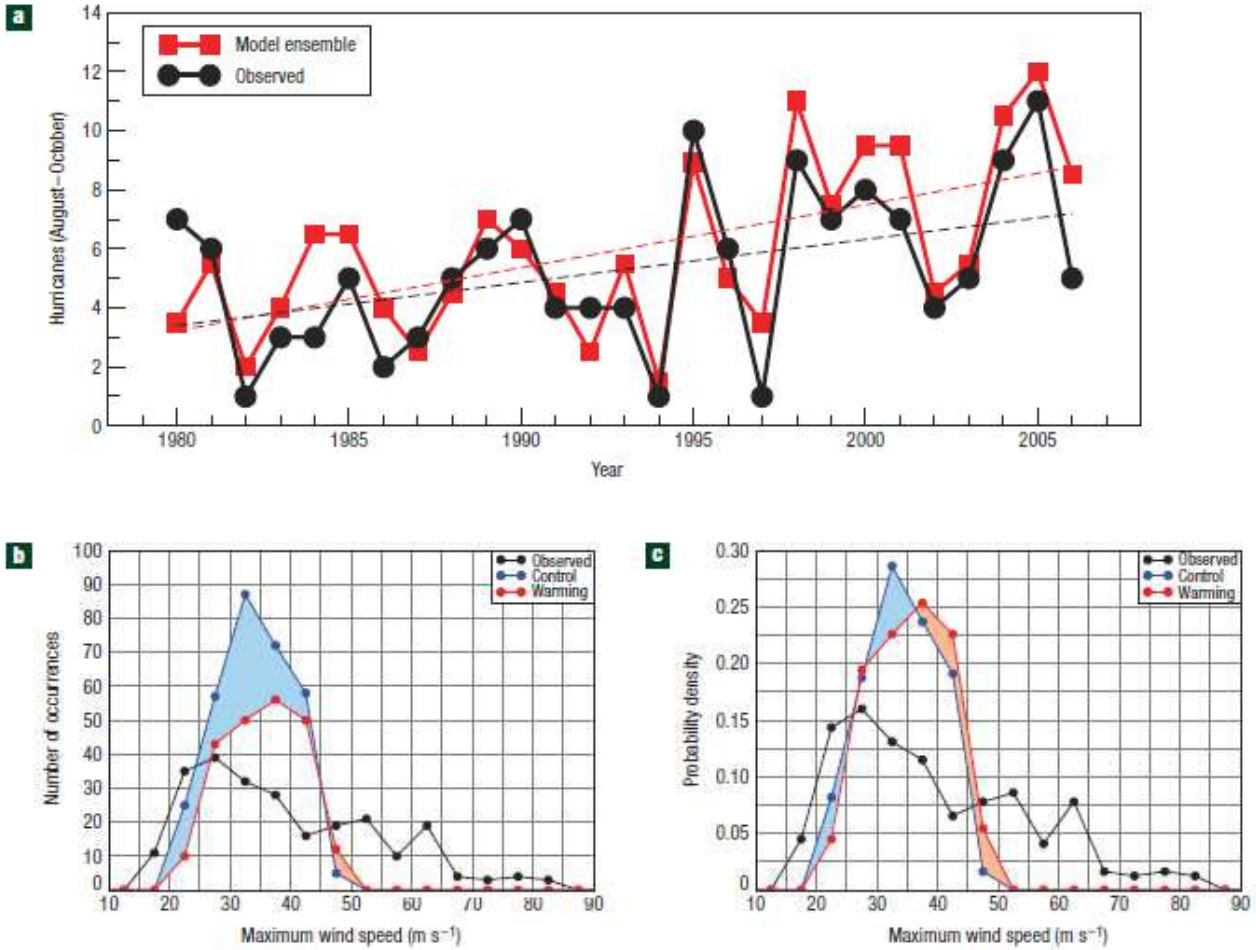

Figure 1 Model versus observed Atlantic hurricane counts and distributions of maximum tropical cyclone wind speeds. a, Annual (August–October) counts of Atlantic hurricanes in observations and for the model using observed SSTs and large-scale nudging of the interior solution towards reanalyses. Correlation = 0.84; linear trends: +0.21 storms yr^{-1} (model) and +0.15 storms yr^{-1} (observed). **b**,**c**, Histograms of maximum wind speeds, m s^{-1} (one value per storm) for each Atlantic storm observed or simulated by the model for 1980–2006 (August–October). The normalized histogram (**c**) was obtained by dividing by the total number of storms observed or simulated during the 27 yr period. This controls for differences in storm frequency between experiments or between the control and observations.

Gualdi et al. (2008) JCLI

Changes in Tropical Cyclone Activity due to Global Warming: Results from a High-Resolution Coupled General Circulation Model

S. GUALDI

Istituto Nazionale di Geofisica e Vulcanologia, Bologna, and Centro Euro-Mediterraneo per i Cambiamenti Climatici, Lecce, Italy

E. SCOCCIMARRO

Istituto Nazionale di Geofisica e Vulcanologia, Bologna, Italy

A. NAVARRA

Istituto Nazionale di Geofisica e Vulcanologia, Bologna, and Centro Euro-Mediterraneo per i Cambiamenti Climatici, Lecce, Italy

(Manuscript received 28 February 2007, in final form 7 April 2008)

T106 (120km) CGCM
Preind, present, 2xCO2, 4xCO2

Gualdi et al. (2008) JCLI

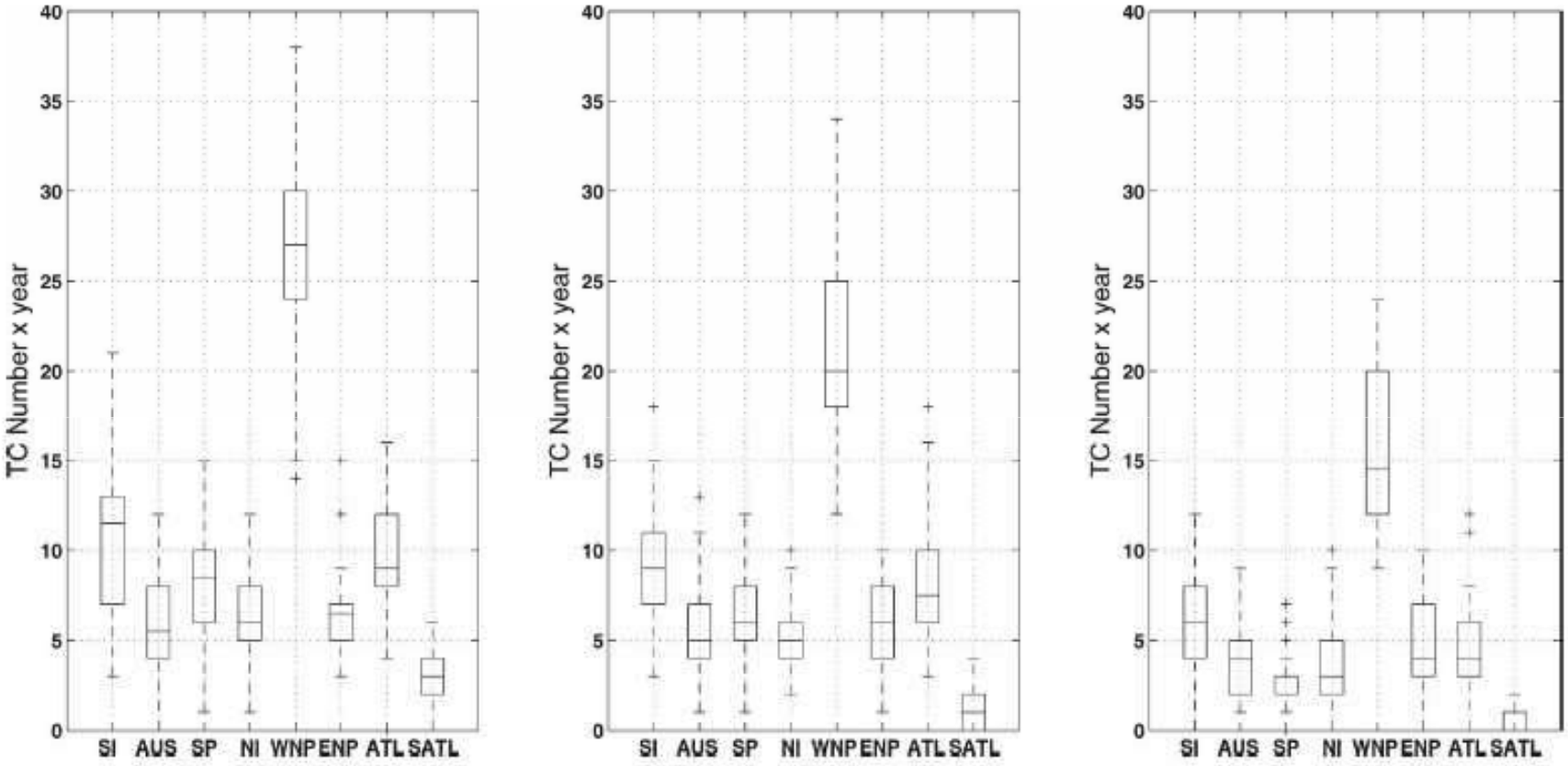

FIG. 12. Box plot of the annual number of TCs in the areas defined in Fig. 4 and for the SATL region: (left) PREIND, (middle) 2CO2, and (right) 4CO2 experiments.

Zhao et al. (2009) JCLI

Simulations of Global Hurricane Climatology, Interannual Variability, and Response to Global Warming Using a 50-km Resolution GCM

MING ZHAO

University Corporation for Atmospheric Research, Boulder, Colorado, and NOAA/Geophysical Fluid Dynamics Laboratory, Princeton, New Jersey

ISAAC M. HELD, SHIAN-JIANN LIN, AND GABRIEL A. VECCHI

NOAA/Geophysical Fluid Dynamics Laboratory, Princeton, New Jersey

(Manuscript received 23 January 2009, in final form 1 June 2009)

50km AGCM GFDL HiRAM
Prescribed SST (HadISST, Reynolds)
Future SST from A1B scenario (CM21, HADCM3, ECHAM5)

Zhao et al. (2009) JCLI

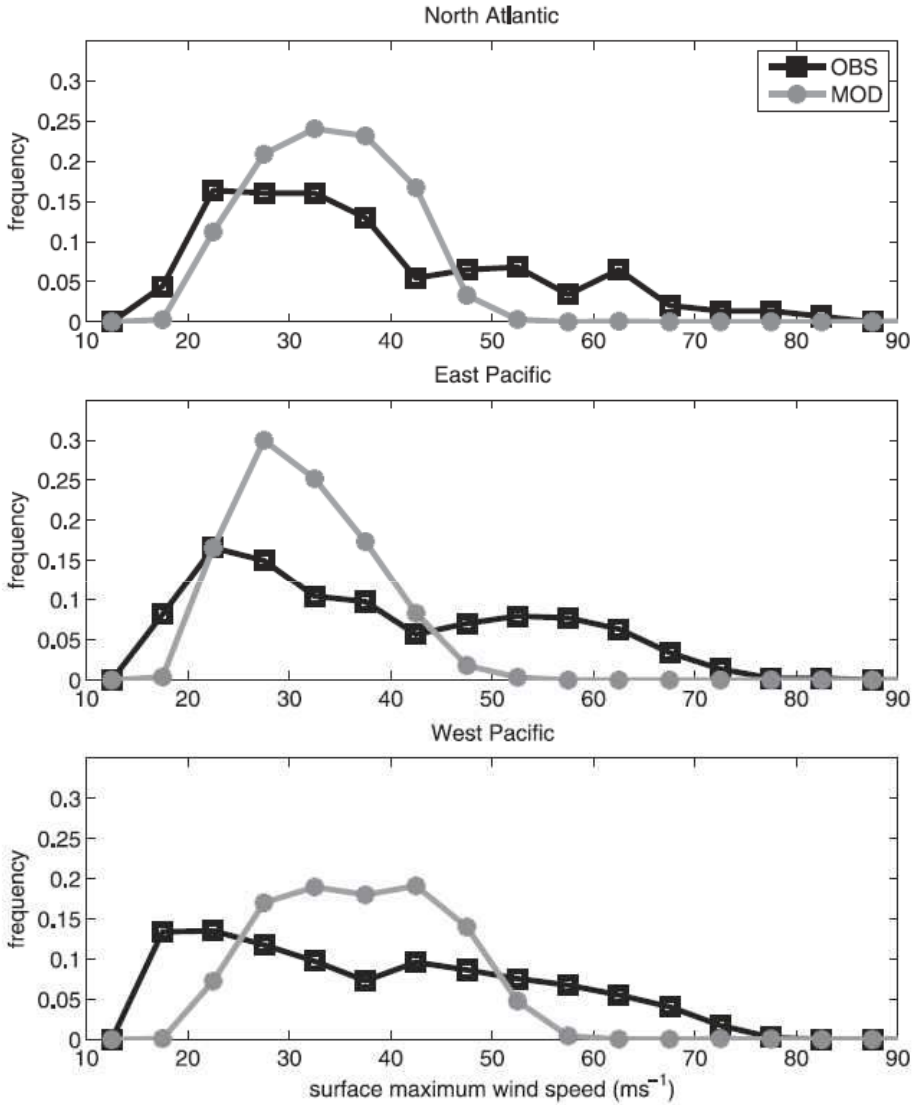

FIG. 6. A comparison of observed and model-simulated tropical storm intensity distribution as characterized by the surface maximum wind speed for the (top) North Atlantic, (middle) east Pacific, and (bottom) west Pacific. IBTrACS observations using 1-min maximum sustained wind at 10 m (black). Model simulation using 15-min (model time step) winds at the lowest model level (gray).

Zhao et al. (2009) JCLI

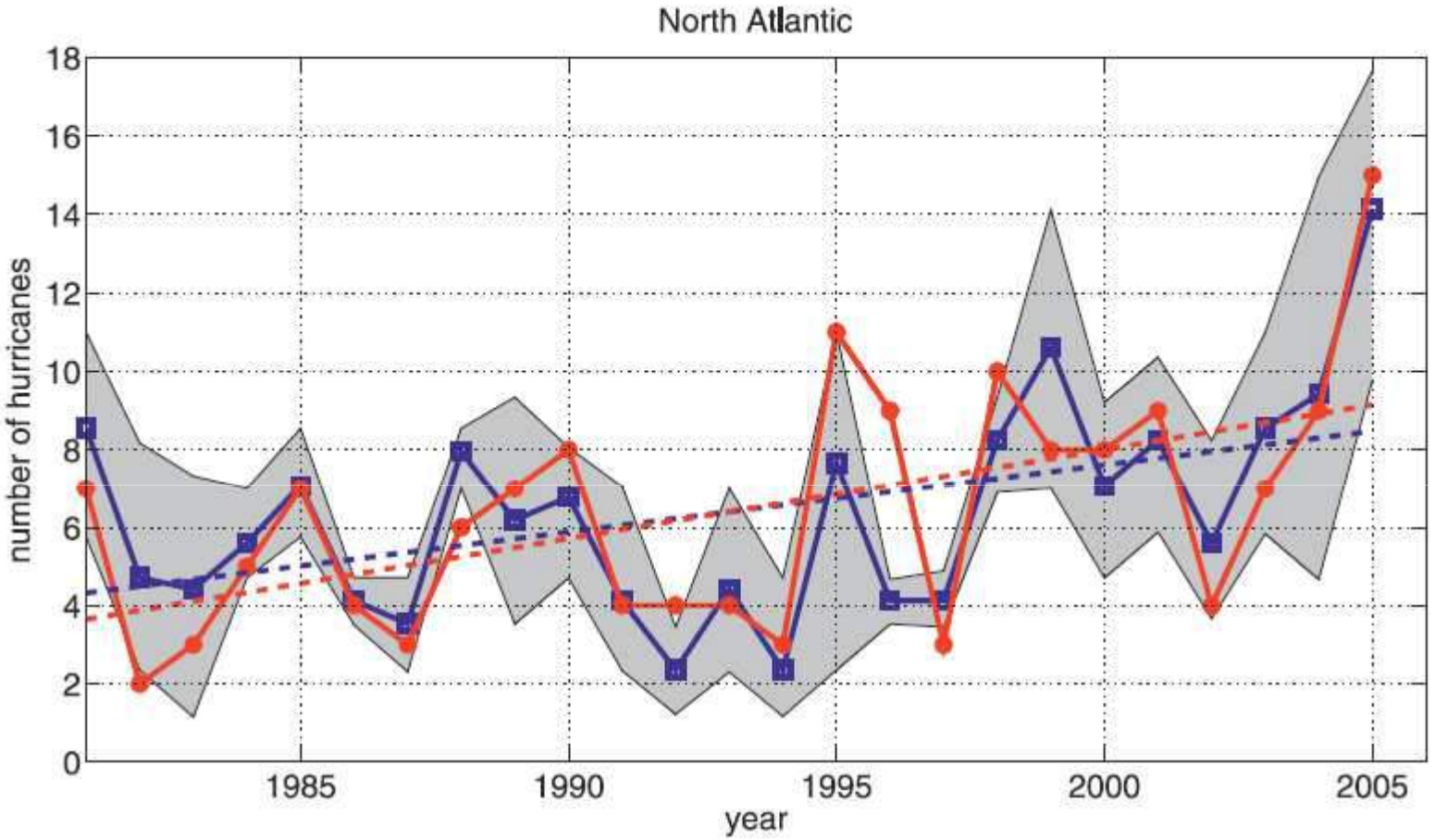

FIG. 7. Interannual variation of hurricane numbers for North Atlantic from 1981 to 2005. IBTrACS observations (Kruk et al. 2010) (red) and four-member ensemble mean (blue); shaded area shows the simulated maximum and minimum number for each year from the four-member integrations. Model time series are normalized by time-independent multiplicative factors so as to reproduce the observed total number. Dotted lines show observed and model (ensemble mean) linear trends.

Zhao et al. (2009) JCLI

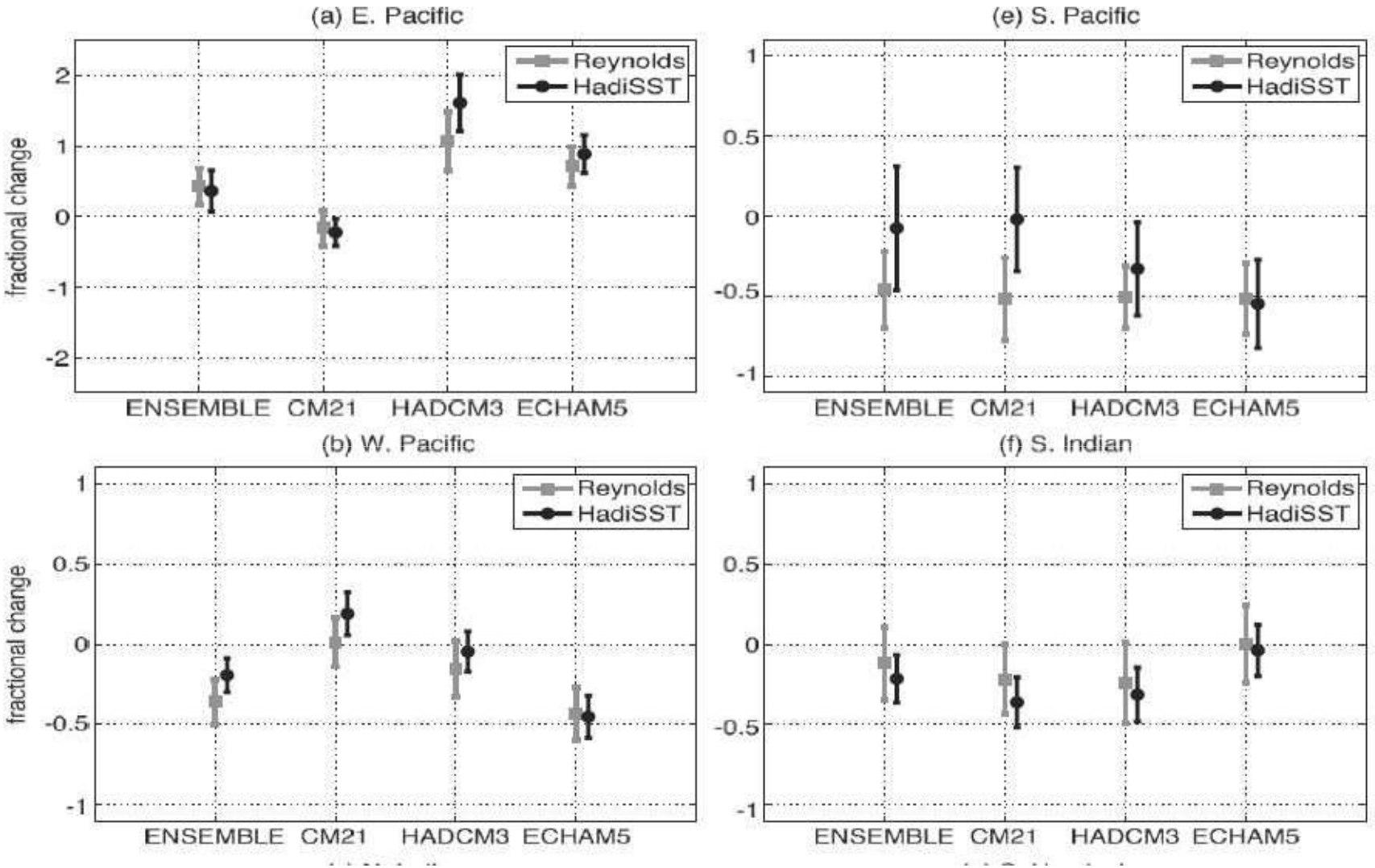

Zhao et al. (2009) JCLI

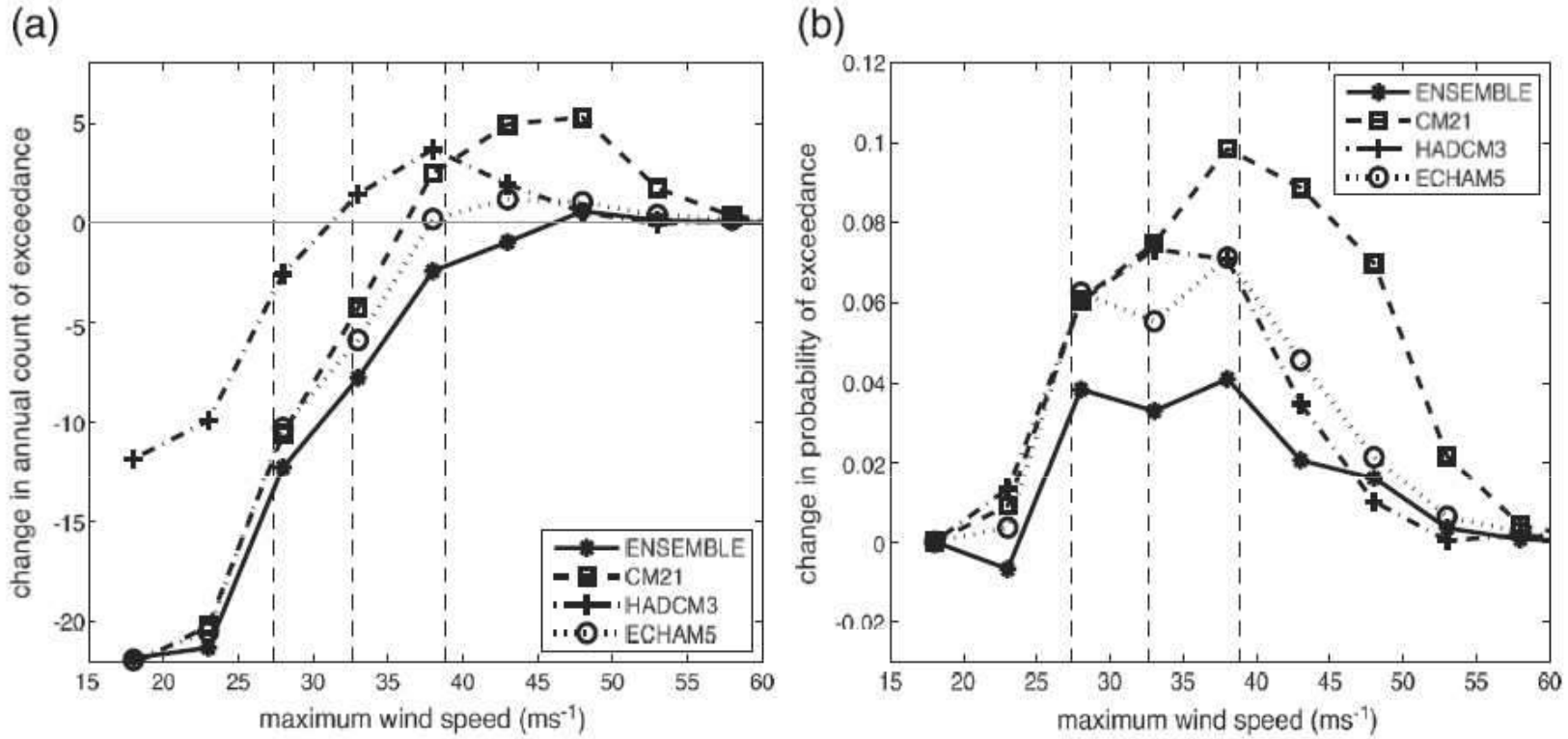

FIG. 18. (a) Change (warming minus control) in annual storm count exceeding a given surface maximum wind for the entire global tropical ocean. Vertical lines show the lower quartile, median, and upper quartile of the controls. (b) As in (a), but showing changes in the probability of exceedance of tropical storm intensity. A positive value indicates the relative increase in the fraction of storms with maximum surface wind speed above the corresponding value.

Sugi et al. (2009) SOLA

A Reduction in Global Tropical Cyclone Frequency due to Global Warming

Masato Sugi[1,2], Hiroyuki Murakami[3] and Jun Yoshimura[2]

[1] *Research Institute for Global Change, JAMSTEC, Yokohama, Japan*

[2] *Meteorological Research Institute, JMA, Tsukuba, Japan*

[3] *Advanced Earth Science and Technology Organization, MRI, Tsukuba, Japan*

Experiments	Resolution	ΔSST	Integration	Ratio(%) of TC frequency Future/Present								
				Global	NH	SH	N Indian	NW Pacific	NE Pacific	N Atlantic	S Indian	S Pacific
C	TL959, 20km	MRI CGCM2.3	10yr	70	72	68	48	62	66	134	72	57
A0	TL959, 20km	MRI CGCM2.3	20yr	71	68	73	61	64	61	122	72	76
A1	TL959, 20km	MRI CGCM2.3	20yr	75	75	75	71	71	70	123	75	73
A2	TL959, 20km	MIROC-H	10yr	73	85	58	132	128	50	82	76	10
A3	TL959, 20km	CMIP3	25yr	80	79	81	85	74	75	105	95	58
B1	TL319, 60km	MRI CGCM2.3	25yr	80	79	83	88	66	69	158	78	92
B2	TL319, 60km	MIROC-H	25yr	94	100	84	179	164	58	106	110	31
B3	TL319, 60km	CMIP3	25yr	79	81	75	133	86	67	104	82	64
B4	TL319, 60km	CSIRO	25yr	78	71	89	93	113	51	63	78	110

Sugi et al. (2009) SOLA

Regional TC Frequency Change and SST

Experi-ments	Resolution	ΔSST	Integra-tion	Ratio(%) of TC frequency Future/Present								
				Global	NH	SH	N Indian	NW Pacific	NE Pacific	N Atlantic	S Indian	S Pacific
O	TL959, 20km	MRI CGCM2.3	10yr	70	72	68	48	62	66	134	72	57
A0	TL959, 20km	MRI CGCM2.3	20yr	71	69	73	61	64	61	122	72	78
A1	TL959, 20km	MRI CGCM2.3	20yr	75	75	75	71	71	70	123	75	73
B1	TL319, 60km	MRI CGCM2.3	25yr	80	79	83	88	66	69	158	78	92
A3	TL959, 20km	CMIP3	25yr	80	79	81	85	74	75	105	95	58
B3	TL319, 60km	CMIP3	25yr	79	81	75	133	86	67	104	82	64
B2	TL319, 60km	MIROC-H	25yr	94	100	84	179	164	58	106	110	31
A2	TL959, 20km	MIROC-H	10yr	73	85	58	132	128	50	82	76	10
B4	TL319, 60km	CSIRO	25yr	78	71	89	93	113	51	63	78	110

Bender et al. (2010) Science

Modeled Impact of Anthropogenic Warming on the Frequency of Intense Atlantic Hurricanes

Morris A. Bender,[1*] Thomas R. Knutson,[1] Robert E. Tuleya,[2] Joseph J. Sirutis,[1]
Gabriel A. Vecchi,[1] Stephen T. Garner,[1] Isaac M. Held[1]

Downscaling N. Atlantic hurricanes simulated by ZETAC model
using GFDL and GFDN Hurricane Models
triply nested model with minimum grid distance of 8km

Bender et al. (2010) Science

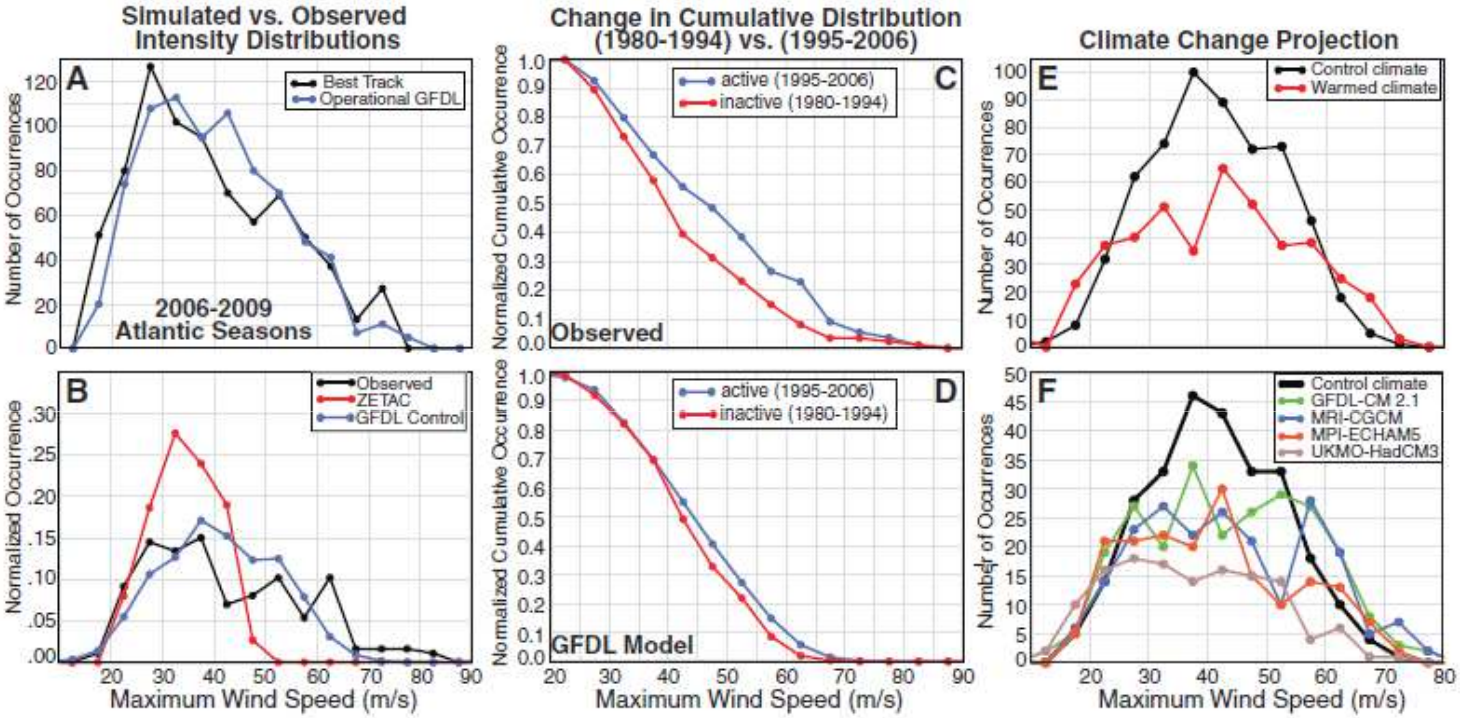

Fig. 1. Simulated and observed histograms of maximum surface wind speed (m/s) in the Atlantic basin. (**A**) Simulated versus observed maximum winds for every 120-hour forecast made (at 6-hour intervals) during the 2006 to 2009 hurricane seasons, using the GFDL operational model run by NOAA's NWS (excluding depressions). (**B**) Normalized intensity histogram (dividing by the total number of storms) for the ZETAC regional model (red), the combined GFDL (NWS) and GFDN (Navy) downscalings (blue), and the observed (black) for the 27 seasons (1980 to 2006) of the control simulations. (**C** and **D**) Observed (C) and simulated (D) cumulative maximum wind distribution (CDFs) comparing the period 1995 to 2006 (blue) to 1980 to 1994 (red). (**E**) Comparison of control (black) and warm climate (red) distributions (combined GFDL and GFDN models) based on the 18-member CMIP3 ensemble A1B scenario climate change. (**F**) Comparison of control (black) and warm climate (colors) distributions for the GFDL and GFDN models based on the four individual CMIP3 model A1B warming scenarios. To save computer resources, the four supplemental experiments (F) were only run for the 13 odd years during 1981 to 2005.

Bender et al. (2010) Science

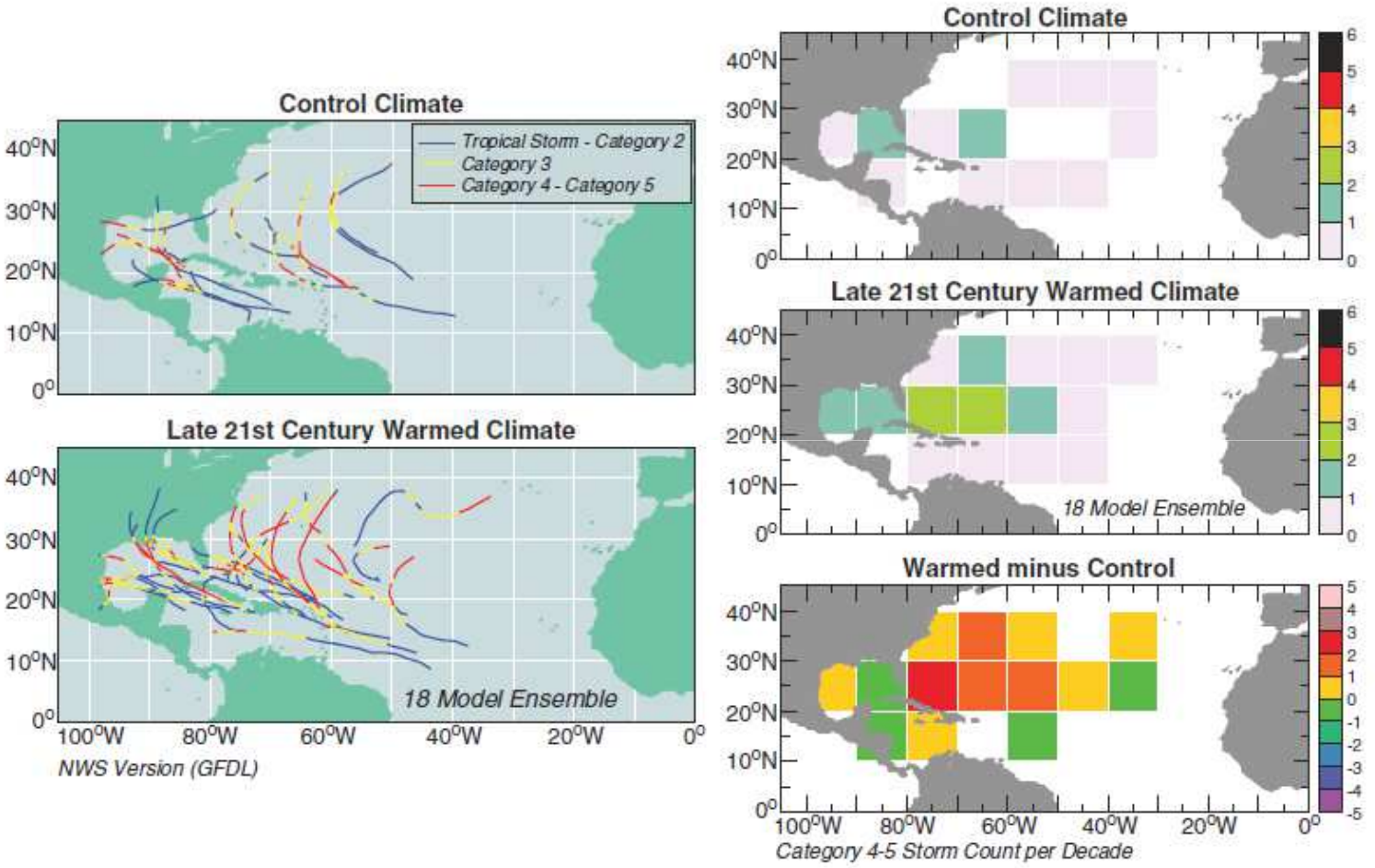

Fig. 3. (**Left**) Tracks for all storms reaching category 4 or 5 intensity, for the control and the warmed 18-model ensemble conditions, as obtained using the GFDL/NWS hurricane model. (**Right**) The spatial distribution of category 4 and 5 occurrences (scaled by storm counts per decade) for the combined control (average of the GFDL and GFDN model versions, top right); the combined CMIP3 18-model ensemble warmed climate results (middle right); and the difference between the warmed climate and control intense hurricane occurrences (bottom right). (The tracks for both the GFDL and GFDN models are presented in fig. S7 for comparison.)

Knutson et al. (2010) Nature GS

nature geoscience

REVIEW ARTICLE

PUBLISHED ONLINE: 21 FEBRUARY 2010 | DOI: 10.1038/NGEO779

Tropical cyclones and climate change

Thomas R. Knutson[1]*, John L. McBride[2], Johnny Chan[3], Kerry Emanuel[4], Greg Holland[5], Chris Landsea[6], Isaac Held[1], James P. Kossin[7], A. K. Srivastava[8] and Masato Sugi[9]

Whether the characteristics of tropical cyclones have changed or will change in a warming climate — and if so, how — has been the subject of considerable investigation, often with conflicting results. Large amplitude fluctuations in the frequency and intensity of tropical cyclones greatly complicate both the detection of long-term trends and their attribution to rising levels of atmospheric greenhouse gases. Trend detection is further impeded by substantial limitations in the availability and quality of global historical records of tropical cyclones. Therefore, it remains uncertain whether past changes in tropical cyclone activity have exceeded the variability expected from natural causes. However, future projections based on theory and high-resolution dynamical models consistently indicate that greenhouse warming will cause the globally averaged intensity of tropical cyclones to shift towards stronger storms, with intensity increases of 2–11% by 2100. Existing modelling studies also consistently project decreases in the globally averaged frequency of tropical cyclones, by 6–34%. Balanced against this, higher resolution modelling studies typically project substantial increases in the frequency of the most intense cyclones, and increases of the order of 20% in the precipitation rate within 100 km of the storm centre. For all cyclone parameters, projected changes for individual basins show large variations between different modelling studies.

Knutson et al. (2010) Nature GS

nature geoscience

REVIEW ARTICLE

PUBLISHED ONLINE: 21 FEBRUARY 2010 | DOI: 10.1038/NGEO779

Tropical cyclones and climate change

"High-resolution dynamical models consistently indicate that greenhouse warming will cause the global average intensity of tropical cyclones to shift towards stronger storms, by 2-11%. "

"Existing modelling studies also consistently project decreases in the globally averaged frequency of tropical cyclones, by 6–34%."

"For all cyclone parameters, projected changes for individual basins show large variations between different modelling studies."

Murakami et al. (2012) CD

Clim Dyn (2012) 39:2569–2584
DOI 10.1007/s00382-011-1223-x

Future changes in tropical cyclone activity projected by multi-physics and multi-SST ensemble experiments using the 60-km-mesh MRI-AGCM

Hiroyuki Murakami · Ryo Mizuta · Eiki Shindo

60km MRI-AGCM, ensemble experiment
CMIP3 SST change cluster,
AS, YS and KF convection scheme

Murakami et al. (2012) CD

4 SST anomaly patterns

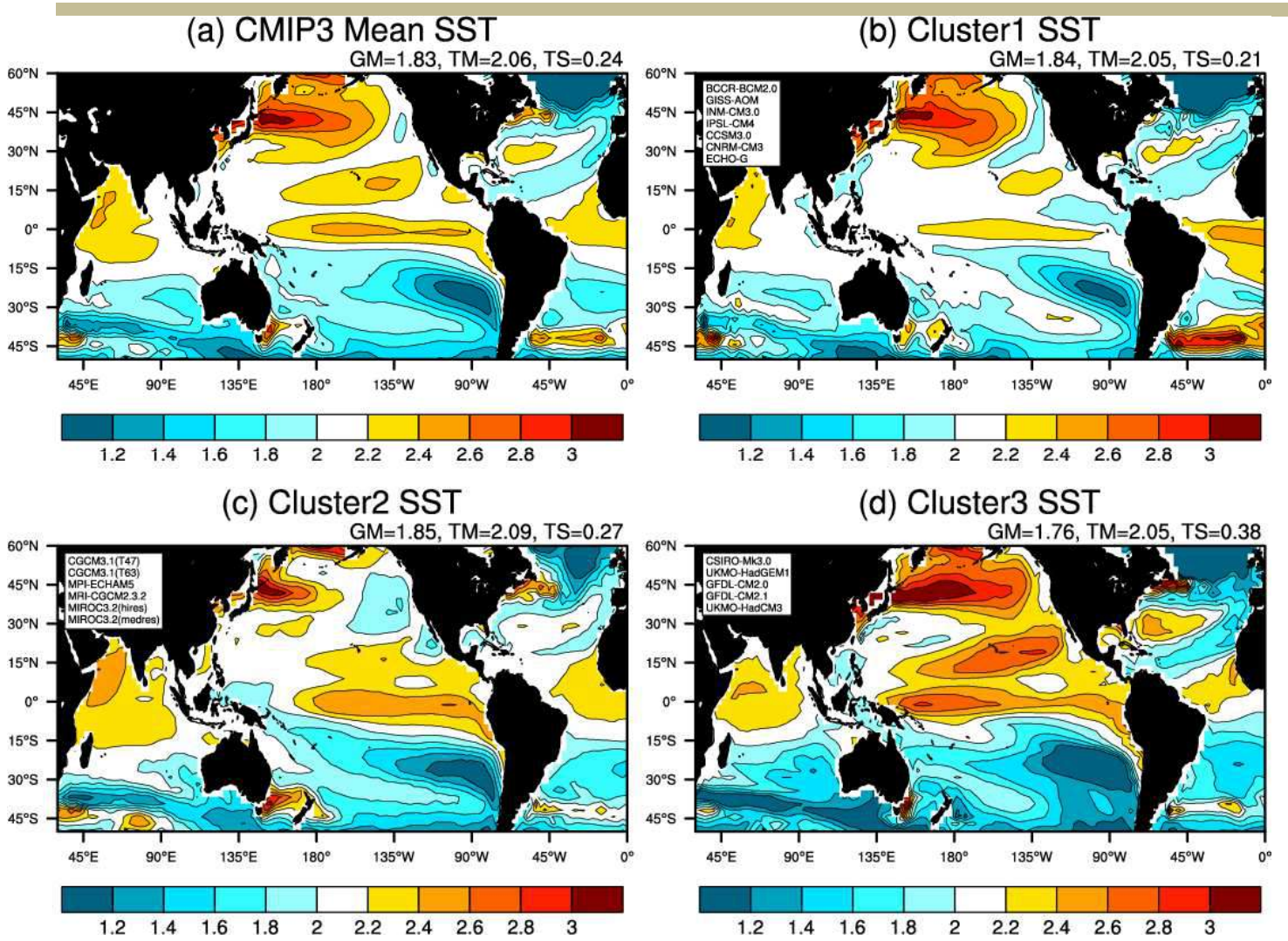

Cluster 1 shows small spatial variance in tropics, while Cluster 3 SST shows large spatial variance in tropics.

Murakami et al. (2012) CD

Future changes in TC Genesis Frequency (TGF) [%]

Y: Yoshimura, K:Kain-Fritsch, A: Arakawa Shubert

0: CMIP3 mean SST, 1:Cluster 1, 2:Cluster 2, 3: Cluster 3, G: Global uniform

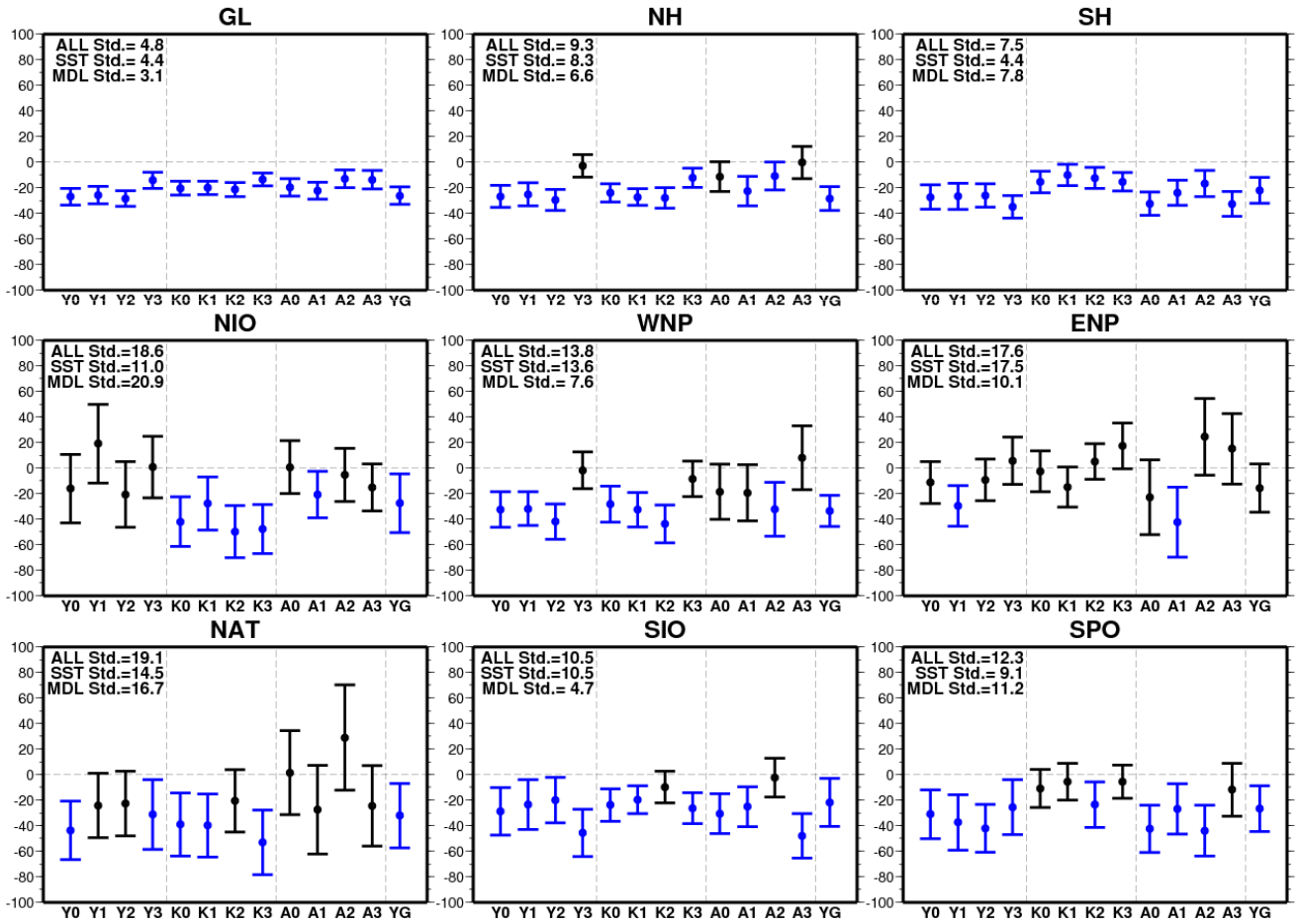

Small uncertainty in the GL, NH, SH scale reduction of TC number

Large uncertainty in the ocean basin scale changes in TC number

Murakami et al. (2012) JCLI

Future Changes in Tropical Cyclone Activity Projected by the New High-Resolution MRI-AGCM*

HIROYUKI MURAKAMI

Japan Agency for Marine-Earth Science and Technology, Meteorological Research Institute, Tsukuba, Ibaraki, Japan

YUQING WANG

Department of Meteorology, and International Pacific Research Center, University of Hawaii at Manoa, Honolulu, Hawaii

HIROMASA YOSHIMURA AND RYO MIZUTA

Meteorological Research Institute, Tsukuba, Ibaraki, Japan

MASATO SUGI

Japan Agency for Marine-Earth Science and Technology, Meteorological Research Institute, Tsukuba, Ibaraki, Japan

EIKI SHINDO, YUKIMASA ADACHI, SEIJI YUKIMOTO, MASAHIRO HOSAKA, SHOJI KUSUNOKI, TOMOAKI OSE, AND AKIO KITOH

Meteorological Research Institute, Tsukuba, Ibaraki, Japan

(Manuscript received 3 August 2011, in final form 31 October 2011)

20km MRI-AGCM, CMIP3 ensemble mean SST change,
AS and YS convection scheme

Murakami et al. (2012) JCLI

熱帯低気圧の経路

観測　現在（1979-2003）

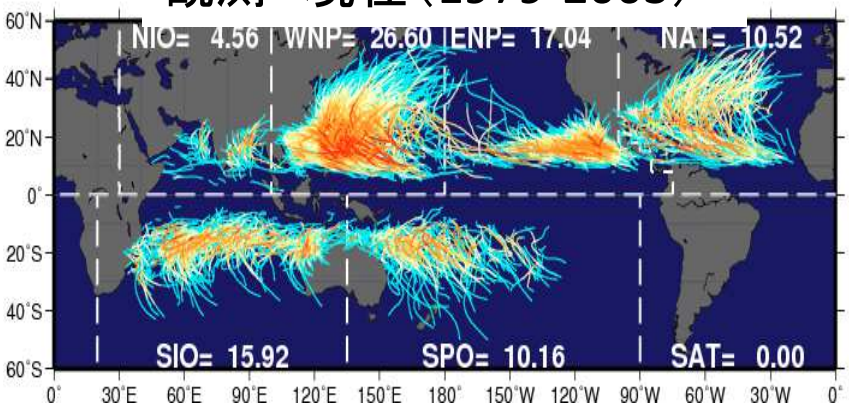

旧モデル　現在（1979-2003）

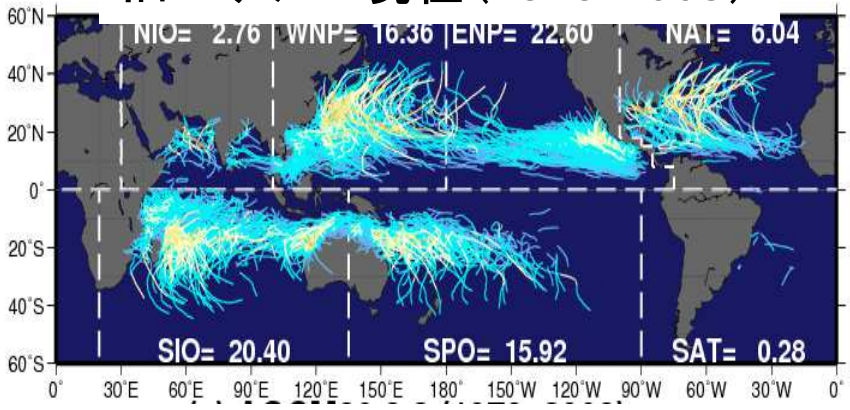

新モデル　現在　(1979-2003)

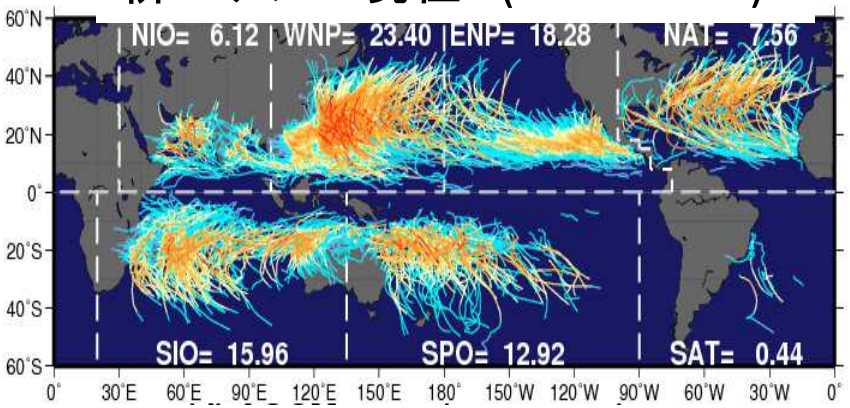

新モデル　将来(2075-2099)

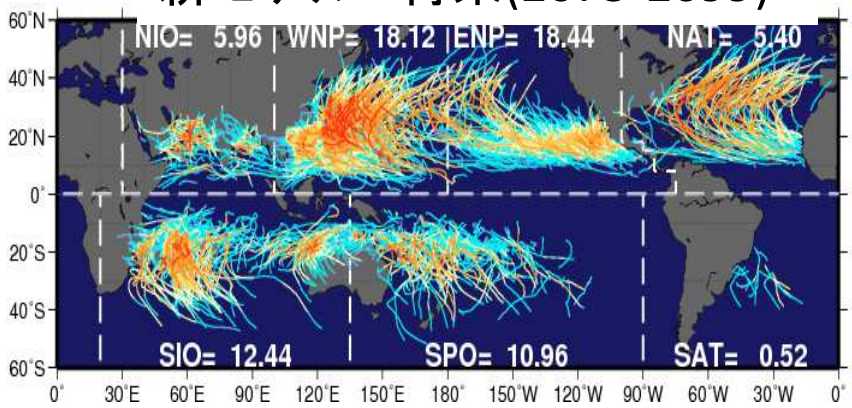

TD　TS　C1　C2　C3　C4　C5

Murakami et al. (2012) JCLI

生涯最大風速別TC頻度

旧モデル V3.1

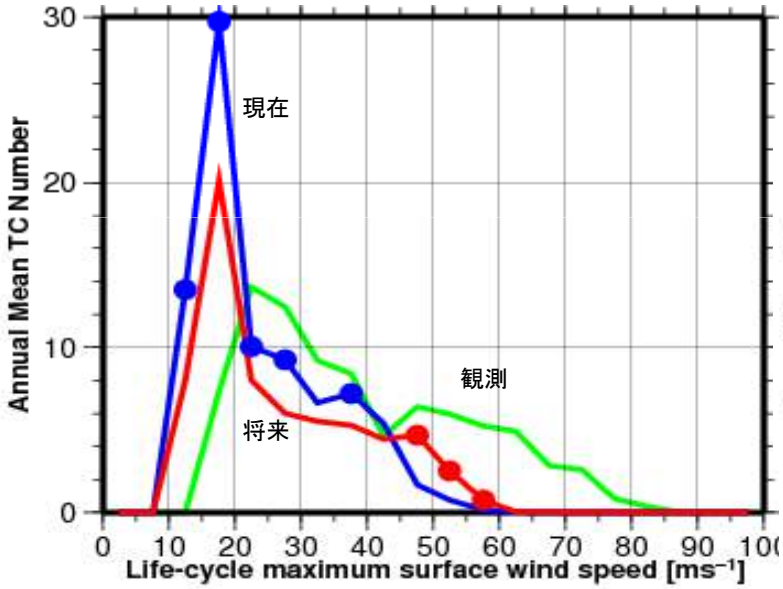

新モデル V3.2

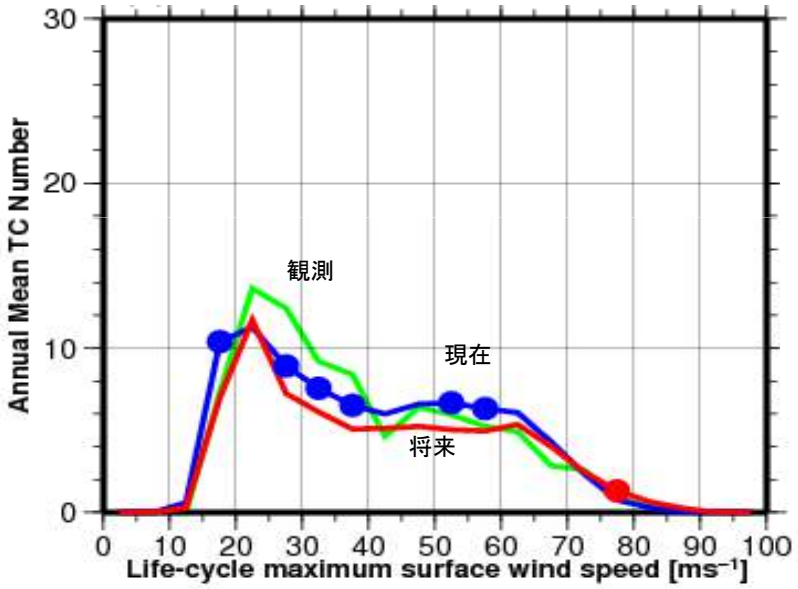

観測

現在

将来

有意水準95%で増加

有意水準95%で減少

Changes in Tropical Cyclones IPCC AR5 (2013) Figure 14.17

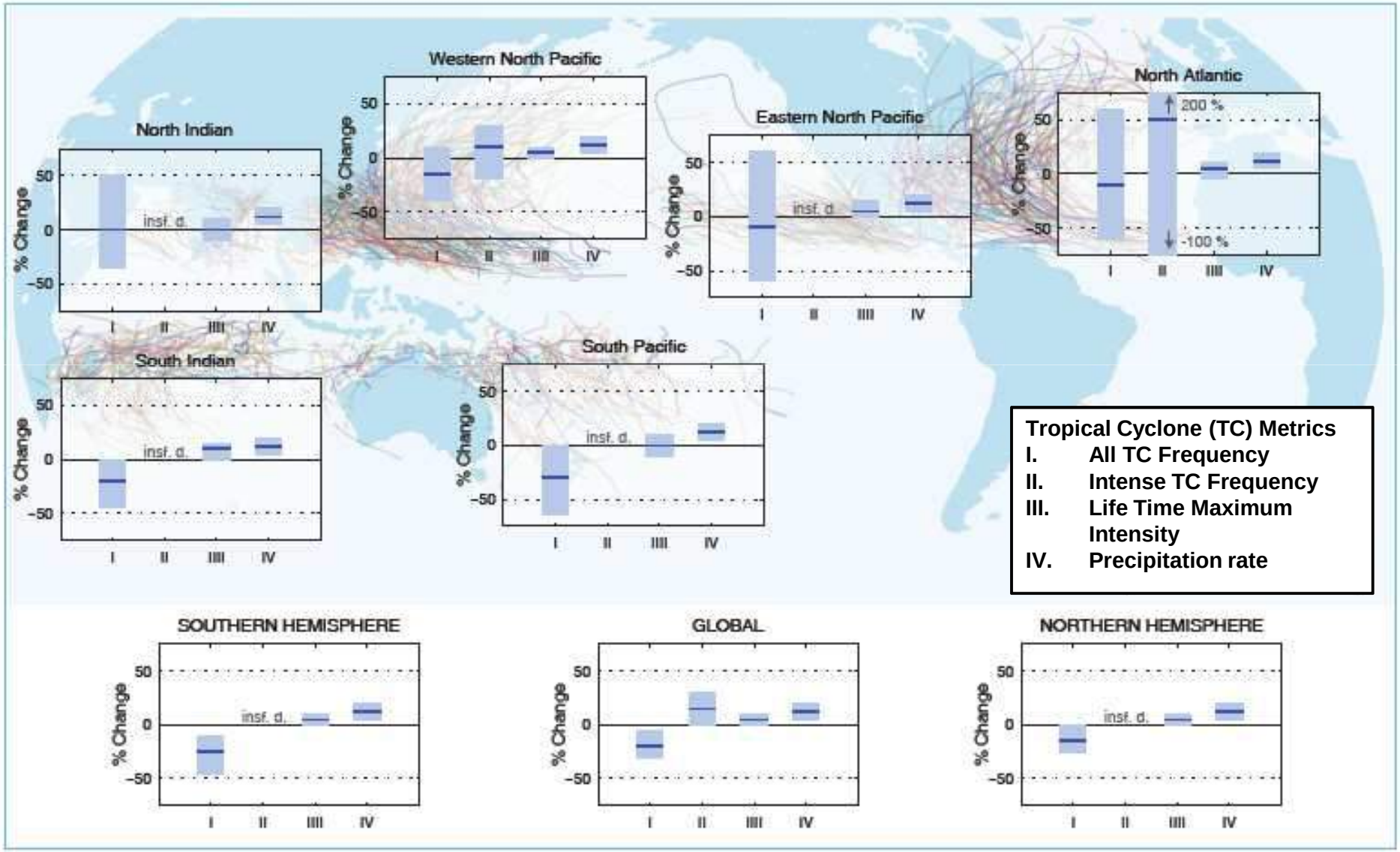

非常に強い台風の数の将来変化

[Cat4+Cat5 TC, V_{max}≥ 59m/s] 5ºx5º Box 10年当たりの数を表示

観測 (BEST TRACK)

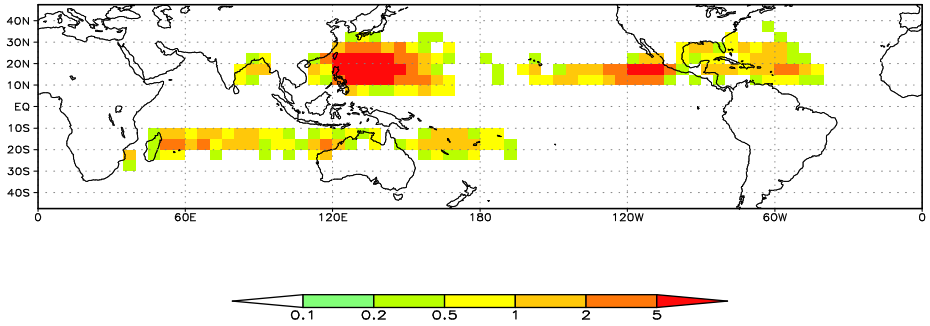

現在（11メンバー）

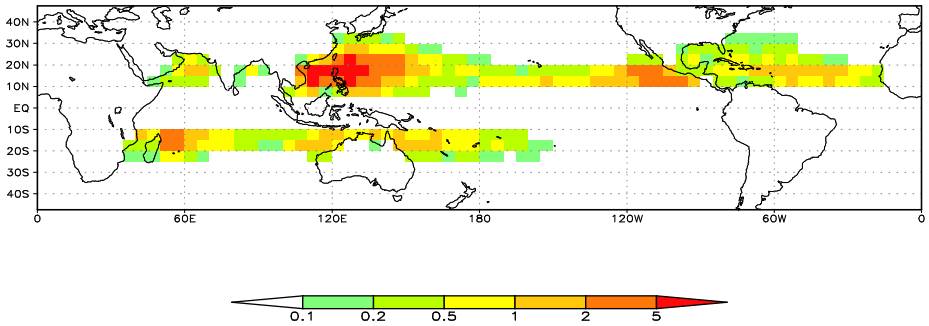

将来（29メンバー）

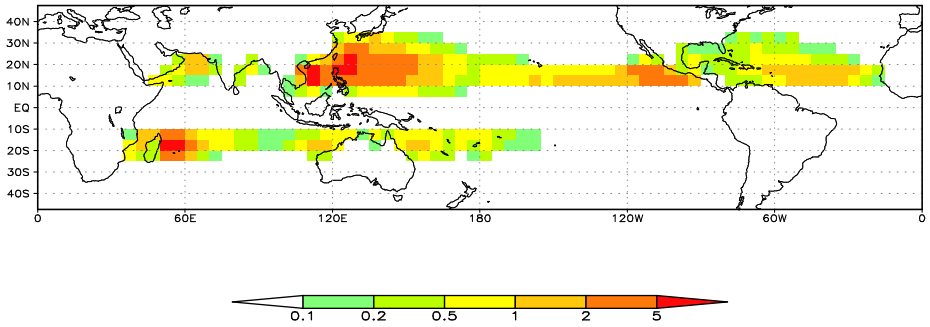

将来変化

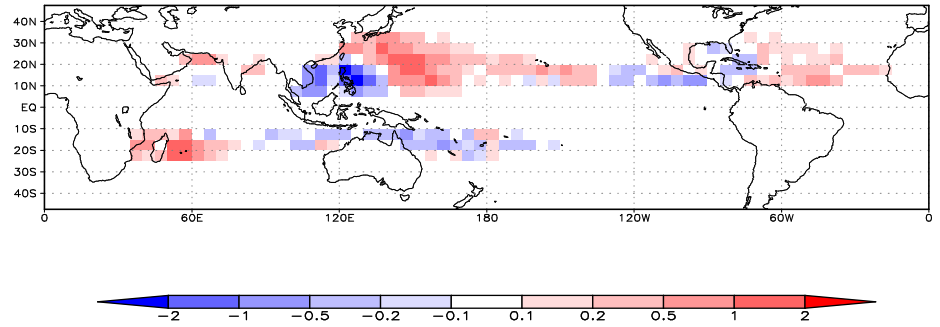

非常に強い台風の数は多くの地域で増加傾向であるが、北西太平洋西部とオーストラリア周辺、および北東太平洋と北大西洋西部では減少傾向。

今後の課題

予測の不確実性の低減

- SSTの予測 （とくに地域的な変化の予測）
- 物理過程 （とくに対流スキーム）
- 解像度 （とくに強い台風）
- 海洋とのカップリング （とくに強い台風）

変化のメカニズムの理解 (→Part2)

- 台風の発生・発達のメカニズム
- 最大可能強度（MPI）理論
- 発生ポテンシャル（GPI）